DEVELOPMENT OF HYDRODYNAMICALLY ENGINEERED CARTILAGE IN RESPONSE TO INSULIN-LIKE GROWTH FACTOR-1 AND TRANSFORMING GROWTH FACTOR-BETA1: FORMATION AND ROLE OF A TYPE I COLLAGEN-BASED FIBROUS CAPSULE

A Dissertation
Presented to
The Academic Faculty

By

Yueh-Hsun Yang

In partial Fulfillment
Of the Requirements for the Degree
Doctor of Philosophy in Bioengineering
in the
School of Biomedical Engineering

Georgia Institute of Technology

August 2013

DEVELOPMENT OF HYDRODYNAMICALLY ENGINEERED CARTILAGE IN RESPONSE TO INSULIN-LIKE GROWTH FACTOR-1 AND TRANSFORMING GROWTH FACTOR-BETA1: FORMATION AND ROLE OF A TYPE I COLLAGEN-BASED FIBROUS CAPSULE

Approved by:

Dr. Gilda Barabino, Advisor
Department of Biomedical Engineering
Georgia Institute of Technology

Dr. Suzanne Eskin
Department of Biomedical Engineering
Georgia Institute of Technology

Dr. Robert Guldberg
Department of Mechanical Engineering
Georgia Institute of Technology

Dr. Jaroslava Halper
Department of Pathology
University of Georgia

Dr. Todd McDevitt
Department of Biomedical Engineering
Georgia Institute of Technology

Date Approved: June 17, 2013

To my family

ACKNOWLEDGEMENTS

I wish to express my sincere gratitude and appreciation to many people who have given me professional and valuable advice for my Ph.D. study and research. First, I would like to thank my advisor, Dr. Gilda Barabino, for her patience, guidance, mentoring and enthusiasm. Throughout my Ph.D. career at Georgia Institute of Technology, Dr. Barabino was always there to show her support and to encourage me at many difficult times. She also trained me to think independently and helped me grow and become a confident researcher and person, which will be beneficial not only for my future career but for the rest of my life. I would like to extend my appreciation to Dr. Suzanne Eskin, Dr. Robert Guldberg, Dr. Jaroslava Halper and Dr. Todd McDevitt for serving on my thesis committee and for their generous comments and commitment to my project. Special mention goes out to Dr. Halper and Mrs. Mary Ard at University of Georgia, who kindly hosted me and provided me with all the informative and technical support while I was working on a part of the experiments in the electron microscopy laboratory there for several months.

I would also like to thank the professional staffs at Institute for Bioengineering and Bioscience at Georgia Institute of Technology. Ms. Sha'Aqua Asberry in the histology laboratory provided extensive technical support, Ms. Angela Lin taught me how to operate the mechanical testing equipment, Ms. Nadia Boguslavsky helped me with flow cytometry analyses, and Mr. Andrew Shaw assisted me in confocal microscopy. This project would not have been successful without their help. I am grateful to have the fantastic lab mates who have been in this journey with me and supported me for the past

couple of years. I deeply appreciate the guidance and assistance from Dr. Tanya Farooque, a former graduate colleague, and Dr. Eileen Finnegan, a former postdoctoral mentor, who taught me cell culture and many other techniques and generously shared their successful and unsuccessful experience with me when I first joined the program so that I could avoid a lot of unnecessary failure.

I would like to acknowledge the funding source, National Science Foundation (NSF0602608), which made it possible for me to carry out this work. And last, but not least, I would like to show my sincere appreciation to the numerous calves from which I isolated knee chondrocytes for my experiments. I would not have earned my Ph.D. degree without their sacrifice.

Finally, I wish to express my greatest gratitude to my parents, Mr. Beng-Yung Yang and Mrs. Chiu-Lien Lin, in Taiwan, who have always worried about me, but have still supported me from eight thousand miles away since I left home eight years ago. Their love has been the most powerful strength that carries me through every challenge not only throughout my graduate career but in my whole life. To Dad and Mom, I would like to share this accomplishment with you and hope that I did not and will not disappoint you.

TABLE OF CONTENTS

LIST OF TABLES

LIST OF FIGURES

LIST OF ABBREVIATIONS

ANOVA: analysis of variance

BM: basal medium

BMP: bone morphogenetic protein

CC: capsule-containing

CF: capsule-free

CFD: computational fluid dynamics

DMMB: 1-9-dimethylmethylene blue

ECM: extracellular matrix

EDTA: ethylenediaminetetraacetic acid

ELISA: enzyme-linked immunosorbent assay

ERK: extracellular regulated kinase

FBS: fetal bovine serum

FGF-2: basic fibroblast growth factor

GAG: glycosaminoglycan

HEPES: N-(2-hydroxyethyl)piperazine N'-2-ethanesulfonic acid

hgDMEM: high glucose Dulbecco's modified eagle medium

IGF-1: insulin-like growth factor-1

IGF-1R: insulin-like growth factor-1 receptor

IL: interleukin

ITS: insulin-transferrin-selenium

LbL: layer-by-layer

MMP: matrix metalloproteinase

MSC: mesenchymal stem cell

ND: non-detectable

NEAA: non-essential amino acid

OA: osteoarthritis

PBS: Dulbecco's phosphate-buffered saline

PCL: polycaprolactone

pDAB: p-dimethylaminobenzaldehyde

PDGF: platelet-derived growth factor

PGA: polyglycolic acid

PIV: particle image velocimetry

PLA: poly-L-lactic acid

pSmad2: phospho-Smad2

pSmad3: phosphor-Smad3

PTOA: post-traumatic osteoarthritis

RA: rheumatoid arthritis

SEM: scanning electron microscopy

TEM: transmission electron microscopy

TGF-β: transforming growth factor-β

TGF-βRII: transforming growth factor-β receptor type II

TNF-α: tumor necrosis factor-α

VEGF: vascular endothelial growth factor

WW: wet weight

WWB: wavy-walled bioreactor

SUMMARY

Articular cartilage which covers the surfaces of synovial joints is designed to allow smooth contact between long bones and to absorb shock induced during joint movement. Tissue engineering, a means of combining cells, biomaterials, bioreactors and bioactive agents to produce functional tissue replacements suitable for implantation, represents a potential long-term strategy for cartilage repair. The interplay between environmental factors, however, gives rise to complex culture conditions that influence the development of tissue-engineered constructs. A fibrous capsule that is composed of abundant type I collagen molecules and resembles fibrocartilage usually forms at the outer edge of neocartilage, yet the understanding of its modulation by environmental cues is still limited. Therefore, this dissertation was aimed to characterize the capsule formation, development and function through manipulation of biochemical parameters present in a hydrodynamic environment while a chemically reliable media preparation protocol for hydrodynamic cultivation of tissue-engineered cartilage was established. To this end, a novel wavy-wall bioreactor (WWB) that imparts turbulent flow-induced shear stress was employed as the model system and polyglycolic acid scaffolds seeded with bovine primary chondrocytes were cultivated under varied biochemical conditions.

The results demonstrated that tissue morphology, biochemical composition and mechanical strength of hydrodynamically engineered cartilage were maintained as the serum content decreased by 80% (from 10% to 2%). Transient exposure of the low-serum constructs to exogenous insulin-like growth factor-1 (IGF-1) or transforming growth factor-β1 (TGF-β1) further accelerated their development in comparison with continuous

treatment with the same bioactive molecules. The process of the capsule formation was found to be activated and modulated by the concentration of serum which contains soluble factors that are able to induce fibrotic processes and the capsule development was further promoted by fluid shear stress. Moreover, the capsule formation in hydrodynamic cultures was identified as a potential biphasic process in response to concentrations of fibrosis-promoting molecules such as TGF-β. Comparison between the capsule-containing and the capsule-free constructs, both of which had comparable tissue properties and were produced by utilizing the WWB system in combination with IGF-1 and TGF-β1, respectively, showed that the presence of the fibrous capsule at the construct periphery effectively improved the ability of engineered cartilage to integrate with native cartilage tissues, but evidently compromised its tissue homogeneity.

Characterization of the fibrous capsule and elucidation of the conditions under which it is formed provide important insights for the development of tissue engineering strategies to fabricate clinically relevant cartilage tissue replacements that possess optimized tissue homogeneity and properties while retaining a minimal capsule thickness required to enhance tissue integration.

CHAPTER 1

INTRODUCTION

Articular cartilage is a white, flexible connective tissue that is found at the ends of bones in synovial joints. It contains sparse cells called articular chondrocytes and a well-organized extracellular matrix (ECM) primarily composed of collagens (mainly type II collagen), proteoglycans and water which come together to form a smooth, resilient layer that protects the underlying subchondral bones from external loading. The ability of articular cartilage to resist tensile forces is attributed to the presence of collagen fibrils within the tissue, which construct a highly cross-linked solid framework. Proteoglycans that contain negatively charged glycosaminoglycan (GAG) branches are encapsulated in the established collagen network and interact with water molecules to provide the tissue with its compressive strength. The combination of both solid and fluid constituents allows articular cartilage to bear shearing loads.

Several causes such as aging, disease, mechanical injury and immobilization can trigger cartilage degeneration leading to pain, stiffness and swelling of joints. The lack of blood vessels in articular cartilage, however, largely limits the tissue's ability to repair itself. In addition, delay in diagnosis and treatment usually due to the aneural nature of cartilage may give rise to severe joint damage (Brown, Johnston et al. 2006). Depending on the severity of the defect, several therapeutic approaches aimed to repair or restore cartilage functions have been developed, such as microfracture, cell and tissue graft transplantation and total joint replacement (Brittberg, Lindahl et al. 1994; Hangody, Kish et al. 1998; Kish, Módis et al. 1999; Andres, Mears et al. 2001; Hangody, Feczkó et al.

2001; Sgaglione, Miniaci et al. 2002; Bos and Ellermann 2003; Hand, Lobo et al. 2003; Huntley, Bush et al. 2005; Jakobsen, Engebretsen et al. 2005; Saris, Vanlauwe et al. 2008; Ronn, Reischl et al. 2011). While there has been some success in short-term treatment of cartilage lesions, long-term cartilage restoration remains elusive (Nerem and Sambanis 1995; Temenoff and Mikos 2000), suggesting that these methods are unable to replicate intact native cartilage.

Tissue engineering techniques hold promise for development of functional tissue substitutes and thereby offer a potential long-term solution to cartilage degeneration. Typically, tissue-engineered constructs are assembled by encapsulating cells into biodegradable or biocompatible substrates and are grown *ex vivo* within a chemically and mechanically defined culture environment for a certain period of time. In order to fabricate tissue replacements suitable for implantation, engineered grafts must satisfy specific functional criteria related to their mechanical properties, biochemical composition, tissue ultrastructure, immunological compatibility and integration capability. Recent efforts to design and utilize novel biomaterials and bioreactor systems in combination with various cell sources and growth factors have made significant advances in cartilage tissue engineering (Temenoff and Mikos 2000; Darling and Athanasiou 2003; Chung and Burdick 2008; Nisbet, Forsythe et al. 2009; Mathieu and Loboa 2012), yet engineered constructs that resemble articular cartilage in all aspects have not been achieved. Thus, many challenges still need to be addressed. Examples include how to facilitate functional maturation of constructs by efficiently increasing synthetic activities of encapsulated cells and how to engineer constructs with ultrastructure, such as collagen organization and orientation, similar to that of native cartilage. It is also necessary to

broaden our limited understanding of the complex interplay between mechanical stimuli and bioactive molecules that are sensitive to such stimuli in neocartilage formation through the development of bioreactor systems that imparts different physical stimulations such as compressive (Steinmeyer and Knue 1997; Mauck, Soltz et al. 2000; Davisson, Kunig et al. 2002; Kisiday, Jin et al. 2004; Waldman, Spiteri et al. 2004) and shear (Jin, Emkey et al. 2003; Waldman, Spiteri et al. 2003) deformation, hydrostatic pressure (Hall, Horwitz et al. 1996; Smith, Rusk et al. 1996; Smith, Trindade et al. 2000; Elder and Athanasiou 2009) and hydrodynamic forces (Vunjak-Novakovic, Martin et al. 1999; Martin, Obradovic et al. 2000; Pazzano, Mercier et al. 2000; Emin, Koç et al. 2008). This knowledge will be beneficial in order to optimize the bioprocessing conditions for *in-vitro* cultivation of tissue-engineered constructs.

In natural and reparative healing processes, articular cartilage defects are usually reconstructed with fibrocartilage or scar tissues composed of a large content of type I collagen as opposed to type II found in normal cartilage (Shapiro, Koide et al. 1993; Andres, Mears et al. 2001; Knutsen, Engebretsen et al. 2004; Ronn, Reischl et al. 2011). Although the formation of fibrocartilage at the injury or integration site alleviates pain and swelling of joints, fibrocartilage is mechanically weaker than healthy articular cartilage (Knutsen, Engebretsen et al. 2004; Khan, Gilbert et al. 2008). Inhomogeneity of mechanical strength across the regenerated tissue can lead to at least three types of disruption within the tissue or at the integration site, i.e. opening, in-phase shear and out-of-phase shear fracture (Ahsan and Sah 1999), and recurring tissue degeneration may occur (Shapiro, Koide et al. 1993; Khan, Gilbert et al. 2008). To overcome this hurdle, implanted grafts must have tissue morphology and functional properties comparable to

those of the surrounding host cartilage. Additionally, newly synthesized ECM at the integration site has to be strong enough to maintain the integrity of the regenerated tissue.

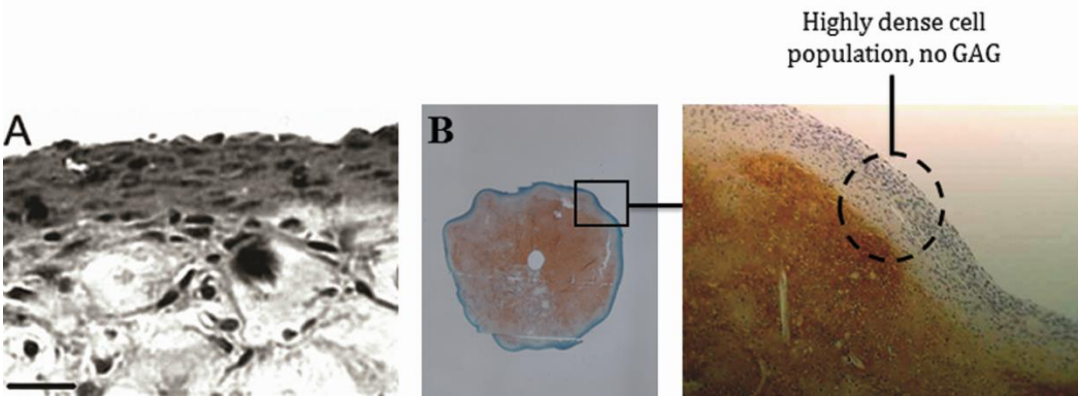

Figure 1.1 Characterization of a fibrous capsule in tissue-engineered cartilage. (A) Immunohistochemical staining of type I collagen (dark). (B) Histological staining of GAG (red) and cytoplasm (green). The capsule contains an increased chondrocyte population and a decreased GAG content. Adapted and modified from (Kisiday, Kurz et al. 2005) and (Bueno, Bilgen et al. 2008).

A unique structure which resembles the matrix composition of fibrocartilage is observed at the periphery of tissue-engineered cartilage (Vunjak-Novakovic, Freed et al. 1996; Kisiday, Kurz et al. 2005; Bueno, Bilgen et al. 2008; Kelly, Fisher et al. 2008). This fibrous cell outgrowth also referred to as the capsule consists mainly of type I collagen and is characterized by increased cell density and decreased (virtually none) GAG deposition (Figure 1.1). It is believed that the formation of a fibrous capsule is attributed to the direct contact of chondrocytes with medium supplements, such as platelet-derived growth factor (PDGF) and transforming growth factor-β (TGF-β), which induce and promote fibrotic processes (Ignotz and Massagué 1986; Lohmann, Schwartz et al. 2000; Kelly, Fisher et al. 2008). Interestingly, a structurally well-organized capsule

is commonly present at the periphery of constructs cultivated under continuous fluid shear conditions (Tsao and Gonda 1999; Vunjak-Novakovic, Martin et al. 1999; Bueno, Bilgen et al. 2005; Bueno, Bilgen et al. 2008). Vunjak-Novakovic and coworkers suggested that when chondrocytes are directly exposed to fluid flow, they tend to deform into a flattened, elongated fibroblast-like shape and thereby synthesize a matrix with increased type I collagen, but decreased GAG contents, which promotes the formation of a solid fibrous capsule (Vunjak-Novakovic, Freed et al. 1996). Nevertheless, the factors that drive and/or modulate the capsule formation and the roles of the capsule in cartilage tissue development and integration have not been fully understood.

Taken together, the objective of this project was to evaluate the combined effects of fluid shear stress and soluble biochemical factors on the capsule formation while a chemically reliable low-serum medium supplemented with shear-sensitive growth factors was developed for hydrodynamic cultivation of tissue-engineered cartilage. A custom-designed wavy-walled bioreactor (WWB) system (Chapter 2.3.2.5) was employed to provide a turbulent flow-induced shear environment for neocartilage development. Moreover, the influence of a fibrous capsule on tissue homogeneity of engineered cartilage and on construct integration with native cartilage tissues was also elucidated. Our central hypothesis was that tissue properties and morphology of engineered cartilage constructs can be modulated through manipulation of environmental factors, i.e. hydrodynamic forces and soluble biochemical cues in this dissertation work. The hypothesis was tested via the following specific aims.

Specific Aim 1: Develop a low-serum culture medium for hydrodynamic cultivation of tissue-engineered cartilage

Fetal bovine serum (FBS) provides a variety of nutrients that are essential for cell growth and has widely been utilized in cell and tissue culture. However, its varied composition composed of undefined constituents can significantly affect experimental results and the use of high serum contents may reduce the clinical relevance of the outcome. It has recently become a practice to replace FBS either partially or completely with serum substitutes such as Nutridoma (Glowacki, Yates et al. 2005) and insulin-transferrin-selenium (ITS) (Kisiday, Jin et al. 2004; Bian, Lima et al. 2008; Kelly, Fisher et al. 2008; Gigout, Buschmann et al. 2009) in order to establish a chemically reliable culture environment. Therefore, the objectives of this aim were to examine the feasibility of reduced FBS contents (0%, 0.2% and 2%, v/v) in combination with ITS (1%, v/v) to support the development of chondrocyte-seeded polyglycolic acid (PGA) scaffolds cultivated under static or hydrodynamic conditions and to investigate the synergistic roles of continuous fluid shear stress and serum in the capsule formation. The results were compared with the traditional high-serum (10% FBS, v/v) cultures.

FBS contains growth factors that are sensitive to mechanical forces. For example, the signaling pathways of TGF-β (Ohno, Cooke et al. 1995; Sakai, Mohtai et al. 1998; Negishi, Lu et al. 2001; Malaviya and Nerem 2002), insulin-like growth factor-1 (IGF-1) (Jin, Emkey et al. 2003; Kapur, Mohan et al. 2005; Lau, Kapur et al. 2006) and bone morphogenetic protein (BMP) (Lau, Kapur et al. 2006) are known to be responsive to shear stress, suggesting that these bioactive agents may play a more critical role in hydrodynamic cultures than in static cultures and can interact synergistically with shear

forces to further accelerate functional maturation of engineered tissues. Thus, we hypothesized that a minimal content of shear-sensitive soluble molecules present in serum is required in cultures supplemented with ITS in order to produce hydrodynamically engineered constructs morphologically, compositionally and mechanically similar to the high-serum constructs. In addition, because FBS also contains fibrosis-promoting molecules such as TGF-β (O'connor-Mccourt and Wakefield 1987) and PDGF (Childs, Proper et al. 1982), we hypothesized that the thickness of a fibrous capsule at the construct periphery increases with increasing serum concentration used in culture. Chapter 3 describes the details of this study.

Specific Aim 2: Determine the effects of transient exposure to exogenous IGF-1 and TGF-β1 on hydrodynamic cultivation of tissue-engineered cartilage

Expression and production of shear-sensitive growth factors by cells increase when the cells are exposed to fluid shear stress (Ohno, Cooke et al. 1995; Sakai, Mohtai et al. 1998; Negishi, Lu et al. 2001; Lau, Kapur et al. 2006), which potentially provides an endogenous source to support neocartialge development. Therefore, the objective of this aim was to evaluate the effects of transient supplementation of exogenous growth factors on tissue properties and morphology of engineered cartilage cultivated under hydrodynamic stimuli. To this end, the low-serum culture medium developed in Specific Aim 1 was further supplemented with TGF-β1, a fibrosis-promoting factor, or IGF-1, a non-fibrosis-promoting factor, both of which have been extensively used in cartilage tissue engineering. For each growth factor, a minimal concentration was selected from their most commonly reported ranges of effective doses for neocartilage cultivation (IGF-

1: 100-300 ng/mL; TGF-β1: 10-30 ng/mL (Blunk, Sieminski et al. 2002; Pei, Seidel et al. 2002; Mauck, Nicoll et al. 2003)) and was applied either for the first two weeks of the culture (transient supplementation) or throughout the entire 4-week cultivation (continuous supplementation). The hypotheses were that (1) hydrodynamically engineered constructs continuously nourished with exogenous growth factors do not necessarily exhibit improved tissue properties over constructs transiently treated with the same bioactive molecules and (2) engineered constructs nourished with a fibrosis-promoting molecule, i.e. TGF-β1 in this study, will form a thicker fibrous capsule compared with the untreated ones. The framework and the outcome of this study are detailed in Chapter 4.

Specific Aim 3: Determine the role of the fibrous capsule in the development of tissue-engineered cartilage cultivated under hydrodynamic stimuli

In Specific Aim 2, treatment with different exogenous growth factors yielded hydrodynamically engineered cartilage with divergent tissue morphologies. Specifically, constructs nourished with IGF-1 retained a solid fibrous capsule whereas exposure to TGF-β1 eliminated the capsule formation regardless of the duration of the supplementation. Based on the distinguishable tissue morphologies, we hypothesized that the capsule-containing (IGF-1) constructs exhibit compromised tissue homogeneity and have a less strong inner core compared with the capsule-free (TGF-β1) constructs. To test this hypothesis, a central core was punched out of each of the 4-week constructs and tissue homogeneity was determined by evaluating radial variations in tissue properties (inner core versus outer annulus). Furthermore, the ability of the intact hydrodynamic

neocartilage with or without a fibrous capsule to integrate with native cartilage tissues was also assessed using an *in-vitro* cartilage explant model. The detailed experimental design and the results are reported in Chapter 5.

Table 1.1 Dissertation Overview

Chapter	Title	Content
2[†]	Literature Review	a comprehensive overview of articular cartilage biology, cartilage degeneration and relevant therapeutic approaches, and cartilage tissue engineering
3[‡]	Requirement for Serum in Medium Supplemented with Insulin-Transferrin-Selenium for Hydrodynamic Cultivation of Tissue-Engineered Cartilage	studies related to Specific Aim 1
4[††]	Improved Biochemical and Mechanical Properties and Differential Tissue Morphology of Engineered Cartilage in Hydrodynamic Cultivation with Transient Exposure to Insulin-Like Growth Factor-1 and Transforming Growth Factor-β1	studies related to Specific Aim 2
5[††]	Diverse Effects of A Fibrous Capsule on Tissue Homogeneity and Integration Capability of Hydrodynamically Engineered Cartilage	studies related to Specific Aim 3
6	Conclusions and Future Work	the key findings and conclusions drawn from this thesis, and the implications for future research directions

[†]Adapted and modified from Yang, Y.-H. and Barabino, G.A. (*in press*) Environmental Factors in Cartilage Tissue Engineering. *Tissue and Organ Regeneration: Advances in Micro and Nanotechnology*. Editors: Zhang, L.G., Khademhosseini, A. and Webster T.

[‡]Adapted and modified from Yang, Y.-H. and Barabino, G.A. (*2011*) Requirement for Serum in Medium Supplemented with Insulin-Transferrin-Selenium for Hydrodynamic Cultivation of Engineered Cartilage. *Tissue Engineering Part A*. 17(15-16): 2025-2035.

[††]Adapted and modified from Yang, Y.-H. and Barabino, G.A. (*in press*) Differential Morphology and Homogeneity of Tissue-Engineered Cartilage in Hydrodynamic Cultivation with Transient Exposure to Insulin-Like Growth Factor-1 and Transforming Growth Factor-β1. *Tissue Engineering Part A*.

CHAPTER 2

LITERATURE REVIEW[†]

2.1 Articular Cartilage

2.1.1 Composition and Mechanical Properties

Articular cartilage is a lubricant substrate that serves as a cushion between the bones of diarthrodial joints. The main function of articular cartilage is to provide a smooth medium for force transfer between long bones; therefore, its tough, but resilient structure is designed to endure constant cyclic loading and to further protect the underlying bones. Structurally, articular cartilage has no nerves and blood vessels and consists of 65–80 wt. % of water, 10–20 wt. % of collagen fibrils and 5–10 wt. % of proteoglycans (Kuettner 1992; Cohen, Foster et al. 1998). Very few cells, called articular chondrocytes, reside in the cartilage tissue and secrete a matrix primary of collagen and proteoglycan (Figure 2.1). Type II collagen, a triple helix made up of three identical polypeptide chains, contributes about 95% of the total collagen content within articular cartilage (Cole and Malek 2004). These collagen fibrils form a highly cross-linked network to establish a well-organized extracellular architecture and thereby grant cartilage tensile strength (20 MPa). Aggrecan containing branched negatively charged GAG molecules is the predominant proteoglycan in articular cartilage and is encapsulated in the collagen mesh. As a result, the trapped negatively charged components create a

[†]Adapted and modified from Yang, Y.-H. and Barabino, G.A. (*in press*) Environmental Factors in Cartilage Tissue Engineering. *Tissue and Organ Regeneration: Advances in Micro and Nanotechnology*. Editors: Zhang, L.G., Khademhosseini, A. and Webster T.

repelling force and recruit massive water molecules, together which generate a high swelling pressure against external compressive loading (0.5–1 MPa). The shear capability (10 MPa) of articular cartilage is attributed to a combination of both solid and fluid constituents. Taken together, the mechanical behavior of articular cartilage is modulated by three major factors: (1) elasticity of the solid matrix, (2) swelling property of the ionic elements and (3) solid-fluid interactions.

2.1.2 Zonal Organization

Articular cartilage is an anisotropic material made up of four distinct zones along the depth of the tissue. From the articular surface to the subchondral bone, these zones are the superficial (tangential) zone, the middle zone, the deep zone, and the calcified zone (Figure 2.1). The middle zone (40-60% of the cartilage thickness) is the thickest layer in articular cartilage, followed by the deep zone (30% of the cartilage thickness) and then the superficial zone (10-20% of the cartilage thickness). The calcified layer is extremely thin and lies between the deep zone and the subchondral bone to separate articular cartilage from bone, and only very few and small chondrocytes reside in this area. Matrix compositions and organizations are quite different in each zone (Jeffery, Blunn et al. 1991; Hwang, Li et al. 1992; Cohen, Foster et al. 1998; Temenoff and Mikos 2000). Specifically, the superficial zone contains the lowest content of proteoglycans and the highest amount of water while thin collagen fibrils are aligned in the same direction as the articular surface. Abundant flattened chondrocytes are found in this region with their long axes parallel to the joint surface. More rounded chondrocytes occupy the

middle zone composed of more proteoglycans, less water and fewer, but thicker collagen fibrils

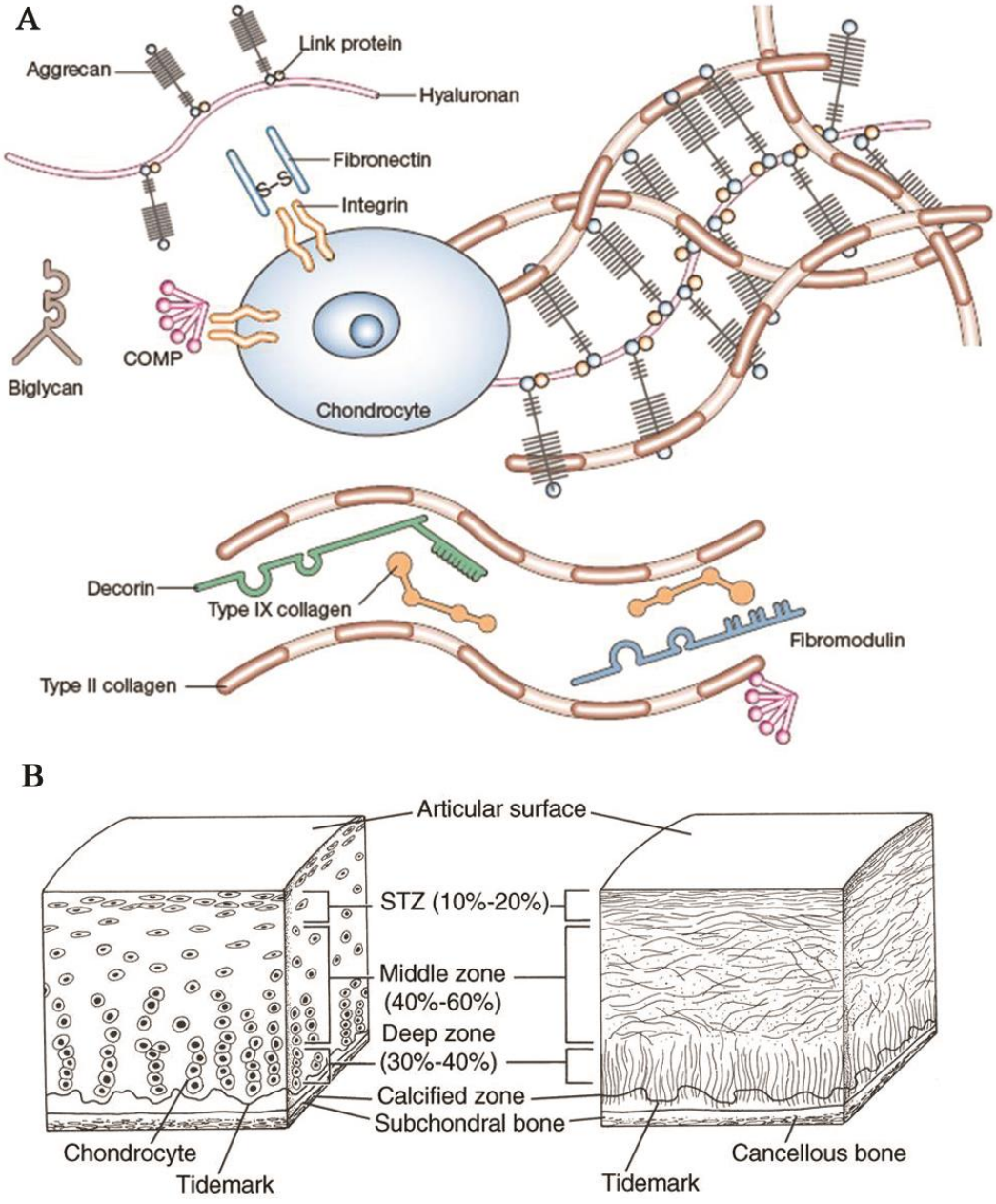

Figure 2.1 Ultrastructure (A) and microstructure (B) of articular cartilage. Adapted and modified from (Chen, Rousche et al. 2006) and (Buckwalter, Mow et al. 1994).

whose orientation is nearly random. The deep zone is comprised of the highest content of proteoglycans, the least water and the largest collagen fibrils that are vertically arranged. Within the deep zone, chondrocytes are rounded and stacked along the thickness of the tissue. Amongst all the layers, chondrocytes within the middle and the deep zones possess higher ECM synthetic activities than those in the superficial zone (Hidaka, Cheng et al. 2006) while the deep zone exhibits the strongest mechanical strength (Klein, Chaudhry et al. 2007).

2.1.3 Cartilage Mechanics

At rest, the synovial fluid transmits hydrostatic pressure to the interstitial water within the cartilage matrix. During normal ambulation, articular cartilage undergoes direct compression thousands of times each day without causing damage. Under a loading period, deformation of cartilage results in changes in environmental conditions experienced by chondrocytes, such as matrix organization, tissue permeability and water content within the tissue (Grodzinsky, Levenston et al. 2000). When cartilage is compressed, water molecules tend to escape from the tissue, yet they cannot instantly leave the tissue due to the reduced permeability such that the interstitial fluid absorbs the majority of mechanical energy and becomes pressurized. As the fluid eventually exits the matrix into the synovial cavity, the gaps in the collagen network shrink and GAG molecules are thereby in closer proximity, producing stronger resistance against compression. The movement of the interstitial fluid precipitates several events. For instance, transient fluid flow generates shear stress that not only directly acts on cells but activates some latent bioactive agents such as transforming growth factor-β (TGF-β)

(Ahamed, Burg et al. 2008). The release of the fluid also enhances the efficiency of the removal of waste produced by chondrocytes and fresh nutrients can be brought back to the tissue as cartilage is relaxed. As a result, this complex mechanism supports the development of articular cartilage and maintains its functionality. Conversely, immobilization of diarthrodial joints can accelerate the deterioration of articular cartilage (Jurvelin, Kiviranta et al. 1986).

2.2 Cartilage Degeneration and Repair

2.2.1 Arthritis, Rheumatoid Arthritis, Osteoarthritis and Post-Traumatic Osteoarthritis

Degeneration of articular cartilage can be induced under several various conditions such as aging, disease and sports or mechanical injury, which leads to pain, stiffness and swelling of joints. Arthritis, a form of musculoskeletal disorders which involves joint inflammation and cartilage breakdown, is the most frequent cause of disability in the United States. It affects 50 million Americans including not only middle-aged and older people but also children, resulting in costs of $128 billion annually (Cheng, Hootman et al. 2010). Rheumatoid arthritis (RA) and osteoarthritis (OA) are the most common forms of arthritis. RA is a systemic autoimmune disease that occurs mostly in women and is generally characterized by the inflammation of the membrane lining the joint. Although RA is primarily diagnosed in synovial joints, it can also induce inflammation throughout the body and affect many other tissues and organs such as heart (Persson 2012). OA is a chronic degenerative disease where the cartilaginous layers covering the ends of the bones gradually wear away, which increases the friction coefficient of the articular surface and yields the exposure of the subchondral bone.

Moreover, in the event that an injury compromises the articular surface, a degenerative condition coined post-traumatic osteoarthritis (PTOA) may soon follow, which if allowed to progress persistently could lead to chronic, debilitating pain and swelling. PTOA results in an estimated cost of $13.5 billion per year in work loss and direct medical costs in the United States alone (Brown, Johnston et al. 2006). Because self-repair of articular cartilage is limited and the damaged tissue is usually reconstructed with fibrocartilage which exhibits weaker mechanical strength than articular cartilage (Knutsen, Engebretsen et al. 2004; Khan, Gilbert et al. 2008), the injury site becomes a nucleating center for the progressive degeneration of the articular surface by altering the native loading state of the joint. The subsequent abnormal wear on the articular surface as a result of this altered loading state, becomes accelerated and ultimately leads to end-stage OA. PTOA can occur as soon as three months after a severe injury and despite advances in surgical treatment and rehabilitation of injured joints, the risk of PTOA has not decreased in the last 50 years (Brown, Johnston et al. 2006). Thus, new therapeutic approaches aimed to regenerate or repair articular cartilage with respect to biological and mechanical functions are sought, which may prevent the onset of PTOA and mitigate future physical and medical costs associated with end-stage OA.

2.2.2 Surgical Therapies

Current strategies for cartilage repair and restoration include abrasion arthroplasty, subchondral drilling, microfracture, cell and tissue graft transplantation and total joint replacement. For large defects, total joint replacement surgeries are required to replace the joint with metal or polymeric materials, yet a revision may need to be performed due

to infection, instability or malpositioning of the implanted joint and worn-out implants (Andres, Mears et al. 2001; Sgaglione, Miniaci et al. 2002; Jakobsen, Engebretsen et al. 2005; Ronn, Reischl et al. 2011). For relatively small lesions, abrasion arthroplasty, subchondral drilling and microfracture are marrow-stimulation methods which promote migration of chondrocyte progenitor cells or mesenchymal stem cells (MSCs) and delivery of growth factors to the defect by creating the access to the subchondral bone (Andres, Mears et al. 2001; Sgaglione, Miniaci et al. 2002; Jakobsen, Engebretsen et al. 2005; Ronn, Reischl et al. 2011). In these approaches, the defect is generally filled with fibrocartilage which relieves pain, but is mechanically compromised. Another option is transplantation of chondrocytes (Brittberg, Lindahl et al. 1994; Saris, Vanlauwe et al. 2008) or cartilage grafts (Hangody, Feczkó et al. 2001; Bos and Ellermann 2003; Hand, Lobo et al. 2003; Huntley, Bush et al. 2005) harvested from non-load bearing regions to the injury site. However, several disadvantages associated with this method have been reported, such as donor site morbidity, limited access to patients' healthy autologous chondrocytes and possible rejection responses to the allogeneic implants. To overcome these obstacles and provide alternative therapeutic strategies, tissue engineering has emerged as a promising approach.

2.2.3 Cartilage Tissue Engineering

The production of tissue-engineered cartilage typically involves cultivation of primary chondrocytes on three-dimensional biodegradable polymer scaffolds or naturally derived hydrogels within controlled environments of bioreactor culture systems (Darling and Athanasiou 2003; Bilodeau and Mantovani 2006) (Figure. 2.2). In order to be

clinically relevant, cartilage substitutes must meet specific functional criteria related to their mechanical properties, biochemical composition, tissue ultrastructure, immunological compatibility and integration capability. However, all of these properties of engineered cartilage are still inferior to those of native tissues. One of the explanations for this gap is that cultured chondrocytes undergo a process of rapid *in-vitro* hypertrophic maturation such that tissue development is impeded (Böhme, Winterhalter et al. 1995). *In vitro*, harvested chondrocytes may only have a limited lifespan and potential to develop

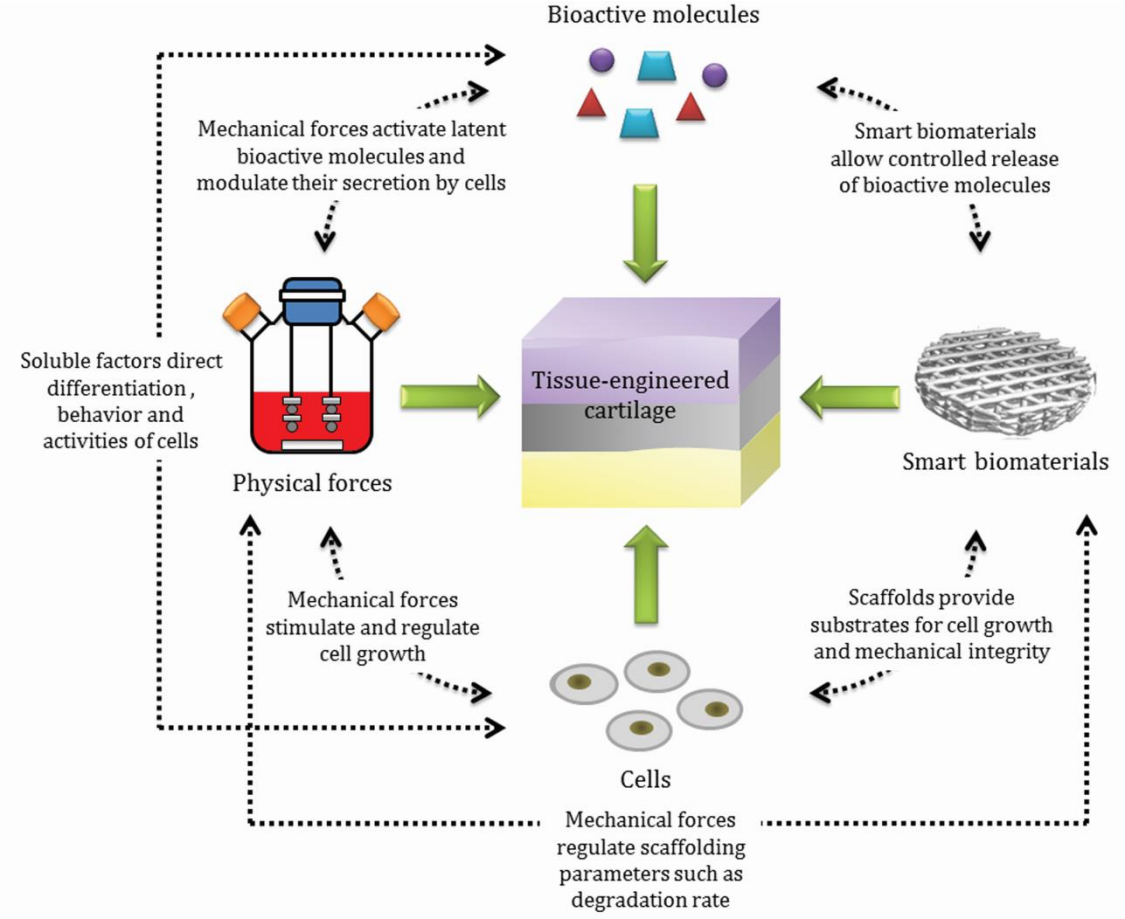

Figure 2.2 Main elements in cartilage tissue engineering: cell sources, biomaterials, bioactive molecules and bioreactor systems.

into mature articular cartilage tissues when they are exposed to culture conditions. Researchers seek to develop novel biomaterials and bioreactor systems in order to improve current tissue engineering strategies that can maximize the efficacy of chondrocytes within their restricted lifetime.

2.3 Environmental Stimuli

Microenvironments define the immediate surroundings of a cell, which encompass essential elements that mediate cellular activities and further tissue formation. These elements include, but are not limited to, soluble molecules, ECM components bound to the cell and adjacent cells. Therefore, the development of functional tissue replacements requires a thorough understanding of the roles environmental factors play in natural and culture environments. Among these factors, biochemical agents are thought to be involved in cell-to-cell communication and signaling, in which extracellular biomolecules, such as growth factors, cytokines and chemokines, transmit chemical signals directly to individual cells and activate a series of chain reactions inside the cells that give rise to particular transcription factors in response to external stimulation and changes in environmental conditions. It is also believed that mechanical stimuli present in the physiological or culture environments can significantly influence cell shape, orientation, apoptosis, gene expression, secretion of signaling molecules as well as synthesis and degradation of ECM components by cells though the mechanisms that transduce mechanical cues into chemical signals that trigger cellular responses are still not fully understood (Grodzinsky, Levenston et al. 2000). It has been reported that there may be several regulatory pathways by which cells can respond to mechanical forces,

including crosstalk between chemo- and mechano-sensitive signaling mediators (Davies 1995; Das, Schurman et al. 1997) and possible mechanisms that alter cellular activities in transcription (Holmvall, Camper et al. 1995; Valhmu, Stazzone et al. 1998; Smith, Trindade et al. 2000), translation and post-translational modifications (Kim, Grodzinsky et al. 1996; Smith, Rusk et al. 1996). The role of biophysical, biochemical and mechanical environmental factors in cartilage tissue engineering will be briefed in this section.

2.3.1 Biomaterials

2.3.1.1 Biophysical Signals

Biomaterials provide a powerful tool to deliver biophysical signals to cultured cells through manipulation of material properties of synthesized substrates, such as elasticity and stiffness, which emulate physiological conditions. For instance, a study reported by McBeath et al. demonstrated that MSC differentiation could be predicted by control of cell shape using a micropatterning technique (Mcbeath, Pirone et al. 2004). Specifically, when human MSCs were cultivated on the surfaces of polydimethylsiloxane substrates coated with large areas of fibronectin that enhanced cell spreading, they experienced strong cytoskeletal tension and tended to differentiate into osteoblasts. Conversely, adipogenic commitment occurred when cells were on small islands of fibronectin and remained round. In addition, Engler and coworkers cultured human MSCs on the surfaces of collagen-modified polyacrylamide hydrogels with the tissue-level elasticity ranged from 0.1 to 40 kPa (Engler, Sen et al. 2006). Cells exhibited the neurogenic, myogenic and osteogenic potential when grown on the soft, intermediate, and

stiff substrates, respectively, in the absence of exogenous inductive molecules. Committed cells could be reprogramed by the addition of soluble inducers during the first week of the cultivation whereas phenotype commitment was irreversible in longer cultures. When nonmuscle myosin II was inhibited, MSCs lost the ability to respond matrix stiffness and were not able to differentiate. These studies substantiate that MSCs can secrete various soluble molecules in response to the microenvironment that alters cellular mechanics and further commit to specialized cell lineages through autocrine signaling.

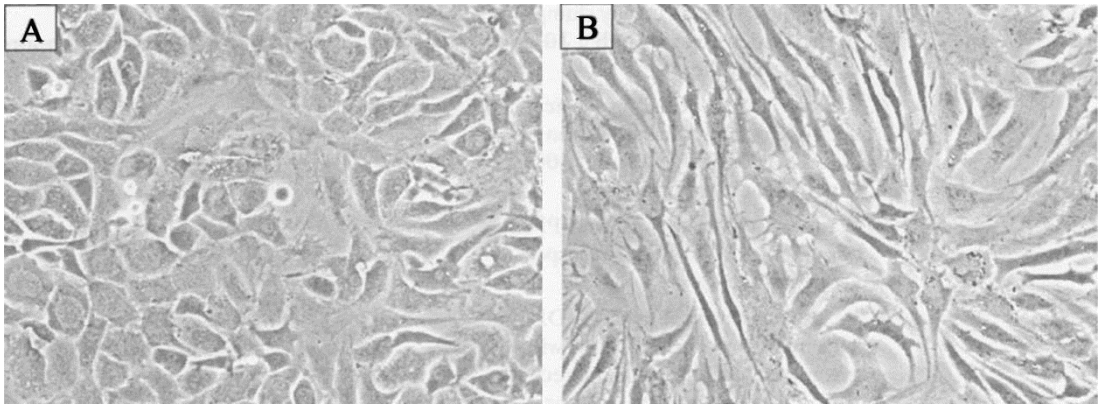

Figure 2.3 Morphology of articular chondrocytes grown on a plastic surface. (A) Primary chondrocytes possess the typical cobblestone shape. (B) Passaged chondrocytes exhibit a fibroblast-like morphology. Reproduced from (Otero, Favero et al. 2012).

2.3.1.2 Hydrogels and Synthetic Meshes

Articular chondrocytes are a rounded, three-dimensional cell type. When expanded in monolayer, they tend to undergo rapid dedifferentiation and can experience phenotypic changes as early as the first passage (Darling and Athanasiou 2005). The dedifferentiated chondrocytes demonstrate a fibroblast-like phenotype and morphology

(Figure 2.3). Therefore, the best approach to culture chondrocytes is to grow them in a three-dimensional environment. Biodegradable and biocompatible materials have been incorporated into tissue engineering strategies to provide three-dimensional substrates and appropriate microenvironments for cell growth and tissue development. These substrates need to mimic the natural environment of cells and are fabricated to meet the requirements for cell survival, matrix biosynthesis, mechanical integrity and integration capacity with host tissues. Among these smart biomaterials are hydrogels and synthetic meshes. Hydrogels are formed by gelation of polymers dissolved in a liquid medium, usually water. Depending on the mechanism of crosslinking, the network structure of hydrogels can be physically or chemically bonded. Hydrogels that are utilized in cartilage repair are commonly composed of agarose (Mauck, Soltz et al. 2000; Hunter and Levenston 2004; Mauck, Yuan et al. 2006; Byers, Mauck et al. 2008; Erickson, Huang et al. 2009; Sheehy, Buckley et al. 2011), alginate (Perka, Schultz et al. 2000; Caterson, Nesti et al. 2001; Kavalkovich, Boynton et al. 2002; Mo, Guo et al. 2009), fibrin (Nixon, Fortier et al. 1999; Perka, Schultz et al. 2000; Hunter and Levenston 2004; Pelaez, Charles Huang et al. 2008), collagen (Yokoyama, Sekiya et al. 2005; Hannouche, Terai et al. 2007; Koga, Muneta et al. 2008; Roy, Boskey et al. 2008), hyaluronic acid (Kavalkovich, Boynton et al. 2002; Liu, Shu et al. 2006; Chung and Burdick 2008; Erickson, Huang et al. 2009) or self-assembling peptides such as KLD-12 (Kisiday, Jin et al. 2002; Kisiday, Kopesky et al. 2008) and Puramatrix (Erickson, Huang et al. 2009). Although hydrogels yield more homogeneous distribution of encapsulated cells and have high flexibility in size and shape, they are usually less porous and exhibit inferior mechanical properties in comparison with meshed scaffolds (Chung and Burdick 2008).

Meshed synthetic scaffolds such as PGA (Freed, Marquis et al. 1993; Obradovic, Martin et al. 2001), poly-L-lactic acid (PLA) (Lohmann, Schwartz et al. 2000; Moyer, Wang et al. 2010) and polycaprolactone (PCL) (Li, Danielson et al. 2003; Shao, Goh et al. 2006) may be preferred in the fabrication of tissue replacements because of their tunable biomechanical properties that can be modified using techniques like soft lithography (Vozzi, Flaim et al. 2003), UV polymerization (Fischer, Dickhut et al. 2010) and electrospinning (Chiu, Luu et al. 2005; Liang, Hsiao et al. 2007). A meshed poly(ethylene oxide) terephthalate/poly(butylene) terephthalate scaffold has been recently fabricated to possess mechanical strength comparable to the level of native cartilage (Moroni, De Wijn et al. 2006). Electrospinning is a novel approach to the manufacture of nanofibrous scaffolds. This type of scaffold provides three-dimensional architecture that mimics the network of fibrillar ECM components in nanoscale and has high porosities and surface-area-to-volume ratios that are suitable for cell adhesion and proliferation (Chiu, Luu et al. 2005; Liang, Hsiao et al. 2007). More importantly, electrospun scaffolds can be engineered to consist of highly aligned nanofibers that will be useful for regeneration of specific tissue types such as tendon and the superficial and the deep zones of articular cartilage (Li, Danielson et al. 2003; Janjanin, Li et al. 2008).

2.3.1.3 Drug/Molecule Delivery Vehicles

Delivery of soluble factors such as growth factors, cytokines and small molecules to cultured cells is mostly through the direct addition of bulk molecules to culture media (Sah, Trippel et al. 1996; Yaeger, Masi et al. 1997; Martin, Vunjak-Novakovic et al. 1999; Blunk, Sieminski et al. 2002; Pei, Seidel et al. 2002; Jin, Emkey et al. 2003; Mauck,

Nicoll et al. 2003; Davies, Blain et al. 2008; Emin, Koç et al. 2008; Duraine, Neu et al. 2009). This method requires excess additives to increase the probability of cells capturing these molecules and continuous supplementation is usually applied, which makes this strategy less economic. Alternatively, growth factors can be embedded in microparticles or scaffolding materials such as hydrogels for local distribution (Holland, Tabata et al. 2005; Park, Temenoff et al. 2005; Defail, Chu et al. 2006; Holland, Bodde et al. 2007; Park, Temenoff et al. 2007; Bouffi, Thomas et al. 2010; Lim, Oh et al. 2010; Spiller, Liu et al. 2012). When loaded microparticles are further encapsulated into scaffolds, it largely reduces the burst release of incorporated molecules (Defail, Chu et al. 2006; Chung and Burdick 2008). In this fashion, the release of growth factors is based on loading density, diffusivity and properties of biomaterials, such as the size of microparticles and degradation rate of hydrogels (Chung and Burdick 2008). Several studies have demonstrated that constructs loaded with TGF-β and/or IGF-1 microcarriers exhibit a higher level of chondrogenesis than the non-loaded ones (Park, Temenoff et al. 2005; Holland, Bodde et al. 2007; Park, Temenoff et al. 2007; Bouffi, Thomas et al. 2010; Spiller, Liu et al. 2012). A novel approach utilizing layer-by-layer (LbL) polyelectrolyte techniques to incorporate proteins into meshed biodegradable scaffolds has been developed. In this system, single or multiple growth factors are coated onto the surfaces of scaffolds based on electrostatic properties of biomolecules in a water-based, room temperature environment (Wood, Chuang et al. 2006; Macdonald, Rodriguez et al. 2008; Macdonald, Rodriguez et al. 2010; Shukla, Fleming et al. 2010; Macdonald, Samuel et al. 2011; Shah, Macdonald et al. 2011) to avoid the use of solvents, heat or other severe conditions that are necessary in the traditional polymer encapsulation process and may

denature the encapsulated proteins (Fu, Pack et al. 2000). The controlled release of growth factors from LbL vehicles can be modulated by simply adjusting the architecture of the nanolayered film and the number of incorporated growth factor layers (Wood, Chuang et al. 2006; Macdonald, Rodriguez et al. 2008; Macdonald, Rodriguez et al. 2010). BMP-2/vascular endothelial growth factor (VEGF)-loaded LbL PCL scaffolds have been shown to successfully recruit host progenitor cells at the implant site to foster *in-situ* development of regenerating bone (Macdonald, Samuel et al. 2011; Shah, Macdonald et al. 2011). To our best knowledge, however, this technique has not been extensively utilized in cartilage repair.

2.3.2 Bioreactor Systems

In order to compensate for low quality of tissue-engineered constructs derived from static cultures, bioreactor systems have been designed to impart mechanical loading to facilitate the development of different types of tissues, such as cardiovascular and musculoskeletal tissues (Darling and Athanasiou 2003; Bilodeau and Mantovani 2006). Bioreactors do their part by providing a well-defined culture environment to control biochemical and mechanical parameters. This section will discuss the common bioreactor systems that have been utilized in cartilage tissue engineering applications.

2.3.2.1 Deformational Loading

Ex-vivo compression, in both confined and unconfined fashions (Figure 2.4A), at certain amplitudes and frequencies has been considered to be capable of replicating joint activities and thereby stimulating chondrocyte and cartilage growth (Gray, Pizzanelli et al.

1989; Sah, Kim et al. 1989; Sah, Doong et al. 1991; Kim, Grodzinsky et al. 1996; Steinmeyer and Knue 1997). However, such loading has been shown to possibly reduce the efficiency at which the synthesized ECM components are encapsulated in the tissue network as a result of frequent flow movement that increases the release of those molecules into the surroundings (Gray, Pizzanelli et al. 1989; Sah, Doong et al. 1991). Given that stimulatory effects of compressive loading on protein synthesis can last for hours (Gray, Pizzanelli et al. 1989; Sah, Kim et al. 1989), tissue constructs are usually exposed to intermittent compression in long-term experiments in order to maximize the retention of ECM components within engineered tissues (Mauck, Soltz et al. 2000; Davisson, Kunig et al. 2002; Kisiday, Jin et al. 2004; Waldman, Spiteri et al. 2004). Studies have demonstrated that dynamic compression can enhance gene expression of aggrecan by cultured chondrocytes (Valhmu, Stazzone et al. 1998) and influence chondrocyte-specific biosynthetic pathways (Kim, Grodzinsky et al. 1996), resulting in improved biochemical and mechanical properties of cell-laden agarose (Mauck, Soltz et al. 2000) and self-assembling peptide (Kisiday, Jin et al. 2004) hydrogels. These dynamically loaded samples can achieve at least 20 to 50% greater ECM deposition and mechanical strength than static tissue constructs (Mauck, Soltz et al. 2000; Kisiday, Jin et al. 2004; Waldman, Spiteri et al. 2004).

Dynamic compression yields a culture condition as complex as the natural environment within the synovial capsule. Under dynamic compressive loading, cells or tissues experience not only volumetric deformation, but also gradients in osmotic stress, hydrostatic pressure, hydrodynamic forces, electric field stimulation and more (Grodzinsky, Levenston et al. 2000). This complexity increases the difficulty in isolating

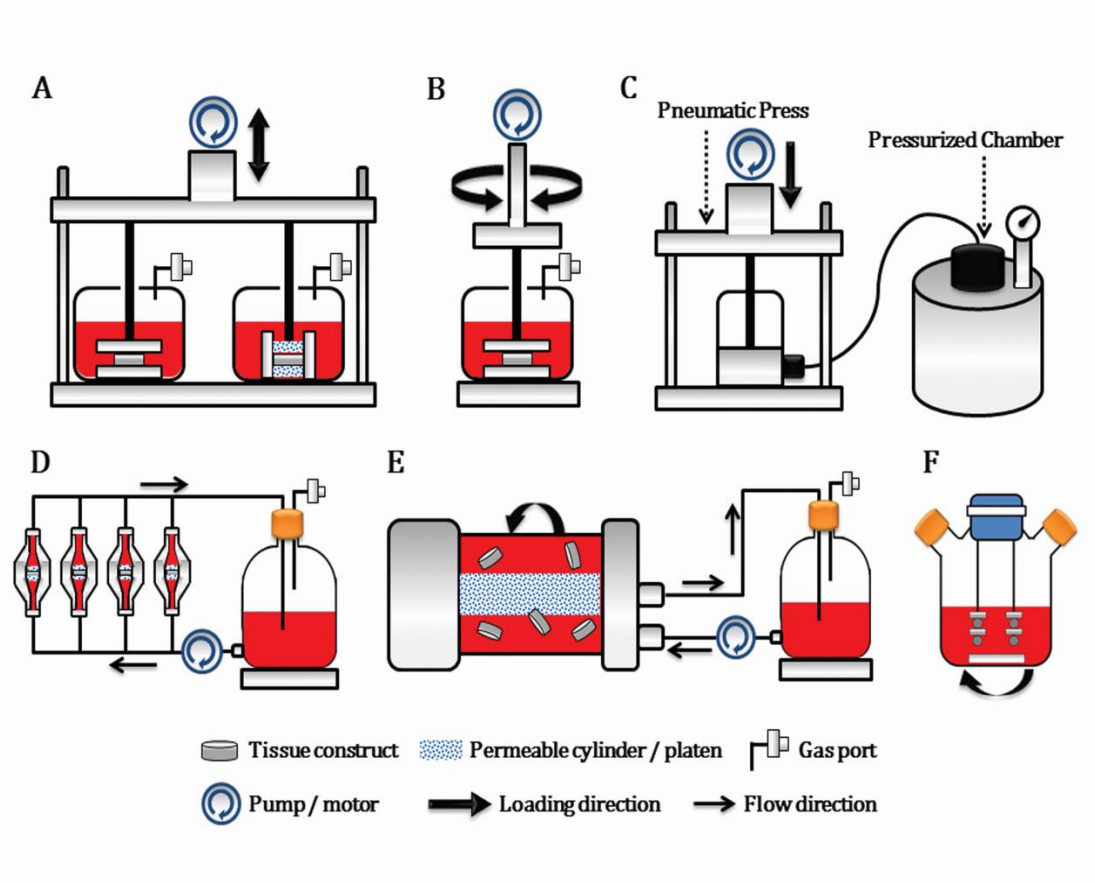

Figure 2.4 Bioreactor systems in cartilage tissue engineering. (A) Confined and unconfined compressive loading. (B) Shear deformation. (C) Hydrostatic pressure. (D) Direct perfusion. (E) Rotating vessel. (F) Spinner flask.

the effects of a single environmental factor on the development of tissue-engineered cartilage. Therefore, the design of bioreactors has shifted to systems that only emulate one of many conditions that take place in the knee or other joints. For example, using parallel impermeable platens (Figure 2.4B), sinusoidal shear deformation has been successfully applied to cartilage explants in a range of 0.5–6% strain amplitude at 0.1 Hz without introducing significant interstitial fluid flow (Jin, Emkey et al. 2003). The shear-loaded cartilage tissues exhibited 35% and 25% greater protein and proteoglycan synthesis, respectively, than the non-loaded tissues in a 24-hour loading period. This enhancement of tissue properties, however, was independent of amplitude and frequency

of applied shear deformation. Similar shear instruments have also been utilized in the long-term cultivation of chondrocyte-seeded substrates. The intermittent dynamic shear deformation resulted in engineered cartilage with a 6-fold higher stiffness than the static controls (Waldman, Spiteri et al. 2003).

2.3.2.2 Hydrostatic Pressure

Bioreactor systems that reproduce physiological levels of hydrostatic pressure in diarthrodial joints have been fabricated in the laboratory by compressing a gas or liquid phase that transmits load through culture media to cells (Figure 2.4C) (Elder and Athanasiou 2009). Hydrostatic pressure in the physiological range of 7 to 10 MPa is preferred in this type of application because loading at such levels stimulates tissue constructs without causing evident deformation of samples and thus maintains the integrity of matrix architecture (Hall, Horwitz et al. 1996; Darling and Athanasiou 2003). A study in which the effects of the loading profile of hydrostatic pressure at 10 MPa on articular chondrocytes was evaluated in a 4-hour loading period demonstrated that, relative to the non-loaded cells, intermittent pressure applied at 1 Hz was found to increase aggrecan and type II collagen mRNA signals by 31% and 36%, respectively, whereas constant pressure did not influence mRNA expression (Smith, Rusk et al. 1996). A follow-up experiment was conducted to investigate the time-dependent effects of intermittent hydrostatic pressure loaded at 10 MPa and 1 Hz for up to 24 hours. A biphasic behavior was detected in mRNA expression of type II collagen by loaded chondrocytes with a peak value at the 4-hour period while aggrecan signals continuously increased with the loading period (Smith, Trindade et al. 2000). Intermittent hydrostatic

pressure was also applied to grow tissue-engineered cartilage and was shown to positively regulate functional maturation of neocartilage (Elder and Athanasiou 2009).

2.3.2.3 Laminar Flow

In addition to direct deformation and hydrostatic pressure, fluid flow also plays a key role in the development of both native and engineered cartilage. *In vivo,* joint movement during normal walking or exercise not only alters pericellular concentrations of cytokines, growth factors, enzymes and more other molecules, driving protein or ion flux in and out of the cartilage tissue, but also forces the exchange of substances between the interstitial fluid within cartilage and the surrounding synovial fluid. Because of the avascular nature of articular cartilage, nutrient delivery to and waste removal from chondrocytes largely rely on this flow-enabled exchange. The individual contributions of diffusion and convection to the transport of neutral and charged proteins within articular cartilage have been examined (Garcia, Frank et al. 1996; Garcia, Lark et al. 1998). These studies suggest that when cartilage is stimulated by fluid flowing at a velocity of 1 μm/s (flow velocity within articular cartilage at normal walking frequencies (Hou, Mow et al. 1992)), the efficiency of mass transfer of solutes is tremendously enhanced. Fluid flow bioreactor systems can be divided into two major categories based on flow profile, i.e. laminar or turbulent flow (Dunkelman, Zimber et al. 1995; Vunjak-Novakovic, Obradovic et al. 1998; Vunjak-Novakovic, Martin et al. 1999; Martin, Obradovic et al. 2000; Pazzano, Mercier et al. 2000; Emin, Koç et al. 2008).

Among the systems that generate laminar flow, direct perfusion systems (Figure 2.4D) push culture media through cell-seeded scaffolds such that cells within constructs

can directly sense hydrodynamic shear stress as fluid flows through the pores. In order to achieve uniform medium flow, constructs have to tightly fit in the perfusion chamber and no gaps between samples and the chamber wall are allowed. Cells under perfusion stimulation become aligned in the direction of the flow, which makes it possible to engineer a tissue with specific cell orientations (Dunkelman, Zimber et al. 1995; Pazzano, Mercier et al. 2000). Although it has been demonstrated that the perfusion flows at both low (1 μm/s) (Pazzano, Mercier et al. 2000) and high (11 μm/s) (Dunkelman, Zimber et al. 1995) velocities significantly increase ECM contents of tissue-engineered cartilage, denser matrix deposition tends to occur near the surface facing the oncoming flow. As a result, the nonhomogeneous matrix distribution along the thickness of the construct affects overall mechanical properties of engineered cartilage. This "one-side effect", however, can be overcome by reversing medium flow periodically during the cultivation (Darling and Athanasiou 2003).

Another representative system that employs laminar flow is the rotating vessel bioreactor (Figure 2.4E) which utilizes fluid flow and gravity to apply a relatively low level of shear stress to cells or tissue constructs suspended in culture media (Vunjak-Novakovic, Martin et al. 1999; Martin, Obradovic et al. 2000; Emin, Koç et al. 2008). Remarkably, a research group has shown that chondrocyte-seeded PGA scaffolds cultivated within a rotating vessel bioreactor were able to develop into robust tissues with equilibrium moduli and GAG contents similar to or better than native cartilage after seven months in culture (Martin, Obradovic et al. 2000). Nevertheless, a major concern with this type of bioreactor is that the path of the suspended constructs within flow is unpredictable such that it is difficult to build a simulation model to optimize the

bioprocessing conditions (Darling and Athanasiou 2003). A hybrid bioreactor combining perfusion and rotating vessel systems was designed, in which cartilage constructs are mounted in the perfusion chamber while the outer wall of the reactor simultaneously spins during the cultivation (Farooque 2008). A computational fluid dynamics (CFD) model was established to define this unique hydrodynamic environment. Experimentally, the hybrid bioreactor system further improved chondrocyte doubling rate and collagen accumulation within engineered tissues in comparison with the system without the perfusion flow. This evidence suggests that development of tissue-engineered cartilage can potentially benefit from enhanced hydrodynamic forces such as those introduced by turbulent flow.

2.3.2.4 Turbulent Flow

Turbulent flow-induced shear environments can be established within a simple mechanically stirred bioreactor system equipped with an impeller or stir bar and referred to as a spinner flask (Figure 2.4F). Under mixing, oxygen and nutrients can be efficiently delivered to cells seeded within and/or on the scaffolds. It has been suggested by Vunjak-Novakovic et al. that mechanically stirred bioreactors can yield the best cell attachment efficiency to meshed synthetic scaffolds during the cell seeding process (Vunjak-Novakovic, Obradovic et al. 1998). The induced hydrodynamic shear stress possesses the ability to organize matrix architecture. Figure 2.5 demonstrates that the orientation of newly synthesized collagen fibrils is in the same direction as fluid flow at the periphery of engineered tissues which is in direct contact with the flow, but is disorderly in the interiors of the constructs. On the other hand, cultured cells can also be damaged when

exposed to extremely high agitation rates (150-300 rpm) (Papoutsakis 1991). Therefore, it is important to find a balance between hydrodynamic parameters and cell/tissue growth.

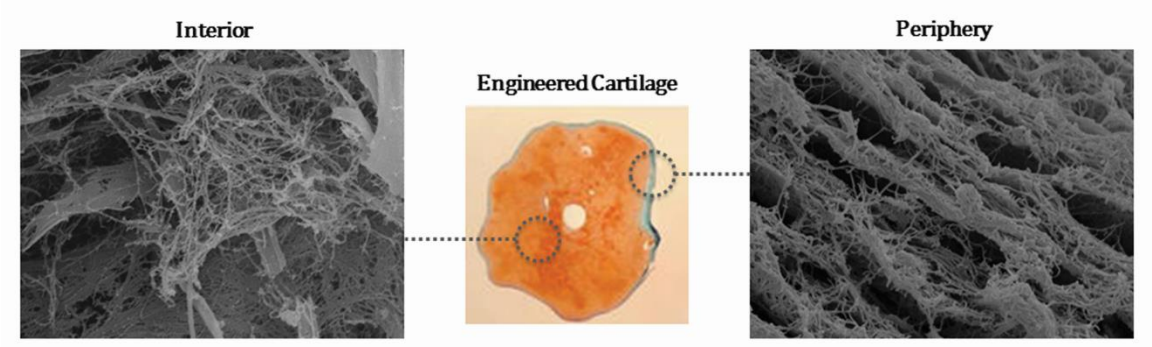

Figure 2.5 Orientation of collagen fibrils in tissue-engineered cartilage cultivated under turbulent flow. Collagen fibrils at the construct periphery are aligned in the same direction whereas those close to the center of the construct are less organized. Scanning electron microscopic images: 6500X.

2.3.2.5 Wavy-Walled Bioreactor (WWB)

A novel WWB system (Figure 2.6A) designed in our laboratory is an alternative version of the conventional spinner flask (Figure 2.6B) whose circular glass wall is modified into a sinusoidal curve. The internal radius (r) of the WWB is a function of the radial angle (θ) and can be expressed in the form of Equation 2.1.

$$r(\theta) = R_{avg} + A\sin(N\theta) \qquad \text{Equation 2.1}$$

where r and θ: cylindrical coordinates

R_{avg}: average internal radius

A: peak amplitude

N: number of lobes

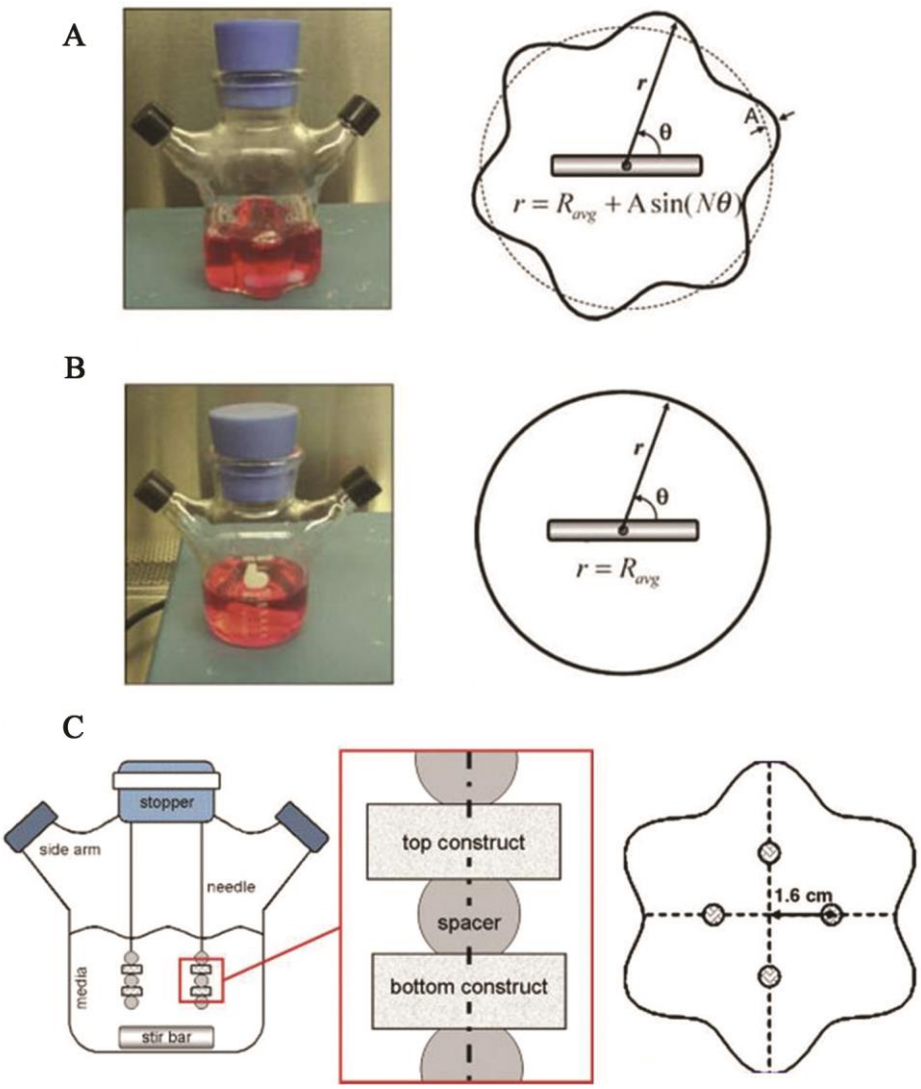

Figure 2.6 Configuration of the wavy-walled bioreactor (A) and the spinner flask (B), and the bioreactor setup for construct cultivation (C).

Mass transport within the WWB is achieved through mixing of culture media. The wavy shape of the WWB was designed to mimic baffles that increase hydrodynamic instabilities and thereby enhance the efficiency of fluid mixing. The initial intent of the WWB design was to cultivate suspended mammalian cells and it has previously been demonstrated by Barabino and coworkers that increased CHO cell proliferation in microcarriers can be accomplished in the WWB when compared with the traditional spinner flask (Barabino, Metghalchi et al. 1993). This WWB prototype had a capacity of 250 mL, an average radius of 3.50 cm, a peak amplitude of 0.65 cm and a total number of 6 lobes. The WWB then underwent several modifications to meet the requirements for cartilage tissue engineering. For example, the peak amplitude was changed from the initial measure, 0.65 cm, to the current version, 0.45cm, in order to avoid the accumulation of cultured chondrocytes at the lobes. The present WWB has a capacity of 120 mL, an average radius of 3.35 cm, a peak amplitude of 0.45 cm and a total number of 6 lobes (Bueno, Bilgen et al. 2004; Bueno, Bilgen et al. 2005). In a scaffold-free, cell aggregation study, the WWB was able to yield the formation of chondrocyte aggregates 45% faster than the spinner flask when both types of the bioreactors were agitated at the same rate (Bueno, Bilgen et al. 2004).

In the cultivation of chondrocyte-seeded scaffolds, the WWB is equipped with four 6-in long, 21 gauge stainless steel needles that are fixed onto a rubber stopper at the equidistant positions (r = 1.6 cm) (Figure 2.6C). Two scaffolds are then threaded onto each of the needles and are separated by a silicon spacer with a diameter of 3 mm, provided a total of eight constructs per bioreactor. The unique hydrodynamic culture environment within the WWB has previously been characterized using computational

fluid dynamics (CFD) simulation which was further validated by particle image velocimetry (PIV) methods (Bilgen, Sucosky et al. 2006; Bilgen and Barabino 2007). This characterization suggests that three hydrodynamic parameters (1) the average shear stress, (2) axial and (3) tangential fluid velocities on the control volume surface that is created around tissue constructs explain more than 99.9% of the variability of the hydrodynamic environment. In comparison with the spinner flask, the WWB yields a 43% higher axial velocity, but 50% lower shear stress applied to the construct surfaces (Bilgen and Barabino 2007). These conditions lead to increased chondrocyte seeding efficiency (Bueno, Laevsky et al. 2007) and improved cell proliferation and ECM deposition within engineered cartilage (Bueno, Bilgen et al. 2005; Bueno, Bilgen et al. 2008). A mathematical model composed of four elements, (1) a CFD model, (2) a kinetic growth model, (3) an artificial neural network that empirically correlates hydrodynamic parameters with kinetic constants and (4) a second artificial neural network that correlates biochemical compositions of constructs with their material properties, was developed to predict the dynamics of tissue growth with respect to their compositional and mechanical properties (Bilgen, Uygun et al. 2009). The model also suggested an optimal agitation rate of 50 rpm for neocartilage cultivation.

2.3.3 Bioactive Molecules

Extracellular biochemical signals are required to both initiate a series of biological reactions associated with specific cellular activities in response to external stimulations and provide essential elements for regulation of cell growth and tissue development. *In vitro*, nutrients assimilated by cells mainly originate from the

constituents present in culture media. These bioactive molecules are transported between culture media and cells and as such are important mediators in the soluble local environment of developing tissues.

2.3.3.1 Fetal Bovine Serum (FBS)

FBS is a typical medium supplement in the cultivation of mammalian cells because it contains rich proteins such as growth factors and cytokines. Although culture media supplemented with high serum contents (10-20%, v/v) have been extensively utilized to grow different types of cells and tissues, contradictory reports on the effects of serum have been documented. These variations may result from highly undefined serum composition and varied concentrations of its constituents when extracted from different individuals, thereby introducing unpredictable experimental outcomes. For instance, while high serum contents have been shown to increase cell doubling rate (Glowacki, Yates et al. 2005) and to effectively support *in-vitro* development of engineered tissues (Freed, Marquis et al. 1993; Mauck, Soltz et al. 2000), serum has also been shown to interfere with particular cellular activities and the function of exogenous growth factors. Specifically, chondrocyte proliferation (Mandl, Van Der Veen et al. 2002) and cartilage matrix production (Glowacki, Yates et al. 2005) in serum-containing cultures were compromised in comparison with serum-starved cultures supplemented with basic fibroblast growth factor (FGF-2) and TGF-β, respectively. It has also been demonstrated that embryonic bodies in culture with FBS had less capability to differentiate into functional neuronal cells (Zhang, Li et al. 2005) whereas serum-free media were shown to induce massive neural differentiation of embryonic carcinoma cells (Pacherník, Bryja

et al. 2005). Furthermore, serum-containing cultures failed to support the differentiation of porcine stromal vascular cells into adipocytes as indicated by reduced glycerol-3-phosphate dehydrogenase activities while the addition of insulin and hydrocortisone to serum-free media facilitated adipose differentiation (Suryawan and Hu 1993). Recent studies also indicated that the presence of serum components led to chondrocyte dedifferentiation (Lin, Willers et al. 2006) and decreased the activity of TGF-β1 in chondrogenesis of synoviocyte pellet cultures (Bilgen, Orsini et al. 2007). Thus, there is a need to reduce the dependency on serum while retaining its beneficial effects in the preparation of chemically defined culture media for cell and tissue engineering.

2.3.3.2 Insulin-Like Growth Factor-1 (IGF-1) and Transforming Growth Factor-β (TGF-β): Shear-Sensitive Growth Factors

Incorporation of soluble factors into tissue engineering strategies as medium supplements is a vital step in the development of engineered cartilage constructs. These molecules include, but are not limited to, growth factors such as IGF-1 (Sah, Trippel et al. 1996; Yaeger, Masi et al. 1997; Jin, Emkey et al. 2003; Mauck, Nicoll et al. 2003; Davies, Blain et al. 2008), TGF-β (Yaeger, Masi et al. 1997; Blunk, Sieminski et al. 2002; Malaviya and Nerem 2002; Pei, Seidel et al. 2002; Mauck, Nicoll et al. 2003; Glowacki, Yates et al. 2005; Davies, Blain et al. 2008; Emin, Koç et al. 2008; Duraine, Neu et al. 2009), FGF-2 (Sah, Trippel et al. 1996; Martin, Vunjak-Novakovic et al. 1999), and BMPs (Khalafi, Schmid et al. 2007; Kim and Im 2008; Shen, Wei et al. 2008; An, Cheng et al. 2010), and other stimulating agents like chondroitin sulfate (Basalo, Chahine et al. 2007; Bian, Kaplun et al. 2009), Genipin (Lima, Tan et al. 2009) and trimethylamine N-

oxide (O'connell, Fong et al. 2012). Among exogenous growth factors, IGF-1 and TGF-β are two of the most common stimulating biomolecules in cartilage biology (Chung and Burdick 2008). In articular cartilage, IGF-1 is one of the main molecules responsible for cartilage homeostasis and balancing matrix synthesis and degradation by chondrocytes. IGF-1 has the potential to maintain the viability of native cartilage (Sah, Trippel et al. 1996), to stimulate gene expression of both aggrecan and type II collagen by chondrocytes (Yaeger, Masi et al. 1997; Davies, Blain et al. 2008) and subsequent biosynthesis of associated protein molecules (Jin, Emkey et al. 2003), and to enhance stiffness of engineered cartilage (Mauck, Nicoll et al. 2003).

The TGF-β family is a more complex group that consists of at least three isoforms, TGF-β1, -β2 and -β3, which are associated with chondrocyte activities. The major functions of TGF-β molecules are to induce ECM deposition and inhibit protease production by cells. Although these isoforms have a high degree of similarity (65-80%) in their structure (Derynck, Lindquist et al. 1988) and most studies have reported an overall stimulatory effect of TGF-β on chondrocyte proliferation and cartilage maturation (Yaeger, Masi et al. 1997; Blunk, Sieminski et al. 2002; Malaviya and Nerem 2002; Pei, Seidel et al. 2002; Mauck, Nicoll et al. 2003; Glowacki, Yates et al. 2005; Davies, Blain et al. 2008; Emin, Koç et al. 2008; Duraine, Neu et al. 2009), they may still serve different biological roles. For instance, it has been found that the distribution of these three isoforms in the pathological joint is quite discrete. Specifically, abundant TGF-β1 molecules were localized in the superficial chondrocytes of osteophyte cartilage (Uchino, Izumi et al. 2000) while TGF-β2 was present within lining layer and pannus over the joint surface and TGF-β3 was only observed in the sparse cells within the deeper layers

of the synovia in an arthritic mouse model (Mu¨Ssener, Litton et al. 1997). Moreover, in fracture healing, TGF-β1 was expressed in early callus and the expression further increased during chondrogenesis and endochondral ossification whereas no stable trend was detected in both TGF-β2 and -β3 expression throughout the healing process (Rosier, O'keefe et al. 1998). Nevertheless, the total expression of TGF-β isoforms in mRNA level was found to increase in the early phase of osteoarthritic cartilage (Van Der Kraan, Glansbeek et al. 1997). This evidence substantiates their functional roles in cartilage regeneration mechanisms.

IGF-1 (Blunk, Sieminski et al. 2002; Pei, Seidel et al. 2002; Jin, Emkey et al. 2003; Mauck, Nicoll et al. 2003) and TGF-β (Blunk, Sieminski et al. 2002; Pei, Seidel et al. 2002; Mauck, Nicoll et al. 2003; Emin, Koç et al. 2008) are two of the bioactive molecules that are sensitive to mechanical stimuli such as shear stress, meaning that they are capable of interacting synergistically with mechanical forces to further accelerate functional maturation of engineered tissues. Differential responses to varied levels of shear or other mechanical loads have been observed. For example, Gooch and coworkers showed that engineered cartilage stimulated by exogenous IGF-1 exhibited increased ECM deposition when they were cultivated under laminar flow induced within a rotating vessel bioreactor, but not in a spinner flask that imparts turbulent flow (Gooch, Blunk et al. 2001). Several groups have also reported that IGF-1 and/or TGF-β in combination with shear stress resulted in accelerated cell proliferation, enhanced ECM synthesis and better tissue development (Ohno, Cooke et al. 1995; Malaviya and Nerem 2002; Jin, Emkey et al. 2003). Furthermore, the production of these shear-sensitive molecules by cells can be promoted when the cells are cultivated under fluid shear conditions (Ohno,

Cooke et al. 1995; Sakai, Mohtai et al. 1998; Negishi, Lu et al. 2001; Kapur, Mohan et al. 2005). In addition, TGF-β in particular is synthesized in a latent form by cells, which can be activated when exposed to shear conditions, and the activation largely depends on the magnitude of applied shear stress (Ahamed, Burg et al. 2008). These findings speak to the complexity of fluid shear stress in the modulation of not only tissue morphology and properties but also synthesis, activation and function of the shear-sensitive growth factors.

2.4 Summary

The limited self-repair ability of injured or diseased articular cartilage persists as a challenge for orthopedic medicine. Tissue engineering approaches combining cells, bioactive molecules and biocompatible/biodegradable scaffolds in scalable bioreactor systems for fabrication of functional tissue replacements hold promise. The ultimate and clinical goals of cartilage tissue engineering are to replace damaged cartilage with tissue-engineered constructs that are mechanically strong and functionally reliable and are able to integrate with the host tissues to support the integrity of the entire regenerating tissue.

Successful creation of functional tissue substitutes suitable for implantation requires a thorough understanding of environmental factors that control and regulate cellular behavior and tissue formation. Recent efforts to develop engineering tools such as novel biomaterials and bioreactor systems have made remarkable progress in cartilage tissue engineering by improving the quality of engineered constructs. Yet, the knowledge of the formation and the role of a type I collagen-based fibrous capsule, a unique structure only present at the periphery of tissue-engineered cartilage, is still limited. In this dissertation, we employed a simple tool, the WWB system, to investigate the

modulation of the capsule formation by the interplay between fluid shear stress and biochemical factors through the systematic development of a chemically reliable culture environment that is favorable for hydrodynamic cultivation of tissue-engineered cartilage. IGF-1 and TGF-β1 were chosen to be incorporated into the system because of their shear-sensitive nature. We further aimed to answer the question of whether or not the presence of the fibrous capsule at the construct periphery would hinder neocartilage development. Exploiting the synergy between mechanical and biochemical stimuli is an important step toward the optimization of bioprocessing conditions for the achievement of clinically relevant cartilage tissue replacements.

CHAPTER 3

REQUIREMENT FOR SERUM IN MEDIUM SUPPLEMENTED WITH INSULIN-TRANSFERRIN-SELENIUM FOR HYDRODYNAMIC CULTIVATION OF TISSUE-ENGINEERED CARTILAGE[‡]

3.1 Introduction

Achievement of viable engineered tissues through *in vitro* cultivation in bioreactor systems requires a thorough understanding of the complex interplay between mechanical forces and soluble biochemical cues. Bioreactors that impart various mechanical stimuli have been utilized to support the development of different tissue types such as cardiovascular tissues (Barron, Lyons et al. 2003; Hahn, Mchale et al. 2007), tendon (Angelidis, Thorfinn et al. 2009), bone (Cartmell, Porter et al. 2003; Yu, Botchwey et al. 2004; Duty, Oest et al. 2007), and cartilage (Vunjak-Novakovic, Martin et al. 1999; Mauck, Soltz et al. 2000; Darling and Athanasiou 2003; Gemmiti and Guldberg 2006; Elder and Athanasiou 2009). In cartilage tissue engineering, bioreactor systems have been designed to provide deformational loading, hydrostatic pressure and hydrodynamic forces. The use of dynamic compressive loading to apply physiological levels of strain has been shown to improve mechanical and biochemical properties of chondrocyte-laden agarose (Mauck, Soltz et al. 2000) and self-assembling peptide (Kisiday, Jin et al. 2004) hydrogels. In these studies, the compressively loaded samples

[‡]Adapted and modified from Yang, Y.-H. and Barabino, G.A. (*2011*) Requirement for Serum in Medium Supplemented with Insulin-Transferrin-Selenium for Hydrodynamic Cultivation of Engineered Cartilage. *Tissue Engineering Part A*. 17(15-16): 2025-2035.

exhibited an at least 20% increase in GAG accumulation inside the construct, which led to equilibrium compressive moduli improved by about 40-50% in comparison with the non-loaded ones. It has also been demonstrated that temporal hydrostatic pressure applied at a magnitude in the range of 1 to 10 MPa with a frequency between 0.1 and 1 Hz can enhance the deposition of ECM components and the stiffness of engineered cartilage (Elder and Athanasiou 2009). The application of continuous fluid flow-induced shear stress is aimed to improve mass transport mechanisms through fluid mixing and simultaneously provide physical stimuli across or through the cell-seeded construct. Thus far, improved tissue quality has been reported when engineered cartilage constructs are cultivated under fluid shear conditions (Vunjak-Novakovic, Martin et al. 1999; Cartmell, Porter et al. 2003; Bueno, Bilgen et al. 2004; Yu, Botchwey et al. 2004; Bueno, Bilgen et al. 2005; Gemmiti and Guldberg 2006; Bueno, Laevsky et al. 2007; Bueno, Bilgen et al. 2008). Continuous fluid shear bioreactors include customized perfusion systems (Cartmell, Porter et al. 2003; Gemmiti and Guldberg 2006), rotating wall vessels (Vunjak-Novakovic, Martin et al. 1999; Yu, Botchwey et al. 2004), spinner flasks (Vunjak-Novakovic, Martin et al. 1999) and WWBs (Bueno, Bilgen et al. 2004; Bueno, Bilgen et al. 2005; Bueno, Laevsky et al. 2007; Bueno, Bilgen et al. 2008).

Extracellular soluble molecules are an important regulator in both natural and experimental tissue growth environments. *In vitro*, nutrients are delivered to cultured cells mainly through culture media supplemented with a variety of constituents. FBS contains abundant growth factors and cytokines and is traditionally used as a medium supplement in the cultivation of mammalian cells. Although culture media supplemented with high serum contents (10-20%, v/v) have been shown to support the development of

good quality tissue substitutes (Freed, Marquis et al. 1993; Mauck, Soltz et al. 2000), FBS elicits many issues. For instance, FBS composition is highly undefined and the concentration of its constituents may vary when extracted from different donors, thereby introducing unpredictable effects on cultured cells and tissues. The evidence includes its interference with the differentiation of pluripotent and multipotent cells (Suryawan and Hu 1993; Zhang, Li et al. 2005; Bilgen, Orsini et al. 2007). In addition, FBS also contains antibodies and binding proteins that may neutralize exogenous growth factors added to the system (Friedrich, Haring et al. 2009). As a result, it is necessary to minimize the serum concentration while retaining its beneficial effects in the formulation of chemically reliable culture media for cell and tissue engineering.

ITS is a commercially available medium supplement and each of its components, i.e. insulin, transferrin and selenium, is associated with essential cellular activities (Mcquillan, C J Handley et al. 1986; Shapiro and Wagner 1988; Shapiro and Wagner 1989; Venkateswaran, Klotz et al. 2002). Specifically, insulin is a peptide hormone that facilitates cellular uptake of glucose and amino acids from blood. Transferrin, an iron transport protein, is responsible for detoxification of culture media from oxygen radicals and peroxides while selenium forms the active center of the enzymes that reduce oxygen radicals. In cartilage tissue engineering, the standard concentration of ITS (1%, v/v, [10 μg/mL insulin, 5.5 μg/mL transferrin, and 5 μg/mL selenium]) added to culture media is based on the concentration of insulin previously found to stimulate proteoglycan synthesis in cultured cartilage explants (Mcquillan, C J Handley et al. 1986; Kisiday, Kurz et al. 2005). Low-serum or serum-free media supplemented with ITS have been used in the *in-vitro* cultivation of chondrocytes (Mandl, Van Der Veen et al. 2002; Chua,

Aminuddin et al. 2005; Gigout, Buschmann et al. 2009) and engineered cartilage (Fitzsimmons, Sanyal et al. 2004; Kisiday, Jin et al. 2004; Chua, Aminuddin et al. 2005; Kisiday, Kurz et al. 2005; Bian, Lima et al. 2008; Kelly, Fisher et al. 2008). In these studies, ITS has been shown to be suitable as a partial (Kisiday, Jin et al. 2002; Fitzsimmons, Sanyal et al. 2004; Kisiday, Kurz et al. 2005; Kelly, Fisher et al. 2008) or full (Kisiday, Kurz et al. 2005; Bian, Lima et al. 2008) substitute for FBS. For instance, Kelly and coworkers demonstrated that the supplementation of ITS could reduce the FBS content from 20% to 2% while stiffness and biochemical compositions of engineered constructs were either maintained or enhanced (Kelly, Fisher et al. 2008). Moreover, Kisiday et al. revealed that the replacement of FBS with ITS may largely depend on the substrate material since agarose-based cartilage constructs could be grown in a serum-free ITS-supplemented culture medium whereas ITS media alone did not support the development of chondrocyte-laden self-assembling peptide gels (Kisiday, Kurz et al. 2005). Most of these studies, however, were evaluated under loading-free culture conditions or, in a few cases, under conditions of dynamic compressive loading (Kisiday, Jin et al. 2004; Kisiday, Kurz et al. 2005; Kelly, Fisher et al. 2008), none of these studies employed or investigated the role of hydrodynamic forces.

Mechanical and biochemical stimuli can act synergistically to regulate cellular activities, tissue morphology and tissue properties. *In vitro*, improved cell function and tissue formation have been achieved through the combined application of mechanical loading and exogenous growth factors (Ohno, Cooke et al. 1995; Malaviya and Nerem 2002; Jin, Emkey et al. 2003; Lau, Kapur et al. 2006). Some growth factors, like TGF-β, IGF-1 and BMPs, are known to be shear-sensitive, suggesting that their synthesis is

promoted in shear-stimulated cells and further that the up-regulation of their signaling pathways contributes to differential anabolic activities of cells in response to fluid shear stress (Ohno, Cooke et al. 1995; Sakai, Mohtai et al. 1998; Negishi, Lu et al. 2001; Lau, Kapur et al. 2006). This evidence substantiates the potential involvement of these soluble molecules in mechanotransduction mechanisms.

A type I collagen-based fibrous capsule (Chapter 1) that is a unique feature of tissue-engineered cartilage may be one of the representative examples attributed to the combined effects of hydrodynamic forces and soluble biochemical factors. In the present study, by employing the WWB system (Chapter 2.3.2.5), we examined the feasibility of reduced FBS contents (0%, 0.2% and 2%, v/v) in combination with ITS (1%, v/v) to support the development of chondrocyte-seeded PGA scaffolds cultivated under static or hydrodynamic conditions and also focused on the synergistic roles of continuous fluid shear stress and serum in the capsule formation, given that serum contains both shear-sensitive and fibrosis-promoting soluble molecules. The results were compared with the traditional high-serum (10% FBS, v/v) cultures. We hypothesized that (1) a minimal content of shear-sensitive molecules present in serum is required in cultures supplemented with ITS in order to produce hydrodynamically engineered constructs morphologically, compositionally and mechanically similar to the high-serum constructs and (2) the thickness of a fibrous capsule at the construct periphery increases with increasing serum concentration employed in culture.

3.2 Materials and Methods

3.2.1 Materials

High glucose Dulbecco's modified eagle medium (hgDMEM), *N*-(2-hydroxyethyl)piperazine *N*'-2-ethanesulfonic acid (HEPES), L-ascorbic acid, Dulbecco's phosphate-buffered saline (PBS), ethylenediaminetetraacetic acid (EDTA), cysteine, Sigmacote®, 1-9-dimethylmethylene blue (DMMB), chondroitin sulfate, chloramines-T hydrate, p-dimethylaminobenzaldehyde (pDAB), and hydroxyproline were from Sigma (St. Louis, MO). Sodium bicarbonate, L-proline, FBS, penicillin-streptomycin, non-essential amino acid (NEAA), ITS, 0.4% trypan blue solution, 10% formalin, 6-in. long, 21 gauge stainless steel needles, magnetic stir bars, silicone tubing, and robber stoppers were purchased from VWR International (West Chester, PA). Fungizone, collagenase type II, and PicoGreen quantification kit were from Gibco (Carlsbad, CA). Papain enzyme was from Worthington (Lakewood, NJ). PGA biofelt (2 mm thick x 85 mg/mL bulk density, 97% void volume) was from Concordia Medical (Warwick, RI). Knee joints of 1- to 2-week-old bovine calves were obtained from Research 87 (Marlborough, MA).

3.2.2 Bioreactor and Scaffold Preparation

Conventional spinner flasks were purchased from Bellco Glass, Inc. (Vineland, NJ) and sent to G. Finkenbeiner, Inc. (Waltham, MA) for WWB fabrication based on the configuration described in Chapter 2.3.2.5. Briefly, a WWB was assembled by fitting them with two Teflon side-arm caps, a magnetic stir bar (0.8 cm diameter x 4 cm long), and a rubber stopper. Four 6-in. long, 21 gauge needles were inserted through the stopper at equidistant positions. The interiors of bioreactors, needles, and stir bars were then

treated with Sigmacote® to form a thin silicone film that prevents cell adherence. After evaporation of Sigmacote®, the assembled bioreactors were washed gently, air-dried and steam-sterilized.

10-mm diameter PGA discs were sterilized by three successive 15-min submersions in sterile 70% ethanol and three subsequent 15-min rinses with sterile deionized water followed by a 30-min exposure to ultraviolet light. Two sterilized PGA discs were threaded onto each of the 21 gauge needles and separated by a 3-mm diameter silicone spacer, resulting in a total of eight PGA scaffolds per bioreactor. The WWBs were then filled with 120-mL hgDMEM supplemented with 10% FBS, 100 U/mL penicillin, 100 U/mL streptomycin, 10 mM HEPES, 0.4 mM L-proline, 0.1 mM NEAA, 3.6 mg/mL sodium bicarbonate, 2.5 μg/mL fungizone and 50 μg/mL ascorbic acid, and were allowed to stabilize overnight with a stir bar spinning at 50 rpm inside a humidified, 37°C, 5% CO_2 incubator. The two side-arm caps were loosened for gas exchange.

3.2.3 Cell Isolation, Cell Seeding and Tissue Culture

Isolation of primary chondrocytes was based on the work done by Freed et al (Freed, Marquis et al. 1993). Briefly, articular cartilage sections were harvested aseptically from the femoropatellar groove of freshly slaughtered 1- to 2-week-old calves. Tissue explants were then minced into 1-2 mm^3 cubes, followed by digestion with type II collagenase in hgDMEM at a concentration of 1.5 mg/mL for 17 hours. The supernatant of the digested tissues was collected and centrifuged at 1000 rpm for 12 min to obtain chondrocyte pellets. Pellets were washed three times with 0.02% EDTA in PBS and chondrocytes were then resuspended in the medium specified above. Cell number and

viability were determined using a trypan blue exclusion assay. The average cell viability remained greater than 90%. A small aliquot of chondrocytes in suspension was then added to each of the sterilized bioreactors at a density of five million live cells per scaffold. Cell seeding was allowed to proceed for 3-4 days until 95% of the chondrocytes achieved attachment.

At the end of the seeding period, media were completely removed from the bioreactors and replaced with fresh hgDMEM supplemented with four different combinations of FBS and ITS: (A) 0% FBS + 1% ITS, (B) 0.2% FBS + 1% ITS, (C) 2% FBS + 1% ITS and (D) 10% FBS. This point was considered as day zero. Cell-seeded PGA scaffolds were then cultured in the WWB agitated by a stir bar at 50 rpm inside an incubator for 28 days, and culture media were renewed every 3 days thereafter. Constructs were aseptically removed from the bioreactors at specific time points for evaluation. A static control experiment without fluid agitation was carried out under the same culture conditions as the hydrodynamic study. Figure 3.1 shows a schematic overview of the experimental design.

3.2.4 Biomechanics

Equilibrium compressive moduli of constructs were determined using an unconfined compression test. During examination, a preload of 0.01 N was applied to samples until equilibrium was achieved. A stress relaxation test was carried out at strains of 5, 10, 15, 20 and 25%, after which samples were allowed to equilibrate. Equilibrium moduli were obtained from the slope of the plot of equilibrium force normalized to the cross-sectional area of the construct versus the strains.

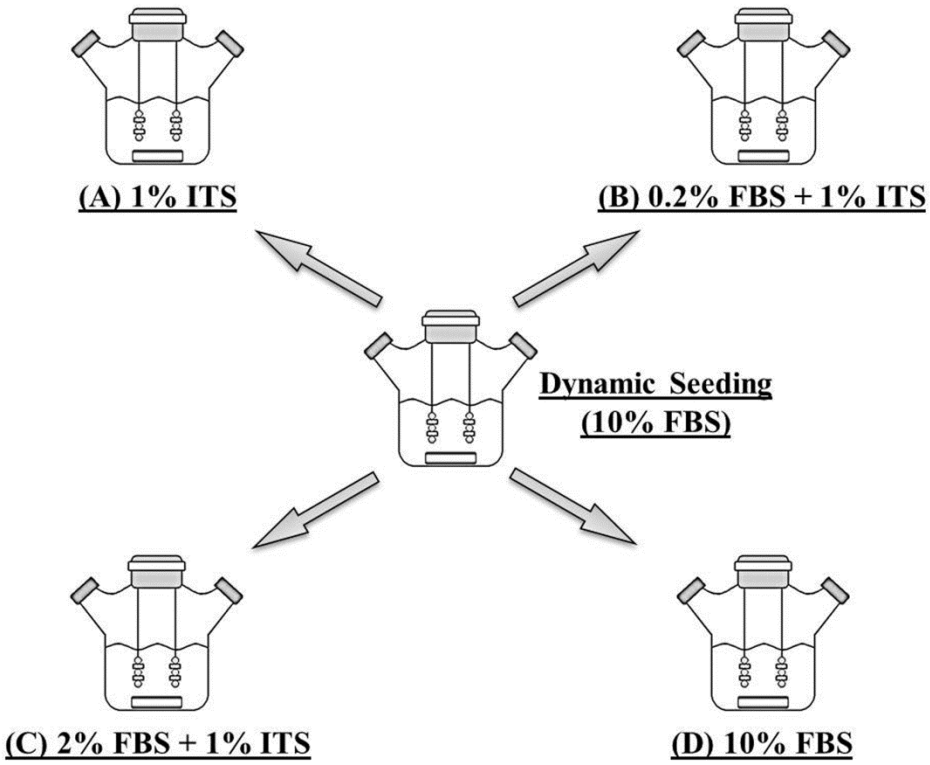

Figure 3.1 Schematic overview of the experimental design. Dynamic cell seeding process was performed in the WWB for 3-4 days and the culture medium was supplemented with 10% FBS. Cell-seeded constructs were then cultivated with (A) 1% ITS, (B) 0.2% FBS + 1% ITS, (C) 2% FBS + 1% ITS, or (D) 10% FBS in the WWB for an additional 28 days in the presence (hydrodynamic groups) or absence (static groups) of continuous fluid shear stress.

3.2.5 Biochemistry

Prior to biochemical analyses, engineered tissues were weighed (wet weight), frozen, lyophilized using a speed vacuum for 24 hours, weighed (dry weight), and digested with papain enzyme in a PBS/EDTA/cysteine solution for 17 hours at 60°C. DNA was quantified using a PicoGreen dsDNA kit employing a fluorescence spectrometer and the number of chondrocytes per construct was calculated by assuming

7.7 pg of DNA per chondrocyte (Kim, Sah et al. 1988). Sulfated GAG contents retained inside the construct were assessed spectrophotometrically at 525 nm using a DMMB dye-binding assay (Farndale, Buttle et al. 1986). Chondroitin sulfate was used to create a standard curve and a ratio of chondroitin sulfate to GAG of 1 was assumed. Total collagen contents were determined using an orthohydroxyproline colorimetric assay, assuming a 1:10 orthohydroxyproline-to-collagen concentration ratio (Woessner 1961). The concentration of hydroxyproline was measured spectrophotometrically at 550 nm after acid hydrolysis and reaction with chloramine-T and pDAB. GAG and total collagen contents are presented in values normalized to the wet weight of constructs.

3.2.6 Histology

In preparation for histology, constructs were fixed in 10% formalin, embedded in paraffin (Histocentre 2, Shandon), and sectioned in 5-7-μm thick slices (Isomet 1000 Precision Saw, Buehler). The slices were fixed on glass slides and then stained with hematoxylin and eosin for cells, safranin-O and fast green for GAG, and Masson's trichrome for collagen. Color images were captured using a standard light microscope (Nikon E600, Japan).

3.2.7 Measurement of Capsule Thickness

Safranin-O and fast green images captured at 10X magnification were collected for image analysis to quantify the thickness of a fibrous capsule. The images were converted to grayscale using the RGB split function in ImageJ software (NIH), followed by background subtraction and threshold selection. Irrelevant artifacts were then removed

and the processed images were sent to NIS-Elements AR 3.0 software (Nikon) for image analysis (0.49 μm / pixel). The average thickness of a capsule was calculated by normalizing the area of the capsule to its length averaged from the two long sides.

3.2.8 Statistical Analyses

The hydrodynamic study was repeated three times using the same batch of primary chondrocytes collected from three calves, while cells employed in the duplicate static experiments were mixed from three other donors. In each set of experiments, two (hydrodynamic) or three (static) constructs were harvested from each group at each time point for analysis of macroscopic, mechanical and biochemical properties or for histological evaluation. Samples collected from identical experiments were assessed together ($n = 6$) and biochemical assays were performed in duplicate. Twenty histological images per group, which were randomly selected from the slides that represented the six 28-day construct blocks, were used for image analysis of capsule thickness ($n = 20$). Statistical data are presented as means ± one standard deviation and statistical analyses were performed by Student's *t*-test (two-tailed) for comparison between two groups or by one-way or two-way analysis of variance (ANOVA) in conjunction with the Bonferroni post test for multiple comparisons. Statistical significance was achieved when *p*-values were less than 0.05.

3.3 Results

3.3.1 Static Controls

To substantiate the importance of shear-sensitive soluble factors in hydrodynamic cultivation of tissue-engineered cartilage, a static control study preceded the hydrodynamic experiments. Briefly, at the end of the cultivation, similar biochemical compositions were observed in the serum-free, low-serum, and high-serum groups (Figure 3.2). The average values were 8.58 ± 1.52 million cells per construct, 0.69 ± 0.13% of wet weight in collagen content and 1.16 ± 0.18% of wet weight in GAG content, respectively. The histological specimens (Figure 3.3) revealed that a fibrous capsule which is characterized by increased cell density and decreased GAG accumulation was only observed at the outer edge of the 2% FBS + ITS and the 10% FBS constructs. These thin capsules were about 12.73 μm and 20.79 μm thick in the 2% FBS + ITS and the 10% FBS groups, respectively (Table 3.1).

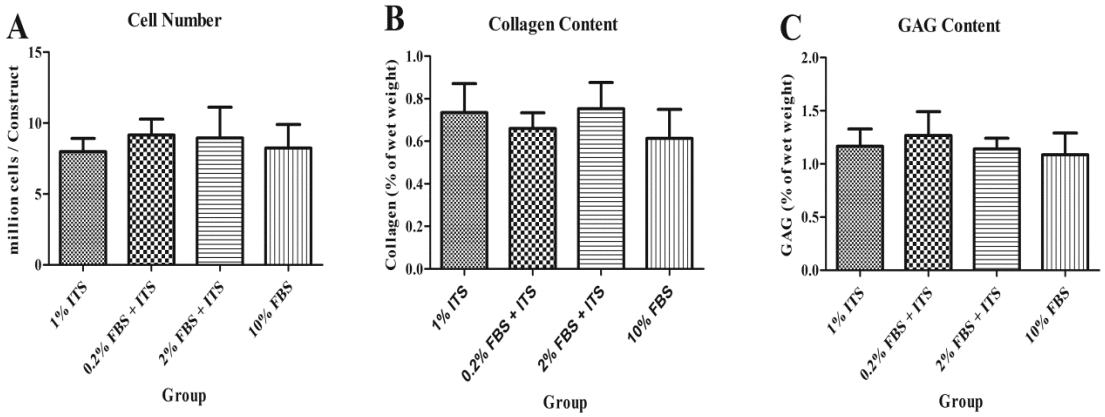

Figure 3.2 Cell number (A), total collagen content (B) and GAG content (C) of 28-day constructs cultivated with different media in the absence of hydrodynamic stimuli. Reduced serum (0-2%) media supplemented with 1% ITS were able to maintain the levels of construct properties achieved in the high-serum (10%) group. No statistical significance was observed among the experimental groups; $p < 0.05$; n = 6.

Table 3.1 Capsule Thickness of 28-Day Static Constructs

Culture Condition	1% ITS	0.2% FBS + ITS	2% FBS + ITS	10% FBS
Capsule Thickness (µm)	ND	ND	12.73 ± 4.44	20.79 ± 3.10[†]

[†]Statistical significance versus the 2% FBS + ITS group; $p < 0.001$; n = 20. ND: non-detectable.

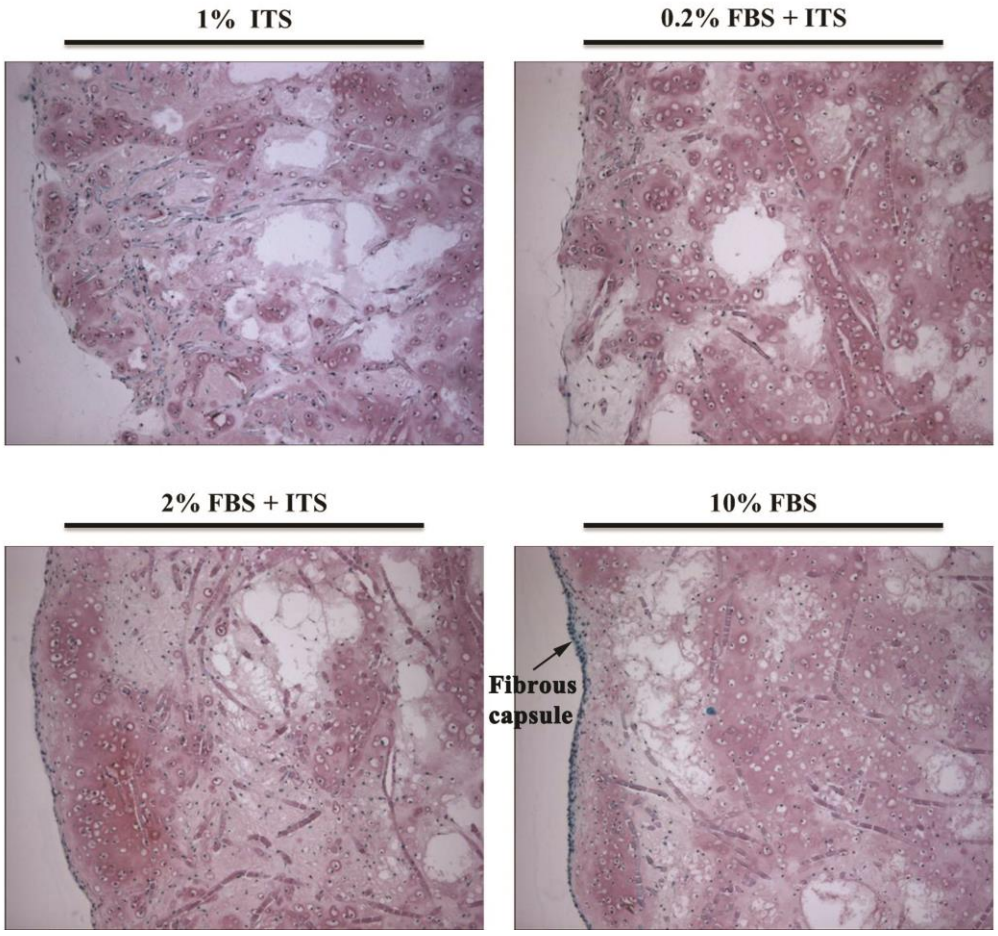

Figure 3.3 Light microscopy images of 28-day static constructs stained with safranin-O and fast green. GAG, nuclei and cytoplasm are stained red, black and green, respectively. The tubular structures represent remaining PGA fibers. The static cultures yielded low ECM deposition and an imperceptible fibrous capsule was only observed in the 2% FBS + ITS and the 10% FBS groups. Images were taken at 10X magnification.

3.3.2 Hydrodynamic Constructs

3.3.2.1 Macroscopic Properties

The wet weight (Figure 3.4A) of constructs remained similar across the experimental groups in the first two weeks of the cultivation whereas the serum-free group had at least a 50% reduction in the average wet weight compared with the serum-containing groups at day 28 ($^{*}p < 0.05$). In addition, the wet weights of the 0.2% FBS + ITS and the 2% FBS + ITS constructs at day 28 were significantly higher than those of the same groups at day 3 ($^{\wedge}p < 0.05$) and day 14 ($^{\#}p < 0.05$).

The dry weight values (Figure 3.4B) of the serum-free constructs at days 14 and 28 were significantly lower than those of the serum-containing groups at the same time points ($^{*}p < 0.05$) and reached its maximum value at day 3 ($^{\&}p < 0.05$). At day 14, the dry weights of the 2% FBS + ITS and the 10% FBS constructs decreased about 25% when compared with the corresponding 3-day values ($^{\$}p < 0.05$). At day 28, the 2% FBS + ITS group was the only experimental group which showed significantly greater dry weight than that measured at day 14 ($^{\#}p < 0.05$).

At day 14, the water content (Figure 3.4C) of the serum-free group was higher than those of the 2% FBS + ITS and the 10% FBS groups ($^{*}p < 0.05$). Overall, the water contents of all the constructs, except for the serum-free samples, increased over time, and significantly greater contents were measured at day 28 when compared with those detected in the beginning of the culture ($^{\wedge}p < 0.05$).

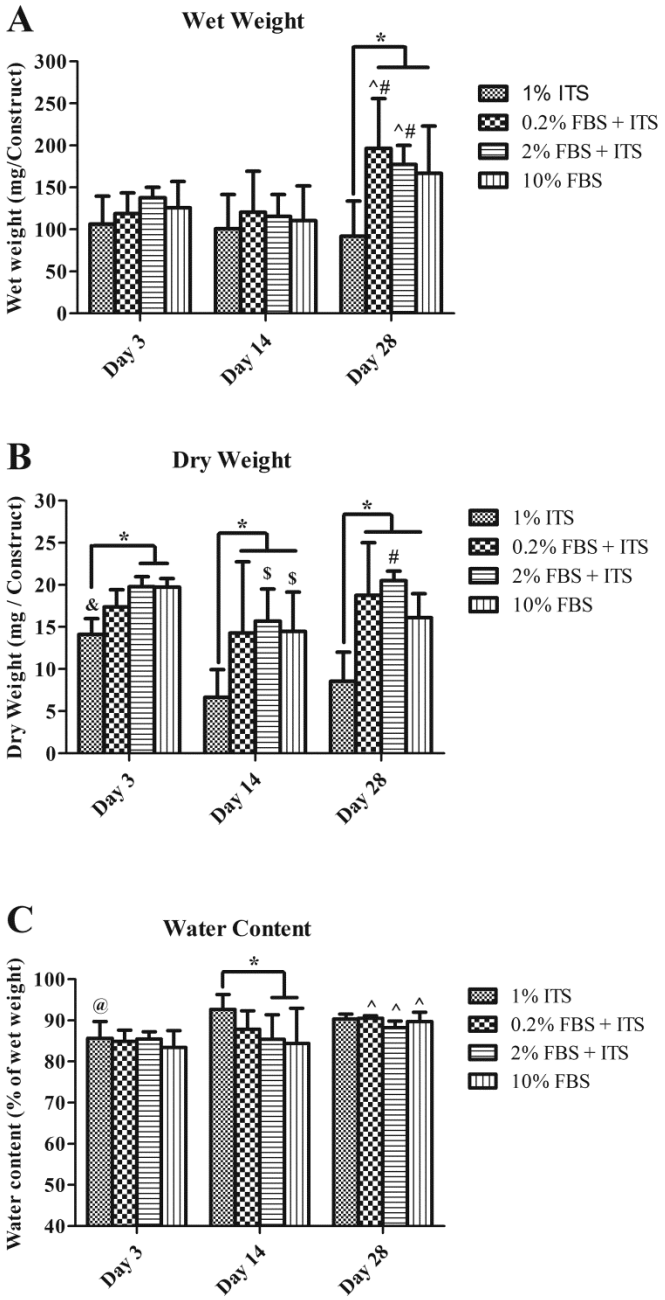

Figure 3.4 Wet weight (A), dry weight (B) and water content (C) of chondrocyte-seeded constructs cultivated with different media in the presence of hydrodynamic stimuli over a 4-week period. *indicates significant difference between the groups; ^and $^{\#}$ indicate significant increase compared with the 3-day and the 14-day values, respectively, within the group; $^{\$}$indicates significant decrease versus the 3-day values within the group; $^{\&}$indicates significant increase compared with both the 14-day and the 28-day values within the group; $^{@}$indicates significant decrease versus both the 14-day and the 28-day values within the group; $p < 0.05$; n = 6.

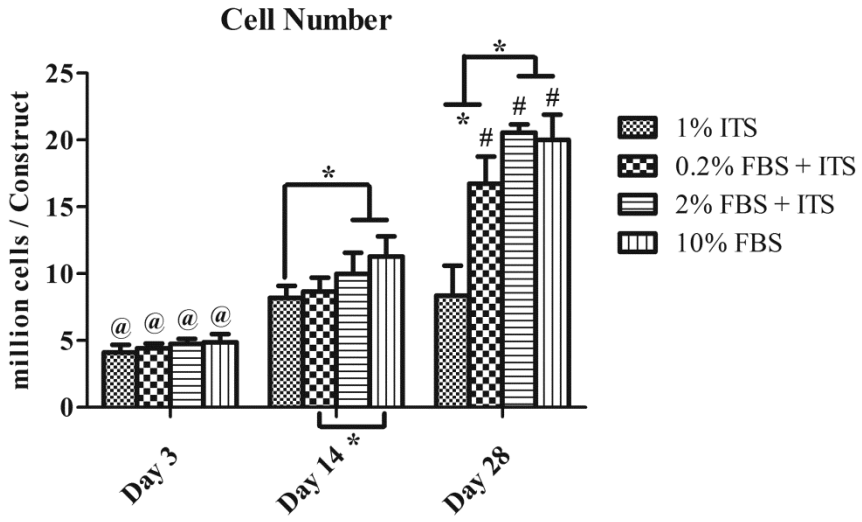

Figure 3.5 Cell number of chondrocyte-seeded constructs cultivated with different media in the presence of hydrodynamic stimuli over a 4-week period. At the end of the cultivation, the 2% FBS + ITS and the 10% FBS cultures yielded higher cell proliferation than the other two groups. *indicates significant difference between the groups; #indicates significantly higher values in comparison with the 14-day values within the group; @indicates significant decrease versus both the 14-day and the 28-day values within the group; $p < 0.05$; n = 6.

3.3.2.2 Cell Proliferation

Three days after the initiation of the culture, the cell number per construct (Figure 3.5) was close to the cell seeding density (five million cells / scaffold) in all the groups and the values were 1- to 3.5-fold lower than those achieved at days 14 and 28 ($^{@}p < 0.05$). At day 14, increased chondrocyte proliferation was detected when the FBS concentration was at least 2%. Specifically, both the 2% FBS + ITS (10.00 ± 1.58 million cells per construct) and the 10% FBS (11.29 ± 1.52 million cells per construct) values were significantly greater than the serum-free value (8.19 ± 0.90 million cells per construct) while the average cell number of the 10% FBS constructs was also higher than

that of the 0.2% FBS + ITS constructs (8.67 ± 1.03 million cells per construct) (*p < 0.05). At day 28, constructs in the 2% FBS + ITS (20.56 ± 0.62 million cells per construct) and the 10% FBS (20.00 ± 1.90 million cells per construct) groups had undergone about two cell population doublings. Conversely, the 0.2% FBS + ITS constructs (16.75 ± 2.01 million cells per construct) exhibited less than two population doublings while the average cell number in the serum-free group (8.37 ± 2.21 million cells per construct) remained unchanged after two weeks in culture.

3.3.2.3 Total Collagen Content

At day 3, no significant differences in collagen production (Figure 3.6) were observed across the groups, and the values were about 2- to 10-fold lower than those at days 14 and 28 ($^{@}p$ < 0.05). At day 14, the collagen contents of the 2% FBS + ITS (1.63 ± 0.24% of wet weight) and the 10% FBS (1.65 ± 0.22% of wet weight) constructs were significantly higher than those of the 0.2% FBS + ITS (1.33 ± 0.10% of wet weight) and the serum-free (1.20 ± 0.10% of wet weight) constructs (*p < 0.05). When compared with the corresponding 14-day values, the collagen contents at day 28 increased at least 38% in the serum-containing groups ($^{\#}p$ < 0.05) while a 46% reduction was detected in the serum-free constructs ($^{\$}p$ < 0.05). At day 28, similar collagen contents were determined in the 2% FBS + ITS (2.46 ± 0.08% of wet weight) and the 10% FBS (2.30 ± 0.08% of wet weight) groups, both of which were significantly higher than the 0.2% FBS + ITS (1.82 ± 0.13% of wet weight) and the serum-free (0.64 ± 0.06% of wet weight) values (*p < 0.05). Overall, the collagen deposition in the serum-free, the 0.2% FBS +

ITS and the 2% FBS + ITS constructs reached about 28%, 79% and 106% of the high-serum value, respectively, at the end of the cultivation.

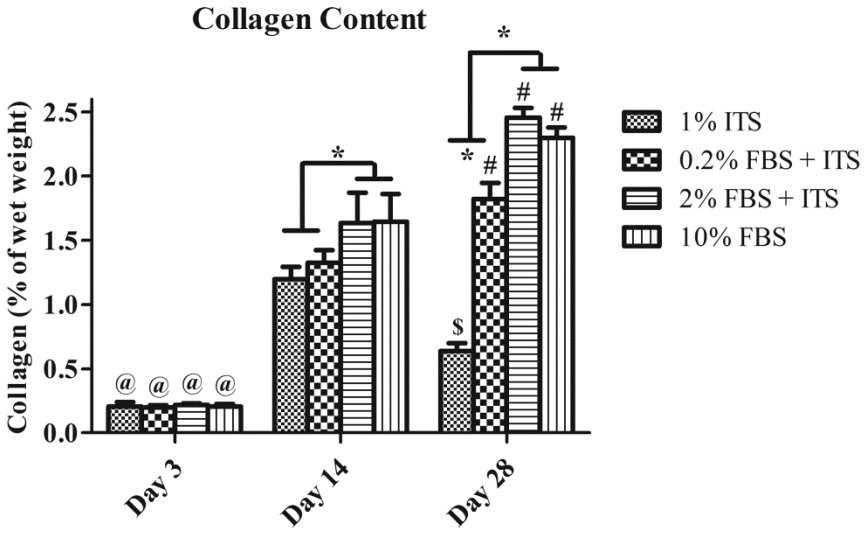

Figure 3.6 Total collagen content of chondrocyte-seeded constructs cultivated with different media in the presence of hydrodynamic stimuli over a 4-week period. At the end of the cultivation, the serum-free constructs had a compromised total collagen content while the 0.2% FBS + ITS and the 2% FBS + ITS values were close to about 79% and 106% of the high-serum level, respectively. *indicates significant difference between the groups; $^{\#}$and $^{\$}$ indicate significantly higher and lower values, respectively, in comparison with the 14-day values within the group; $^{@}$indicates significant decrease versus both the 14-day and the 28-day values within the group; $p < 0.05$; n = 6.

3.3.2.4 GAG Content

Similar to total collagen content, GAG accumulation (Figure 3.7) was comparable across all the experimental groups at day 3, with values reaching approximately 0.40 ± 0.10% of wet weight. These values were 2.5- to 6-fold lower than those measured at days 14 and 28 ($^{@}p < 0.05$). No differences in the GAG content were observed among the groups at day 14, where the values fell in the range of 1.42 ± 0.39% of wet weight.

Differences emerged at day 28, however, as the GAG contents of the 2% FBS + ITS (2.85 ± 0.14% of wet weight) and the 10% FBS (2.99 ± 0.23% of wet weight) groups were both significantly higher than those of the serum-free (1.39 ± 0.20% of wet weight) and the 0.2% FBS + ITS (2.32 ± 0.16% of wet weight) groups (*$p < 0.05$). In comparison with the corresponding 14-day values, the serum-containing constructs increased GAG contents by at least 75% at day 28 ($^{\#}p < 0.05$) while the values held steady for the serum-free group at both time points. Overall, the GAG deposition in the serum-free, the 0.2% FBS + ITS and the 2% FBS + ITS constructs reached about 47%, 78% and 95% of the high-serum value, respectively, at the end of the cultivation.

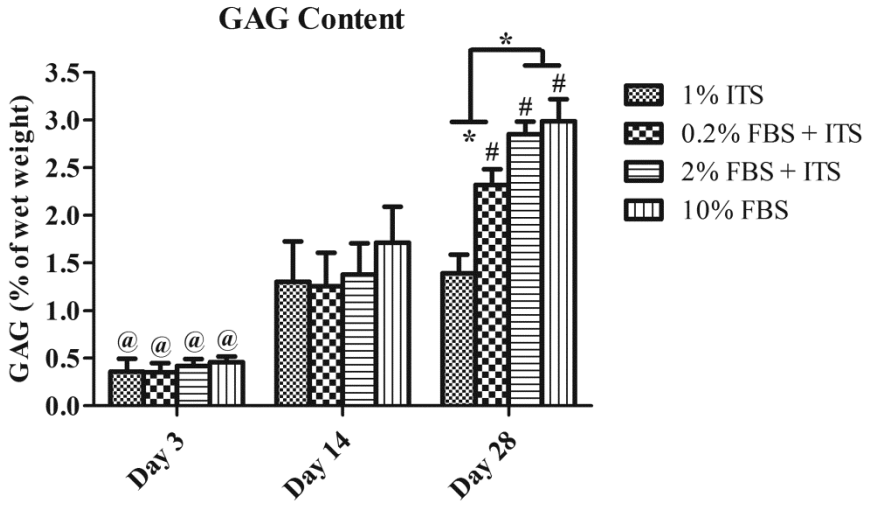

Figure 3.7 GAG content of chondrocyte-seeded constructs cultivated with different media in the presence of hydrodynamic stimuli over a 4-week period. At the end of the cultivation, the serum-free, the 0.2% FBS + ITS and the 2% FBS + ITS constructs exhibited 47%, 78% and 95% of the GAG content achieved by the high-serum constructs, respectively. *indicates significant difference between the groups; $^{\#}$indicates significantly higher values in comparison with the 14-day values within the group; $^{@}$indicates significant decrease versus both the 14-day and the 28-day values within the group; $p < 0.05$; n = 6.

3.3.2.5 Histology

Figure 3.8 includes the histological results of 3-day and 28-day hydrodynamic constructs. No differences were observed in histology of any 3-day constructs. Qualitatively, most chondrocytes initially attached to the outer regions of the PGA scaffolds and fewer cells populated the interiors of the constructs. In addition, abundant large PGA fibers were present in constructs at this early time point.

At day 28, the serum-containing samples were more intensely stained for cells and ECM components in comparison with the serum-free group. Since polymer scaffolds degraded over time, fewer and thinner PGA fibers were observed in the 28-day histological specimens. This degradation, however, was not spatially uniform because polymer fibers were rare at the construct periphery, but were common towards the center of the construct. Interestingly, a fibrous capsule at the periphery of 28-day constructs was not observed when the FBS concentration was equal to or less than 0.2%, whereas the 2% FBS + ITS and the 10% FBS constructs had a solid fibrous capsule with an average thickness of 74.54 μm and 80.84 μm, respectively (Table 3.2).

3.3.2.6 Equilibrium Modulus

At the end of the 4-week cultivation, the serum-free constructs (4.94 ± 1.30 kPa) were mechanically compromised in comparison with the constructs nourished with FBS (^$p < 0.05$). The 2% FBS + ITS (40.43 ± 7.04 kPa) and the 10% FBS (45.43 ± 5.43 kPa) groups demonstrated a comparable level of equilibrium moduli while both the constructs were mechanically stronger than the 0.2% FBS + ITS constructs (19.74 ± 7.09 kPa) (*$p < 0.05$).

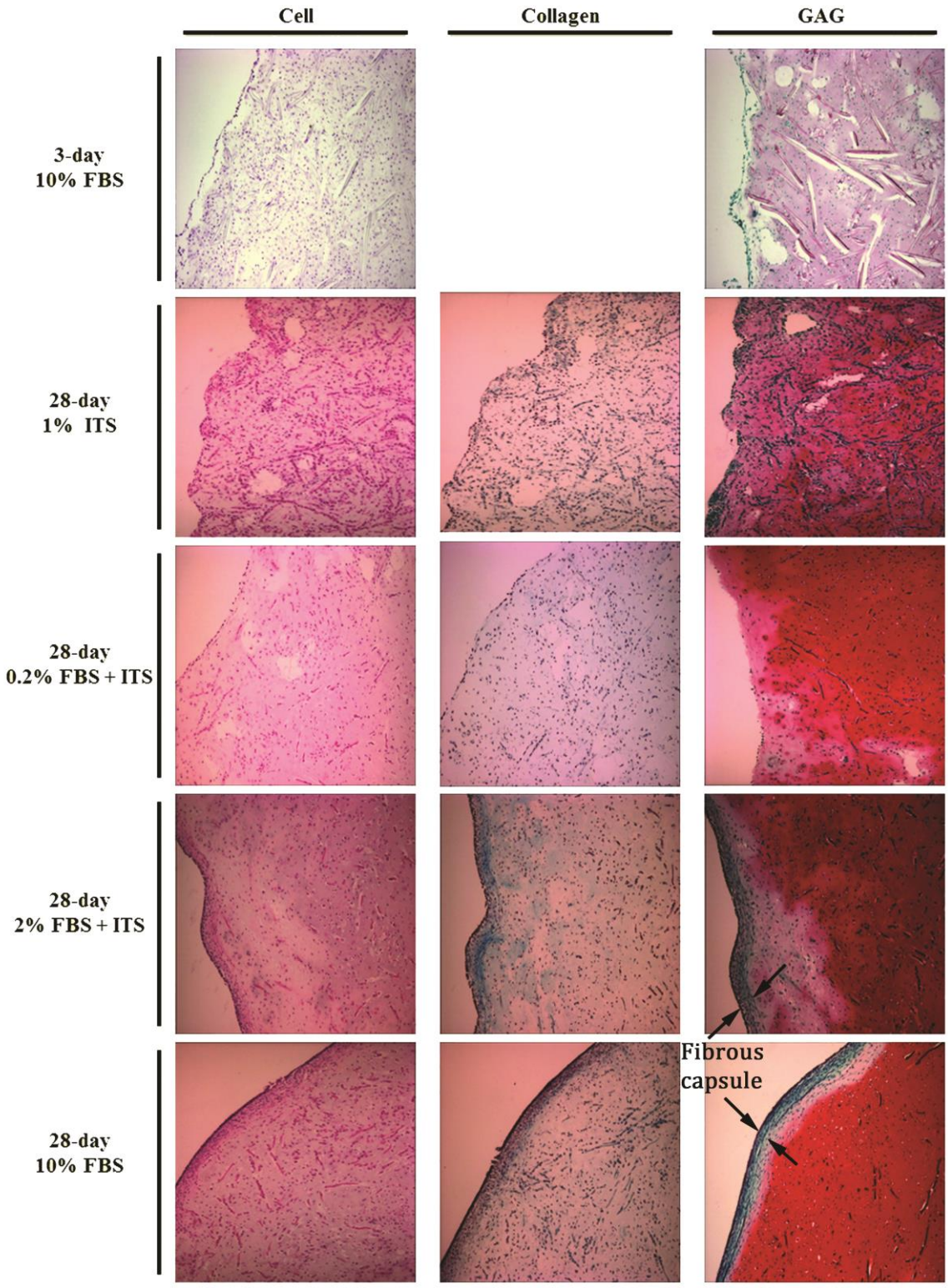
Cell
Collagen
GAG
3-day
10% FBS
28-day
1% ITS
28-day
0.2% FBS + ITS
28-day
2% FBS + ITS
28-day
10% FBS
Fibrous
capsule

Figure 3.8 Light microscopy images of 3-day (1st row) and 28-day (2nd - 5th rows) hydrodynamic constructs taken at 10X magnification. Hematoxylin and eosin staining (left column): cell nuclei are blue-purple; Masson's trichrome staining (middle column): collagen fibrils are blue and nuclei are black; safranin-O and fast green staining (right column): GAG, nuclei and cytoplasm are stained pink/red, black and green, respectively. The tubular structures are remaining PGA fibers. More intense ECM staining was achieved in the serum-containing groups. A solid fibrous capsule was only observed at the periphery of the 2% FBS + ITS and the 10% FBS constructs.

Table 3.2 Capsule Thickness and Equilibrium Compressive Modulus of 28-Day Hydrodynamic Constructs

Culture Condition	1% ITS	0.2% FBS + ITS	2% FBS + ITS	10% FBS
Capsule Thickness (μm)	ND	ND	74.54 ± 5.93	80.84 ± 8.17†
Equilibrium Modulus (kPa)	4.94 ± 1.30^	19.74 ± 7.09	40.43 ± 7.04*	45.43 ± 5.43*

- Capsule thickness: †statistical significance versus the 2% FBS + ITS group; $p < 0.01$; n = 20. ND: non-detectable.
- Equilibrium modulus: ^significant decrease versus the other groups; *significance increase versus the 0.2 % FBS + ITS group; $p < 0.05$; n = 6.

3.4 Discussion

Our long-term objective is to acquire a broader understanding of the complex interplay between fluid shear stress and soluble biochemical factors in neocartilage development and capsule formation. To this end, we first focused on the serum effects in the present study. Chondrocyte-seeded PGA scaffolds were cultivated with media supplemented with various low-serum contents (0%, 0.2% or 2% FBS) plus 1% ITS or with typical high-serum concentration (10% FBS) in the presence or absence of turbulent flow-induced shear forces generated within the WWB system that provides a defined

hydrodynamic environment (Bilgen, Chang-Mateu et al. 2005; Bilgen, Sucosky et al. 2006; Bilgen and Barabino 2007). In agreement with the previous reports (Fitzsimmons, Sanyal et al. 2004; Kisiday, Jin et al. 2004; Chua, Aminuddin et al. 2005; Kisiday, Kurz et al. 2005; Bian, Lima et al. 2008; Kelly, Fisher et al. 2008), our data reveal that constructs stimulated by ITS-supplemented serum-free or low-serum culture media possessed biochemical properties exactly like those of the high-serum constructs in a 4-week static cultivation process (Figure 3.2). This evidence suggests that ITS is a potential substitute for FBS in the static chondrocyte/PGA culture system and that serum is not a requirement. In general, the properties of static constructs paled in comparison with those of hydrodynamic constructs.

In contrast to static cultivation, we found that ITS alone was not sufficient for hydrodynamic development of neocartilage (Figures 3.5, 3.6 and 3.7). Our observation that hydrodynamic constructs cultured with ITS-supplemented low-serum media had similar biochemical properties to the high-serum constructs implies that some critical constituents in serum are sensitive to fluid shear stress and thus promote shear-stimuli-induced cell proliferation and ECM production. Our results also suggest that the presence of these shear-sensitive components is required to support hydrodynamic cultivation of tissue-engineered cartilage. Shear-sensitive soluble molecules associated with chondrocyte activities include TGF-β (Ohno, Cooke et al. 1995; Negishi, Lu et al. 2001; Malaviya and Nerem 2002), IGF-I (Jin, Emkey et al. 2003), IL-6 (Mohtai, Gupta et al. 1996) and matrix metalloproteinase (MMPs) (Yokota, Goldring et al. 2003).

When stimulated by fluid shear stress, the 2% FBS + ITS constructs exhibited biochemical (Figures 3.5, 3.6 and 3.7) and mechanical (Table 3.2) properties comparable

to those of the high-serum engineered tissues. This is in agreement with a previous study carried out by Kelly et al., where dynamic compressive loading was applied to chondrocyte-laden agarose gels grown under low-serum conditions (Kelly, Fisher et al. 2008). Both studies suggest that, under mechanical loading, the biochemical stimuli in the 2% FBS + ITS group are not compromised relative to the high-serum condition. Similarly, the 0.2% FBS + ITS hydrodynamic constructs demonstrated total collagen (Figure 3.6) and GAG (Figure 3.7) contents that were close to 79% and 78% of the corresponding high-serum levels. From the standpoint of eliminating or minimizing the deleterious effects introduced by serum on *in-vitro* generation of tissue substitutes, the 0.2% FBS + ITS formula would yield a more reliable culture environment than the 2% FBS + ITS combination. Yet, the 2% FBS + ITS culture medium may be preferred due to the significantly superior mechanical strength (Table 3.2) of the construct grown under this specific condition. To further elucidate the requirement for ITS in the low-serum hydrodynamic cultivation of tissue-engineered cartilage, a follow-up experiment was conducted, in which chondrocyte-seeded scaffolds were cultivated with 1% ITS, 2% FBS or 2% FBS + ITS. The results (Figure 3.9) indicate that the properties of hydrodynamic constructs decreased when ITS was removed from culture media, suggesting that ITS is an essential supplement in the 2% FBS + ITS recipe in order to support WWB cultivation of neocartilage. In addition, the evidence that a fibrous capsule remained in the 2% FBS constructs (Figure 3.10) suggests that FBS rather than ITS plays a more predominant role in the capsule formation.

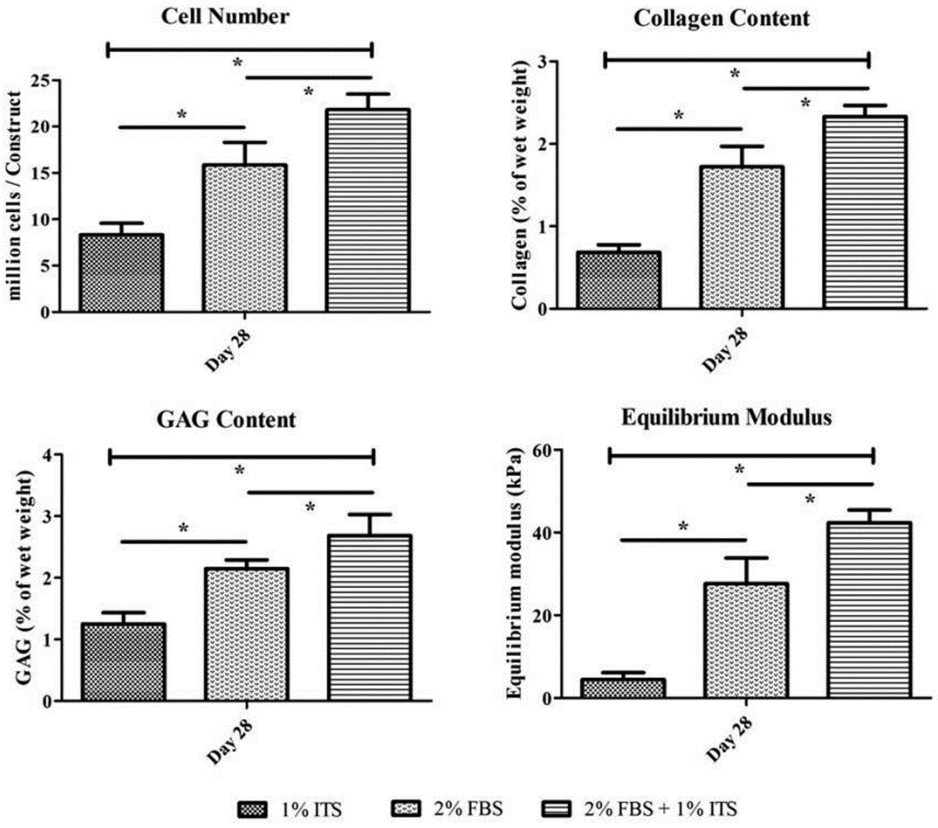

Figure 3.9 Biochemical and mechanical properties of 28-day hydrodynamic constructs cultivated with 1% ITS, 2% FBS or 2% FBS + 1% ITS. *indicates significant difference between the groups; $p < 0.05$; n = 6.

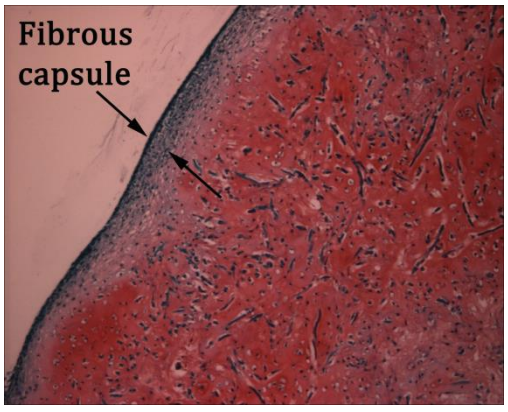

Figure 3.10 Safranin-O and fast green staining of 28-day hydrodynamic constructs cultivated with 2% FBS in the absence of ITS (10X magnification).

Our data also reveal that, at days 3 and 14, the wet weight of hydrodynamic constructs remained similar in serum-free, low-serum and high-serum groups whereas the dry weight of the serum-free constructs decreased drastically when compared with the serum-containing groups (Figure 3.4). This reduction in dry weight was likely due to the rapid degradation of and/or shear-induced damage to PGA scaffolds since the total dry weight of a construct is the sum of cell, ECM and PGA contents and similar biochemical compositions were detected in all the groups at day 3 and in the serum-free and the 0.2% FBS + ITS constructs at day 14. We recognize that this PGA degradation may be mainly attributed to hydrolysis (Agrawal, Athanasiou et al. 1997) instead of other variables such as material porosity and permeability, temperature and loading (Agrawal, Mckinney et al. 2000) because a significant increase in the water content of the serum-free constructs was determined in the first two weeks of the cultivation, which possibly accelerated PGA degradation. However, it is difficult to validate this degradation process using the WWB since a scaffold is anchored in the bioreactor by a stainless steel needle and a 3-mm silicone spacer. As polymers degrade with time, the scaffold becomes fragile and can easily separate from the needle. It is also noteworthy that both wet and dry weights of the serum-free constructs were significantly lower than those of the serum-containing groups at the end of the cultivation, which may result from the combined effects of early and rapid PGA degradation, poor cell proliferation and insufficient ECM deposition.

In both static (Figure 3.3) and hydrodynamic (Figure 3.8) studies, a fibrous capsule was not induced when engineered tissues were cultured with the FBS concentration equal to or less than 0.2%. This outcome agrees with other reports in the literature, in which different chondrocyte/hydrogel systems were tested (Kisiday, Jin et al.

2002; Kisiday, Kurz et al. 2005; Kelly, Fisher et al. 2008), and suggests that the formation of a fibrous cell outgrowth can be reduced by decreasing the serum content in culture. A basic mechanism that accounts for the capsule formation is the direct contact of chondrocytes at the construct periphery with sufficient amounts of certain serum constituents that induce and facilitate fibrosis, such as TGF-β and PDGF (Ignotz and Massagué 1986; Lohmann, Schwartz et al. 2000; Kelly, Fisher et al. 2008). As a result, the drastic reduction in capsule formation/thickness when the FBS concentration decreased from 2% to 0.2% or lower suggests that concentrations of these fibrosis-promoting molecules did not reach the level required for induction of a capsule.

A fibrous capsule is more significant in hydrodynamic constructs than in those cultivated under loading-free or dynamic compressive loading conditions (Vunjak-Novakovic, Martin et al. 1999; Kelly, Fisher et al. 2008). As indicated in Chapter 1, this observation can result from the direct exposure of articular chondrocytes to continuous fluid flow, which own a flattened, elongated cell shape and thereby demonstrate a fibroblast-like phenotype (Vunjak-Novakovic, Freed et al. 1996). Another possible explanation is that some of the fibrosis-promoting soluble factors are also sensitive to fluid shear stress, such as TGF-β (Ignotz and Massagué 1986; Malaviya and Nerem 2002), and thus further facilitate the capsule formation in hydrodynamic cultivation of tissue-engineered cartilage. Additional studies on identification of such molecules and on how these factors modulate capsule formation and development are necessary. Taken together, our results suggest that the serum content can function as a switch to initiate the process of the formation of a fibrous capsule while hydrodynamic forces promote its development. Furthermore, although it has been suggested that the removal of this type I collagen-

based fibrous capsule may be preferred in order to eliminate the interference induced in biochemical assays due to a nonchondrocytic phenotype (Kisiday, Kurz et al. 2005), a similar fibrous layer was observed in both *in-vivo* (Fujisato, Sajiki et al. 1996) and *in-vitro* (Vinardell, Thorpe et al. 2009) cartilage repair models. This evidence implies that the fibrous capsule may enhance the integration of native and engineered cartilage tissues.

Successful tissue engineering strategies must produce tissue replacements that meet the requirements for clinical implantation with respect to their biological, mechanical and functional compatibilities with host native tissues. Engineered constructs derived from static cultures only exhibit limited potential to satisfy such criteria due to the compromised mechanical and biochemical properties, which makes them unsuitable tissue substitutes (Bilodeau and Mantovani 2006). The application of turbulent flow-induced hydrodynamic forces that is aimed to improve mass transport mechanisms of nutrients and waste and simultaneously to deliver mechanical stimuli provides an alternative approach to the cultivation of three-dimensional cell-biomaterial complexes (Freed and Vunjak-Novakovic 1995; Vunjak-Novakovic, Martin et al. 1999; Bilgen, Chang-Mateu et al. 2005). However, hurdles attributed to culture media containing high concentrations of unreliable serum constituents remain unsolved in hydrodynamic cultivation of tissue-engineered cartilage. In addition, the combined effects of serum and continuous fluid shear stress on the formation of a fibrous capsule that is commonly present in hydrodynamically engineered cartialge have not been thoroughly addressed. Therefore, in the current study, we replaced FBS partially or completely with ITS to investigate the serum effects on neocartilage development and capsule formation in the presence or absence of fluid shear stress induced within the WWB.

One of our major findings indicates that, other than insulin, transferrin, and selenium, a minimal content of serum is required to support hydrodynamic cultivation of neocartilage in order to produce engineered constructs morphologically, compositionally and mechanically comparable to the traditional high-serum constructs. The neocartilage development supported by the low-serum culture medium may result from the presence of shear-sensitive soluble molecules in serum whose expression is up-regulated by fluid shear stress and in turn enhances cellular functions and tissue growth. Conversely, under the serum-free condition, the removal of these shear-sensitive cues from the culture system leads to inferior development of hydrodynamic cartilage constructs. This evidence implies that cultured constructs may not benefit from continuous fluid shear stress in the absence of shear-sensitive soluble molecules and thereby improved tissue quality cannot be achieved. It has been suggested by Malaviya et al. that such regulatory mechanism is not solely mediated by a single factor, but by the synergy between all the shear-sensitive cues (Malaviya and Nerem 2002). Furthermore, our results also demonstrate that the formation of a solid fibrous capsule requires not only sufficient fibrosis-promoting soluble molecules but also hydrodynamic forces. Specifically, the process of the capsule formation can be activated by certain soluble factors present in the culture environment and further promoted by fluid shear stress. Additional studies are necessary to determine the soluble biomolecules that are sensitive to fluid shear stress and are involved in the fibrosis of neocartilage and to understand how they modulate tissue properties and morphology of engineered constructs. In conclusion, this chapter substantiates the importance of shear-sensitive signals derived from serum constituents in hydrodynamic

cultivation of tissue-engineered cartilage and identifies potential mechanisms that contribute to the capsule formation.

CHAPTER 4

IMPROVED BIOCHEMICAL AND MECHANICAL PROPERTIES AND DIFFERENTIAL TISSUE MORPHOLOGY OF ENGINEERED CARTILAGE IN HYDRODYNAMIC CULTIVATION WITH TRANSIENT EXPOSURE TO INSULIN-LIKE GROWTH FACTOR-1 AND TRANSFORMING GROWTH FACTOR-β1[††]

4.1 Introduction

Arthritis, a form of musculoskeletal disorders which involves joint inflammation and cartilage breakdown, affects 50 million Americans, resulting in costs of $128 billion annually (Cheng, Hootman et al. 2010). Articular cartilage is a lubricant substrate that serves as a cushion between the bones of diarthrodial joints, but only has a limited ability for self-healing due to its avascular nature. Tissue engineering is a promising technique for restoration of small cartilage defects, which typically involves cultivation of chondrocytes or mesenchymal progenitor cells on three-dimensional biodegradable scaffolds or hydrogels within bioreactor systems that provide chemically and mechanically controllable environmental conditions (Darling and Athanasiou 2003). In order to be clinically relevant, tissue-engineered cartilage must meet specific functional criteria related to their mechanical properties, biochemical composition, tissue ultrastructure, immunological compatibility and integration capability. However, all of

[††]Adapted and modified from Yang, Y.-H. and Barabino, G.A. (*in press*) Differential Morphology and Homogeneity of Tissue-Engineered Cartilage in Hydrodynamic Cultivation with Transient Exposure to Insulin-Like Growth Factor-1 and Transforming Growth Factor-β1. *Tissue Engineering Part A.*

these properties of engineered cartilage constructs are still inferior to those of native tissues.

In-vivo development of avascular cartilage tissues largely relies on the movement of the interstitial fluid which is created by joint deformation during walking or exercise. This fluid movement generates protein or ion flux in and out of cartilage and thus initiates the exchange of trophic and waste substances between the tissue and the surrounding synovial fluid. Garcia et al. demonstrated that mass transfer of proteins and enzymes such as MMP-1 within articular cartilage could be improved by convection when the interstitial fluid flowed at a velocity of 1 μm/s that usually occurs at normal walking frequencies (Garcia, Frank et al. 1996; Garcia, Lark et al. 1998). *Ex vivo*, tissue engineering strategies have utilized agitation of medium fluid to enhance the efficiency of nutrient delivery to and waste removal from cultured cells. Specifically, laminar flow can be generated by perfusion systems (Dunkelman, Zimber et al. 1995; Pazzano, Mercier et al. 2000) and rotating vessel reactors (Vunjak-Novakovic, Martin et al. 1999; Martin, Obradovic et al. 2000; Emin, Koç et al. 2008) while turbulent flow agitation can be established within mechanically stirred bioreactors such as the spinner flask (Vunjak-Novakovic, Freed et al. 1996; Vunjak-Novakovic, Obradovic et al. 1998; Gooch, Blunk et al. 2001) and the WWB (Bueno, Bilgen et al. 2004; Bueno, Laevsky et al. 2007; Bueno, Bilgen et al. 2008).

Growth factors and cytokines are required to support cell growth and tissue development in both natural and culture environments. However, Gooch and coworkers found that treatment with exogenous IGF-1, a shear-sensitive factor (Jin, Emkey et al. 2003; Lau, Kapur et al. 2006), could improve tissue properties of chondrocyte-seeded

PGA scaffolds when they were cultivated within a rotating vessel bioreactor, but not in the spinner flask (Gooch, Blunk et al. 2001). The exact mechanisms that contribute to this finding are still unclear, yet it may be attributed to the complex interplay between shear-sensitive soluble molecules and shear-related parameters such as flow profile and magnitude of shear stress. Other possibilities including scaffold properties, such as porosity, and cell seeding density also need to be considered. Moreover, Gooch's experiments employed a high-serum (10%) content which contains endogenous growth factors, antibodies and binding proteins that may interfere with the function of exogenous growth factors added to the culture systems (Friedrich, Haring et al. 2009). When these biochemical components are exposed to a hydrodynamic environment like that in the Gooch study, it may result in an even more complicated situation. To address this issue, we recently developed a low-serum (2%) ITS-supplemented culture medium for the WWB cultivation of tissue-engineered cartilage and found that the cultivated neocartilage constructs were morphologically, compositionally and mechanically similar to the traditional high-serum constructs (Chapter 3).

Transient supplementation of exogenous growth factors has recently been utilized to facilitate chondrogenesis of chondrocyte- (Lima, Bian et al. 2007; Byers, Mauck et al. 2008) or MSC-laden (Huang, Stein et al. 2009; Kim, Erickson et al. 2012) hydrogels under loading-free or dynamically compressive conditions. In these studies, cell-encapsulated agarose or hyaluronic acid gels transiently exposed to TGF-β3 demonstrated increased cartilage tissue properties relative to those continuously nourished with TGF-β3. As Byers et al. suggested, it may be that cultured cells require substantial time of approximately 2 weeks to adapt themselves to signaling cascades resulting from growth

factor removal from the surroundings before exhibiting stronger potential for ECM synthesis (Byers, Mauck et al. 2008). Yet, this beneficial effect has not been validated in hydrodynamic cultivation of engineered cartilage constructs. To extend our knowledge, the objective of the present study was to evaluate the feasibility of transient exposure of tissue-engineered cartilage to growth factors under continuous fluid shear stress induced within the WWB. Our central hypothesis was that hydrodynamic constructs continuously nourished with exogenous growth factors do not necessarily exhibit improved tissue properties over constructs transiently treated with the same bioactive molecules. We chose IGF-1 and TGF-β1, two of the key stimulating agents in cartilage development, as our model molecules. For each molecule, a minimal concentration was selected from their most commonly reported ranges of effective doses for neocartilage cultivation (IGF-1: 100-300 ng/mL; TGF-β1: 10-30 ng/mL (Blunk, Sieminski et al. 2002; Pei, Seidel et al. 2002; Mauck, Nicoll et al. 2003)). By quantifying the amount of growth factors remaining in waste culture media and the level of expression of the corresponding surface receptors by cultured cells, we explored a possible mechanism that accounts for the "transient" phenomenon. Between the two exogenous growth factors employed in the current study, TGF-β1 is a fibrosis-promoting factor (Ignotz and Massagué 1986; Kelly, Fisher et al. 2008; Dobaczewski, Bujak et al. 2010; Meng, Huang et al. 2010; Fragiadaki, Ikeda et al. 2011) whereas IGF-1 has not been found to necessarily participate in fibrotic processes. We further hypothesized that engineered constructs nourished with exogenous TGF-β1 form a thicker fibrous capsule in comparison with the untreated ones.

4.2 Materials and Methods

4.2.1 Materials

Unless specified otherwise, reagents were purchased from VWR (West Chester, PA), Sigma (St. Louis, MO), Thermo Fisher Scientific (Waltham, MA) or Life Technologies (Grand Island, NY).

4.2.2 Bioreactor and Scaffold Preparation

Conventional spinner flasks were purchased from Bellco Glass, Inc. (Vineland, NJ) and sent to G. Finkenbeiner, Inc. (Waltham, MA) for WWB fabrication based on the configuration described in Chapter 2.3.2.5. Prior to each experiment, the interiors of bioreactors, needles, and stir bars were treated with Sigmacote® to prevent cell adherence. After evaporation of Sigmacote®, the assembled bioreactors were washed gently, air-dried and steam-sterilized.

PGA discs (Biomedical Structures, Warwick, RI) (Ø10 mm x 2 mm thick, 85 mg/mL bulk density, 97% void volume) were sterilized by a series of rinses in sterile 70% ethanol and deionized water, followed by a 30-minute exposure to ultraviolet light. Two of the sterilized PGA discs were threaded onto each of the 21 gauge needles and separated by a silicone spacer, resulting in totally eight scaffolds per bioreactor. The WWBs were then filled with 120-mL hgDMEM and allowed to stabilize overnight with a stir bar spinning at 50 rpm inside a humidified, 37°C, 5% CO_2 incubator.

4.2.3 Cell Isolation, Cell Seeding and Tissue Culture

Articular chondrocytes were isolated from femoropatellar grooves of freshly slaughtered 2-week-old calves (Research 87, Marlborough, MA) by digestion with type II collagenase as previously described (Freed, Marquis et al. 1993). Prior to each experiment, primary chondrocytes harvested from three donors were pooled together. Cell number and viability (> 85%) were determined using a trypan blue exclusion assay. A small aliquot of cells in suspension was added to each of the sterilized WWBs at a density of 5 million live cells per scaffold. The cell seeding process was carried out in the basal medium (BM) and allowed to proceed for 4 days under fluid agitation (50 rpm) until 95% of the cells achieved attachment (Figure 4.1). The BM was defined as the low-serum ITS-supplemented (2% FBS + ITS) culture medium developed in Chapter 3 and was composed of hgDMEM, 2% FBS, 1% ITS, 100 U/mL penicillin/streptomycin, 10 mM HEPES, 0.4 mM L-proline, 0.1 mM NEAA, 3.6 mg/mL sodium bicarbonate, 2.5 µg/mL fungizone and 50 µg/mL ascorbic acid.

At the end of the seeding process, media were completely replaced with fresh BM. This point was considered as day zero. Chondrocyte/PGA complexes were then cultured in the WWBs agitated at 50 rpm for 28 days and media were completely renewed every 3 days thereafter. In the groups nourished with exogenous growth factors, 100 ng/mL IGF-1 or 10 ng/mL TGF-β1 (recombinant human proteins, R&D Systems, Minneapolis, MN) was added to fresh BM during medium exchanges either for the first 15 days of the culture (transient) or throughout the entire 4-week cultivation (continuous). Bioreactors were collected at designated time points (Figure 4.1) and engineered tissues were

harvested for evaluation. For the Smad study, constructs were also cultivated in the WWBs without fluid agitation (static).

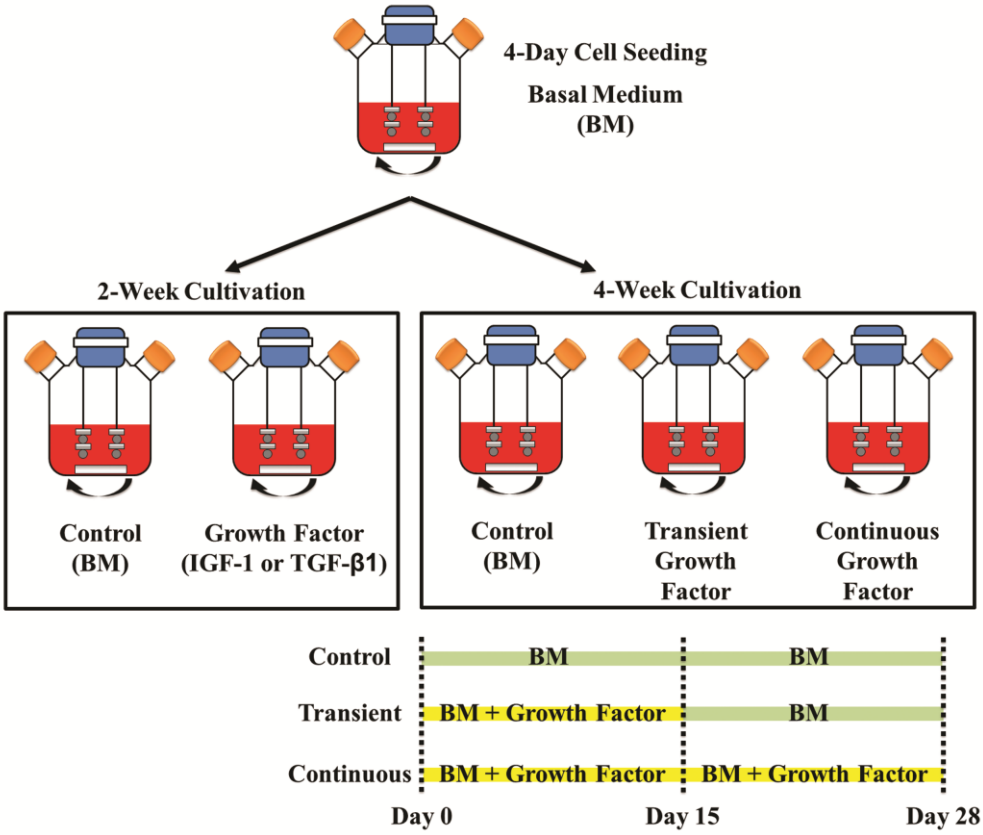

Figure 4.1 Schematic overview of the experimental design. The 4-day cell seeding process was carried out in the basal medium (BM). Chondrocyte-seeded constructs were nourished with IGF-1 or TGF-β1 and cultivated in the WWBs for 4 weeks. For transiently treated constructs, growth factor supplementation was discontinued at day 15 and culture media were switched to the BM for the rest of the cultivation. Bioreactors were collected at either day 14 or day 28.

4.2.4 Biomechanics

Equilibrium compressive moduli of constructs were determined using an unconfined compression test. During examination, a preload of 0.01 N was applied to

samples until equilibrium was achieved. A stress relaxation test was carried out at strains of 5, 10, 15, 20 and 25%, after which samples were allowed to equilibrate. Equilibrium moduli were obtained from the slope of the plot of equilibrium force normalized to the cross-sectional area of the construct versus the strains.

4.2.5 Biochemistry

Prior to the biochemical assays, constructs were weighed (wet weight), frozen, lyophilized and then digested with papain enzyme. DNA weights were quantified using a PicoGreen dsDNA kit and the manufacturer's instructions were followed. Cell numbers were calculated by assuming 7.7 pg of DNA per chondrocyte (Kim, Sah et al. 1988). Sulfated GAG contents were assessed using a DMMB dye-binding assay (Farndale, Buttle et al. 1986). Chondroitin sulfate was used to create a standard curve and a chondroitin sulfate-to-GAG ratio of 1 was assumed. Total collagen amounts were determined using an orthohydroxyproline colorimetric assay, assuming a 1:10 orthohydroxyproline-to-collagen ratio (Woessner 1961). GAG and total collagen contents are presented in values normalized to the wet weight of constructs.

4.2.6 Enzyme-Linked Immunosorbent Assay (ELISA)

Concentrations of IGF-1 and active TGF-β1 in waste media and levels of IGF-1 receptor (IGF-1R) and TGF-β receptor type II (TGF-βRII) in engineered tissues were quantified using DuoSet Enzyme-Linked Immunosorbent Assay Developmental kits (R&D Systems) and the manufacturer's instructions were followed. For detection of IGF-1R and TGF-βRII, one half of each of harvested constructs was lysed and homogenized

in 1% Triton X-100 lysis buffer plus protease inhibitor cocktails, followed by a 15-minute centrifugation at 10,000 × g at 4˚C. The supernatant was collected for ELISA and IGF-1R and TGF-βRII contents were estimated with recombinant human proteins, given the 97% and 91% similarity of amino acid sequence for IGF-1R and TGF-βRII, respectively. The other half was assessed to obtain the DNA amount. Data are presented in values normalized to the corresponding DNA weight.

4.2.7 Western Blot

Proteins were isolated as described in the previous section on ELISA and total protein concentration was determined using a BCA Protein Assay kit. Equal amounts of proteins were electrophoresed on 10% polyacrylamide gels (Bio-Rad, Hercules, CA) and transferred to nitrocellulose membranes. The membranes were then incubated with blocking buffer for 1 hour and purified rabbit antibodies against phospho-Smad2 (pSmad2), phospho-Smad3 (pSmad3) or Smad7 (1:1000) overnight. After several washes, the membranes were treated with IRDye 800CW secondary antibodies (1:5000, Li-Cor, Lincoln, NE) for 1 hour. Images were visualized using an infrared scanner (Odyssey, Li-Cor).

4.2.8 Histology and Immunohistochemistry

Constructs were fixed, embedded in paraffin and sectioned in 5-μm thick slices. The slices were deparaffinized and stained for GAG and collagen using safranin-O/fast green and Masson's trichrome methods, respectively.

IGF-1R and TGF-βRII molecules were stained immunohistochemically. Briefly, deparaffinized sections were incubated with citrate buffer heated to 99°C for 25 minutes to retrieve antigens, followed by a 20-minute cooling at room temperature. The samples were then incubated with 0.3% hydrogen peroxide for 30 minutes, blocking buffer for 20 minutes, and primary rabbit anti-bovine antibodies (1:1500, Abcam, Cambridge, MA) overnight. Finally, the sections were treated with biotinylated secondary antibodies (1:200, Vector Labs, Burlingame, CA) for 30 minutes and streptavidin-conjugated horseradish-peroxidase complex (Vector Labs) for another 30 minutes, followed by the incubation with diaminobenzidine chromogen reagent until optimal staining was developed. Samples incubated with normal rabbit serum substituted for primary antibodies were used as negative controls and no non-specific staining was observed. Color images were captured under a light microscope (Nikon Eclipse Ti, Japan).

4.2.9 Measurement of Capsule Thickness

For image analysis, twenty safranin-O and fast green histological images captured at 10X magnification were collected from each group (six constructs) in order to quantify the thickness of a fibrous capsule. The images were converted to grayscale using the RGB split function in ImageJ software (NIH), followed by background subtraction and threshold selection. Irrelevant artifacts were then removed and the processed images were sent to NIS-Elements AR 3.0 software (Nikon) for image analysis (0.49 μm / pixel). The average thickness of a capsule was calculated by normalizing the area of the capsule to its length averaged from the two long sides.

4.2.10 Statistical Analyses

Statistical data were obtained from experiments repeated three times with two to three replicates per group per time point per experiment and are presented as means ± one standard deviation. Statistical analyses were performed by one-way or two-way ANOVA in conjunction with the Bonferroni post test for multiple comparisons with significance at a p value of less than 0.05.

4.3 Results

4.3.1 Tissue Properties and Morphology

When stimulated by IGF-1 (Figure 4.2) or TGF-β1 (Figure 4.3), 14-day constructs exhibited increased cell proliferation, GAG and collagen deposition and mechanical strength in comparison with the untreated ones ($*p < 0.05$). Specifically, relative to the control group, the properties of the engineered tissues treated with either growth factor were improved by at least 29% in cell number, 47% in GAG content, 24% in collagen content and 34% in equilibrium modulus.

At day 28, although treatment with exogenous growth factors did not necessarily result in a higher cell content, the nourished groups yielded engineered tissues biochemically and mechanically stronger than those in the control group while transient exposure to growth factors further enhanced construct properties in both the IGF-1 (Figure 4.2) and the TGF-β1 (Figure 4.3) cases ($*p < 0.05$). Specifically, the transient IGF-1 constructs had predominant collagen (3.66 ± 0.20% of wet weigh vs. 2.52 ± 0.19% [control] and 2.80 ± 0.18% [continuous]) and GAG (4.21 ± 0.11% of wet weight vs. 2.43 ± 0.25% [control] and 2.83 ± 0.21% [continuous]) accumulation and equilibrium moduli

(87.82 ± 8.48 kPa vs. 39.43 ± 7.63 kPa [control] and 52.73 ± 3.36 kPa [continuous]). Similar trends were recognized in the TGF-β1 experiments in which the highest biochemical contents (4.30 ± 0.13% of wet weight in collagen and 3.67 ± 0.15% of wet weight in GAG) and mechanical stiffness (136.43 ± 29.99 kPa) were detected in the transient group though GAG contents of the transient and the continuous TGF-β1 constructs were not statistically different. However, the difference in tissue quality between the transient and the continuous TGF-β1 groups largely decreased relative to the IGF-1 groups.

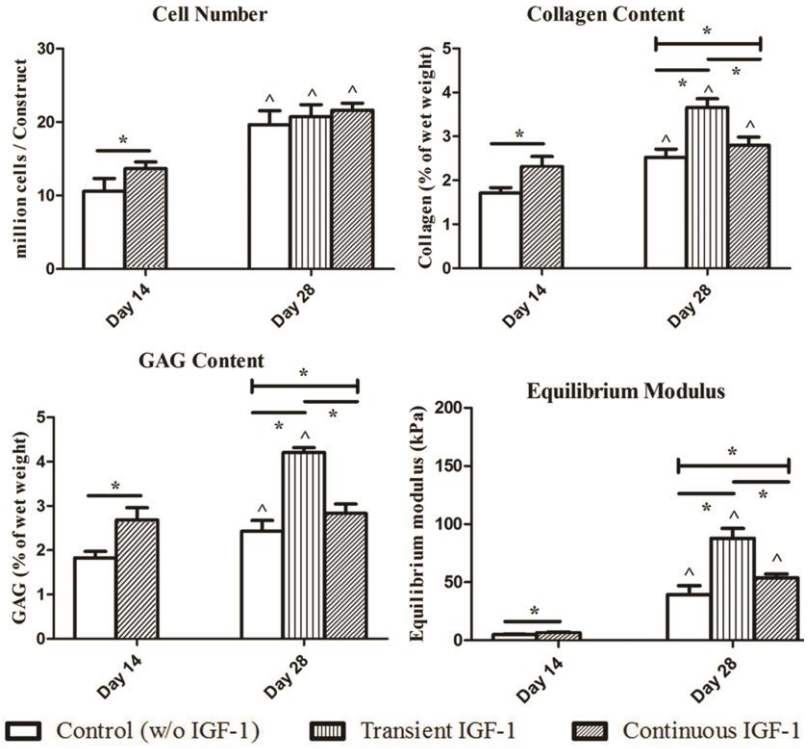

Figure 4.2 Cell number, total collagen content, GAG content and equilibrium compressive modulus of hydrodynamic constructs in the IGF-1 study. ^represents significant difference from the corresponding 14-day value; *indicates statistical significance between the groups; $p < 0.05$; n = 7.

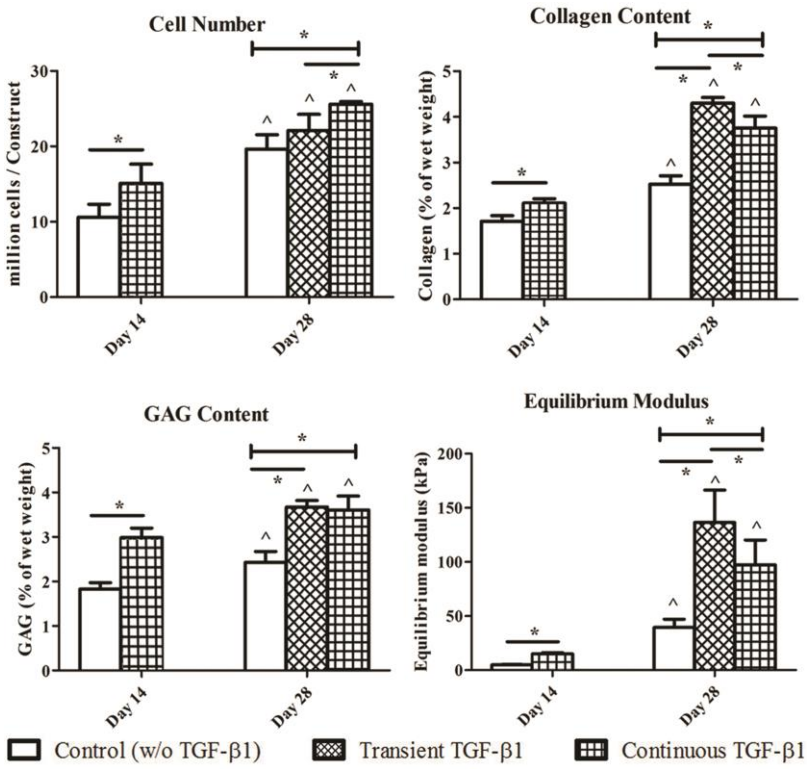

Figure 4.3 Cell number, total collagen content, GAG content and equilibrium compressive modulus of hydrodynamic constructs in the TGF-β1 study. ^represents significant difference from the corresponding 14-day value; *indicates statistical significance between the groups; $p < 0.05$; n = 7.

At the end of the cultivation, a fibrous capsule which is usually characterized by increased cell density and decreased (virtually none) GAG deposition and consists mainly of type I collagen (Vunjak-Novakovic, Freed et al. 1996; Kisiday, Kurz et al. 2005; Bueno, Bilgen et al. 2008; Kelly, Fisher et al. 2008) was observed at the periphery of both the control and the IGF-1 constructs (Figure 4.4), and a similar thickness of the capsule was measured in these groups (Table 4.1). Conversely, exposure to TGF-β1 eliminated the capsule formation regardless of the duration of the supplementation.

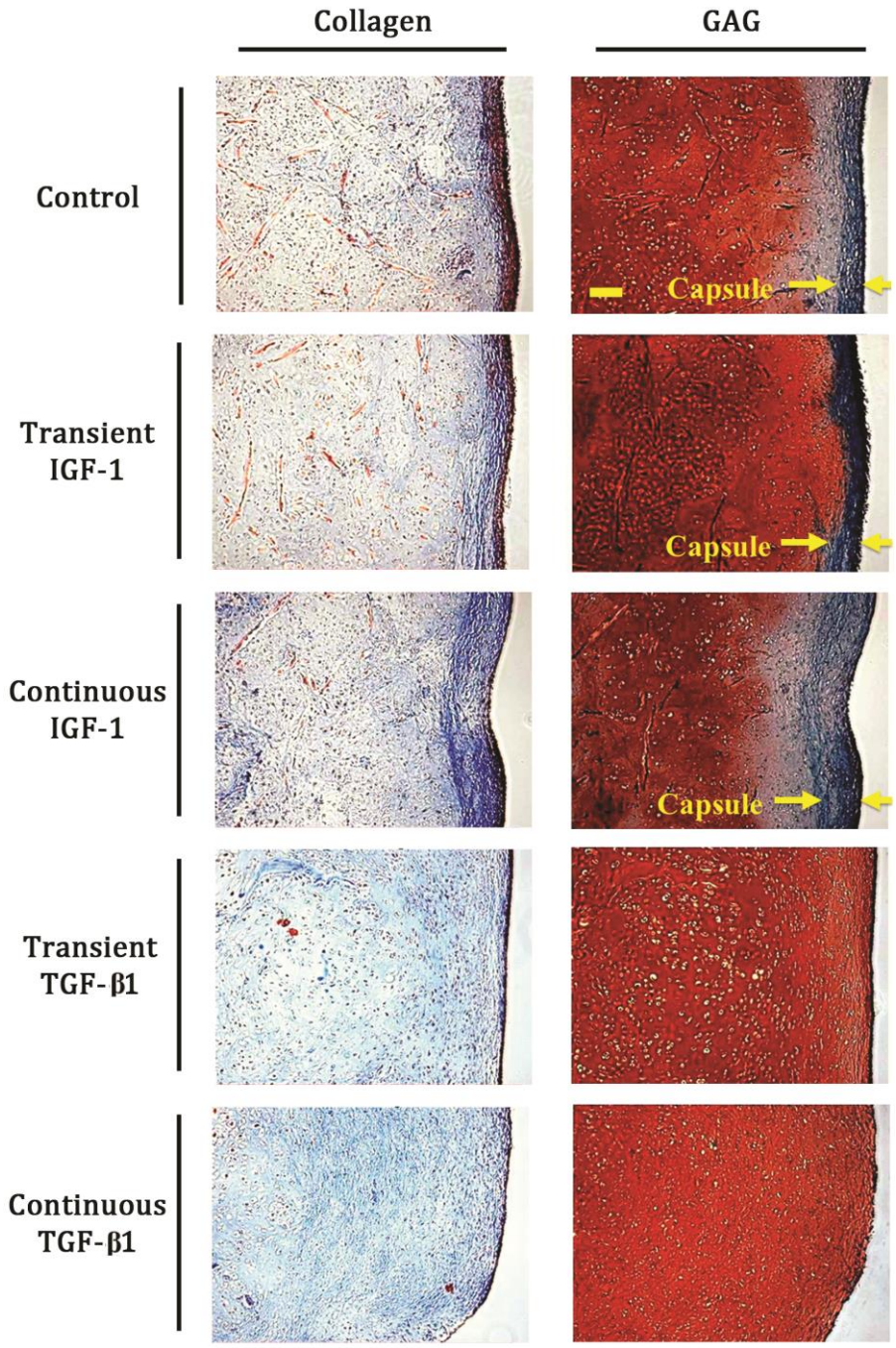

Figure 4.4 Histological images of 28-day hydrodynamic constructs taken at 10X magnification. Left column: collagen is stained blue. Right column: GAG and cytoplasm are stained red and green, respectively. Arrows indicate the structure of the fibrous capsule which only appeared at the periphery of the control and the IGF-1 hydrodynamic constructs. Scale bar = 100 μm.

Table 4.1 Capsule Thickness of 28-Day Hydrodynamic Constructs

Culture Condition	Control (w/o growth factors)	Transient IGF-1	Continuous IGF-1	Transient TGF-β1	Continuous TGF-β1
Capsule Thickness (μm)	78.28 ± 8.56	80.32 ± 10.33	90.39 ± 24.60	ND	ND

n = 20. ND: non-detectable.

4.3.2 IGF-1 and TGF-β1 in Waste Culture Media

IGF-1 or active TGF-β1 levels in waste media were quantified every 3 days to obtain the uptake/release curves of each molecule. The IGF-1 concentration (Figure 4.5A, left) in the continuous IGF-1 group rose over time and reached a steady-state level after 21 days in culture, whereas the TGF-β1 level (Figure 4.5B, left) in the continuous TGF-β1 group gradually decreased in the first two weeks of the cultivation then began to rise at day 18 and continuously increased thereafter. At day 27, the IGF-1 and TGF-β1 concentrations detected in the corresponding continuous groups were 120.68 ± 2.00 ng/mL and 14.90 ± 0.65 ng/mL, respectively. Conversely, the growth factor levels in both the transient groups remained relatively low and constant after two weeks in culture ($^{\&}p < 0.05$). The final IGF-1 and TGF-β1 concentrations measured in the corresponding transient groups at day 27 were 3.57 ± 3.49 ng/mL and 2.74 ± 1.93 ng/mL, respectively. The control group showed extremely low concentrations of IGF-1 (Figure 4.5A, right) and TGF-β1 (Figure 4.5B, right) which were only detectable toward the end of the 4-week cultivation (at day 27, the IGF-1 and TGF-β1 concentrations were 0.17 ± 0.08 ng/mL and 0.21 ± 0.07 ng/mL, respectively).

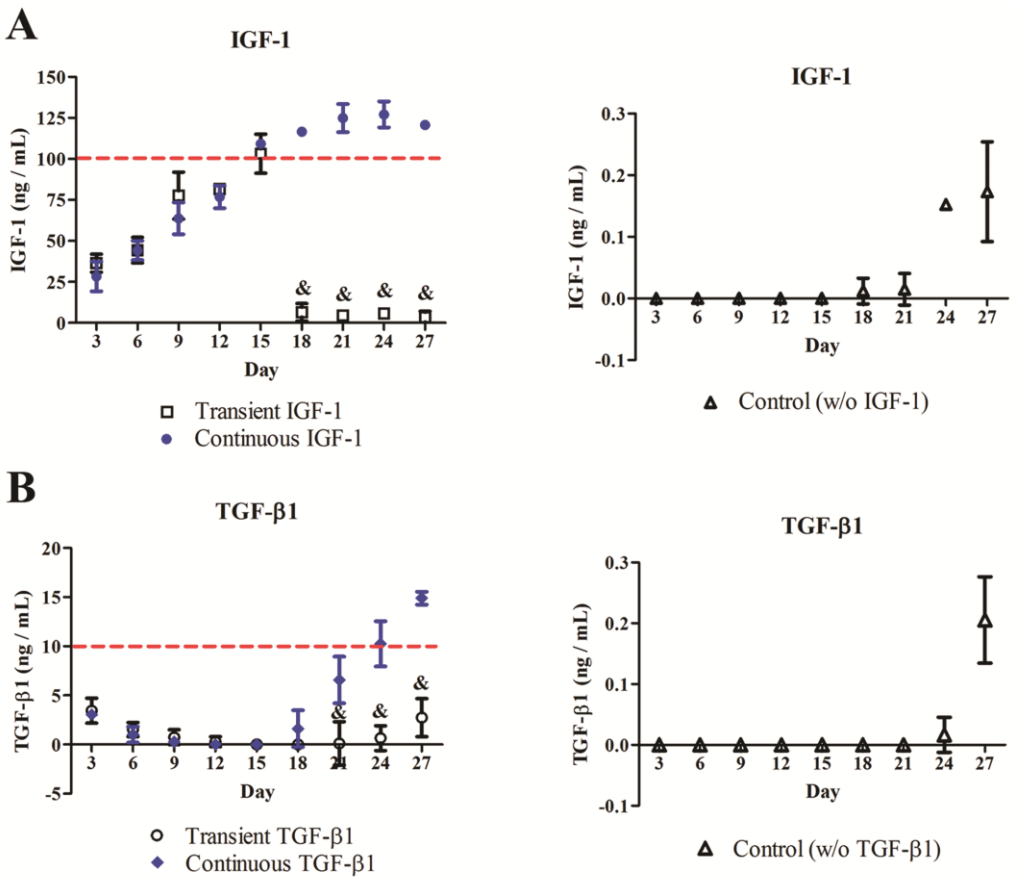

Figure 4.5 Quantification of IGF-1 (A) and TGF-β1 (B) in waste culture media in the IGF-1 and the TGF-β1 experiments, respectively. Dashed lines represent the concentrations of exogenous growth factors initially added to fresh media during medium exchanges in the continuous groups. &indicates significant difference relative to the continuously nourished group at the same time point; $p < 0.05$; n = 6.

4.3.3 IGF-1R and TGF-βRII

Quantification of IGF-1R (Figure 4.6A) and TGF-βRII (Figure 4.6B) in the respective experiments indicated that, at day 14, chondrocytes nourished with either growth factor expressed more receptors than the untreated ones (*$p < 0.05$). Figure 4.6A reveals that reduced IGF-1R expression was determined at day 28 in both the transient (442.86 ± 45.59 pg/µg DNA) and the continuous (300.50 ± 50.08 pg/µg DNA) IGF-1

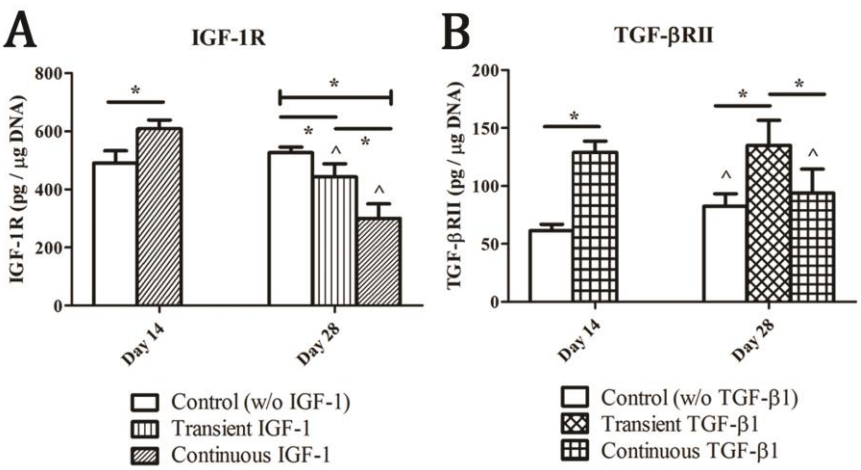

Figure 4.6 Quantitative evaluation of IGF-1 receptor (IGF-1R) (A) and TGF-β receptor type II (TGF-βRII) (B) in the IGF-1 and the TGF-β1 experiments, respectively. IGF-1R and TGF-βRII contents were quantified and estimated with the corresponding recombinant human proteins. ^represents significant difference from the corresponding 14-day value; *indicates statistical significance between the groups; $p < 0.05$; n = 6.

groups compared with the corresponding 14-day value (608.51 ± 30.58 pg/µg DNA) (^$p < 0.05$). At the end of the cultivation, the IGF-1R level in the transient IGF-1 group was found significantly higher than that in the continuous IGF-1 group while both values were compromised relative to the control group (526.08 ± 19.65 pg/µg DNA) (*$p < 0.05$). Immunohistochemistry (Figure 4.7A) confirmed that the untreated (control) samples contained the most intense IGF-1R staining at day 28.

Figure 4.6B demonstrates that chondrocytes transiently exposed to exogenous TGF-β1 expressed TGF-βRII at a level of 135.10 ± 21.61 pg/µg DNA at day 28, which remained similar to the corresponding 14-day value (129.14 ± 9.65 pg/µg DNA), but was significantly higher than the other groups at the same time point (*$p < 0.05$). Qualitatively, the control specimens (Figure 4.7B) were intensely stained for TGF-βRII

in the region close to the edge of engineered tissues whereas both the transient and the continuous TGF-β1 specimens showed weak TGF-βRII signals at the construct periphery, but stronger toward the central portion of the constructs.

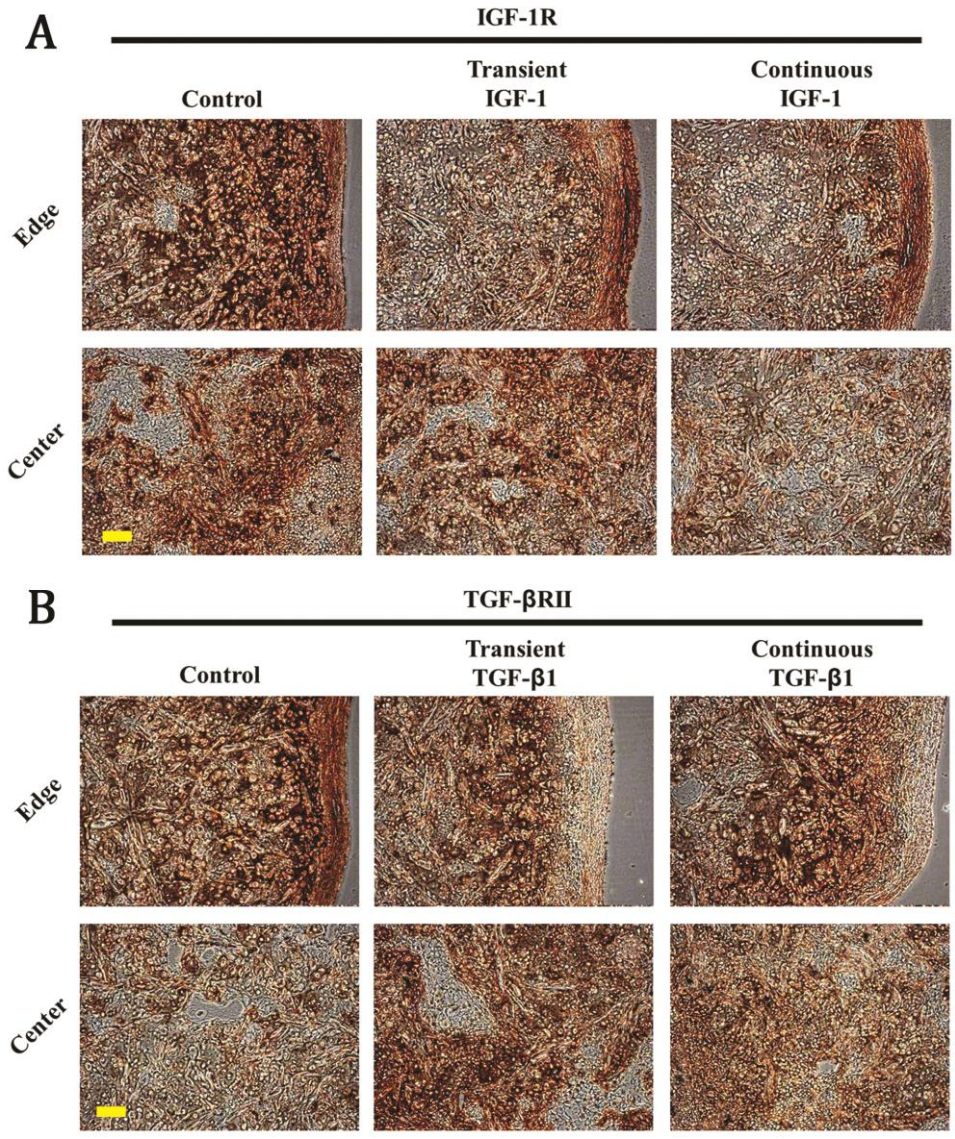

Figure 4.7 Qualitative evaluation of IGF-1 receptor (IGF-1R) (A) and TGF-β receptor type II (TGF-βRII) (B) in the IGF-1 and the TGF-β1 experiments, respectively. IGF-1R and TGF-βRII are stained brown in the corresponding 28-day hydrodynamic constructs. Images were taken under the same optical conditions for each molecule. Scale bar = 100 μm (10X magnification).

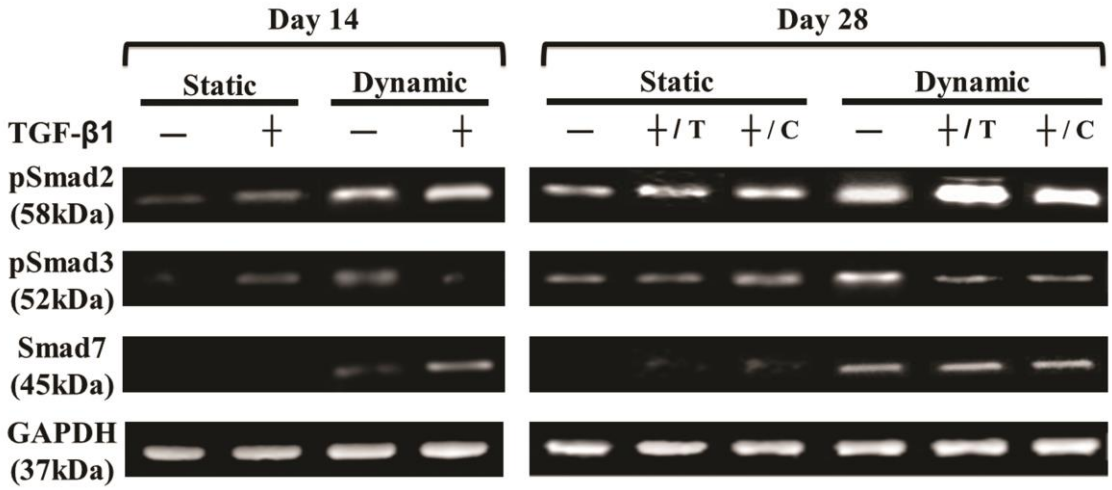

Figure 4.8 Western blot of phospho-Smad2 (pSmad2), phospho-Smad3 (pSmad3), Smad7 and GAPDH. Chondrocyte-seeded constructs were cultivated with (+) or without (-) TGF-β1 in the presence (dynamic) or absence (static) of fluid shear stress induced within the WWB. T: transient; C: continuous.

4.3.4 Smads

Regulation of major intracellular mediators in the TGF-β signaling pathway by TGF-β1 and fluid shear stress was evaluated. In this study, constructs were cultivated with or without TGF-β1 in the presence or absence of hydrodynamic forces. Western blot results (Figure 4.8) revealed that, without TGF-β1, more Smad2 and Smad3 were phosphorylated under hydrodynamic stimuli at days 14 and 28. In both static and dynamic groups, TGF-β1-nourished samples demonstrated more intense pSmad2 than the untreated ones at the same time points. However, relative to the untreated groups, supplementation with exogenous TGF-β1 increased pSmad3 signals under static conditions, but decreased its intensity in the presence of fluid shear stress at both time points. At day 28, the dynamic group with shortened TGF-β1 nourishment (+/T) did not surrender pSmad2 and pSmad3 in comparison with that under continuous TGF-β1

stimulation (+/C). Smad7 was only determined in the dynamic groups. Specifically, stronger Smad7 signals were detected in the TGF-β1-treated group at day 14 whereas similar intensity was observed among the groups at day 28.

4.4 Discussion

In this chapter, chondrocyte-seeded PGA scaffolds were cultured transiently or continuously with IGF-1 or TGF-β1 in the WWBs for 4 weeks. Our results reveal that IGF-1 and TGF-β1 effectively promoted the early development of neocartilage, suggesting that early growth factor supply is required to enhance cell signaling and communication. Yet, engineered tissues did not largely benefit from continuous growth factor stimulation over time, especially in IGF-1 cultures (Figure 4.2). This observation implies that the prolonged exposure to IGF-1 may constrain the development of hydrodynamic constructs. Conversely, discontinuation of growth factors at day 15 eventually led to constructs with better biochemical and mechanical properties (Figure 4.2 and Figure 4.3). Our findings suggest that economical tissue engineering approaches can be developed to produce robust neocartilage through the combination of hydrodynamic bioreactor systems and transient supplementation of exogenous growth factors.

A similar beneficial effect on chondrocyte growth has previously been documented (Lima, Bian et al. 2007; Byers, Mauck et al. 2008). In contrast to the present work demonstrating this “transient” effect under continuous fluid agitation, however, the study reported by Lima and coworkers indicated that the advantage of TGF-β3 removal vanished in neocartilage cultivation with continuous deformational loading (Lima, Bian

et al. 2007). It was speculated that the application of dynamic compressive forces could retain 2-to-3-fold greater concentrations of growth factors inside an engineered construct than free swelling conditions (Mauck, Hung et al. 2003) such that the localized growth factors reached the level where cellular catabolic activities were elicited (Lima, Bian et al. 2007). Such detrimental results were eliminated by delayed compressive stimuli applied after the termination of the TGF-β3 supply, suggesting that preconditioning of chondrocytes with growth factors can facilitate construct development during subsequent exposure to deformational loading (Lima, Bian et al. 2007). Although the contexts of culture systems, for example, type of growth factor, scaffolding material and loading condition and profile are quite different in Lima's and our studies, making direct comparisons challenging, all of these findings indicate the complexity involved in mechanotransductive signaling that cells may elicit in response to various external mechanical stimuli and the corresponding loading protocols.

We further explored the kinetics of growth factor uptake/release by stimulated cells in relation to the duration of exposure to IGF-1 or TGF-β1. Diverse time-dependent trends were identified in the IGF-1 (Figure 4.5A, left) and the TGF-β1 (Figure 4.5B, left) cultures, indicating that the need for each growth factor in articular chondrocytes is governed by differential mechanisms. The final growth factor concentrations in waste culture media measured in all of the groups were higher than those added to fresh media, suggesting that chondrocytes possess the ability to secrete endogenous IGF-1 (Schlechter, Russell et al. 1986; Clemmons, Busby et al. 2002) and TGF-β (Villiger and Lotz 1992; Cheung, Lee et al. 2001) for self-supplementation such that their desire for exogenous growth factors gradually decreases. It has also been demonstrated that both IGF-1 and

TGF-β are shear-responsive molecules, meaning their expression and synthesis can be promoted by fluid shear stress (Negishi, Lu et al. 2001; Lau, Kapur et al. 2006). This evidence may account for the elevated concentrations of IGF-1 and TGF-β1 detected in culture media and implies the unnecessity of the continuous addition of these two growth factors to hydrodynamic culture systems.

The modulation of growth factor secretion into the surroundings by supplementation protocols also altered the expression of the associated surface receptors, i.e. IGF-1R and TGF-βRII. The IGF-1R levels in both the transient and the continuous IGF-1 samples decreased over time (Figure 4.6A) while a similar decline in TGF-βRII was noticed in the continuous TGF-β1 group (Figure 4.6B). It is believed that overdoses of growth factors can suppress the expression of their own receptors (Krupp and Lane 1981; Gebken, Feydt et al. 1999) possibly through enhanced receptor degradation (Kosmakos and Roth 1980). Future inquiries into changes in receptor numbers due to their interactions with other environmental factors such as ECM components (Takeuchi, Nakayama et al. 1996) are necessary. Besides, the inclusion of ITS as part of medium supplements, which contains 10 μg/mL insulin, may also contribute to the IGF-1 accumulation in culture media (Figure 4.5A) and the IGF-1R down-regulation in cells (Figure 4.6A) determined in the current study. Rationally, insulin and IGF-1 are highly similar in molecular structure, both of which are capable of cross-reacting with insulin receptor and IGF-1R (Schumacher, Mosthaf et al. 1991; Dupont, Khan et al. 2001). Although each receptor attracts its own ligand with a 100-to-1000-fold higher affinity than that to the other heterologous molecules (Dupont, Khan et al. 2001), it is possible that insulin present in the BM interfered with the binding between IGF-1 and IGF-1R

such that the disturbed expression of both molecules was observed. The dose of ITS (1%) employed here has been shown to be essential to support the WWB cultivation of tissue-engineered cartilage in the presence of a minimal content of serum (Chapter 3). Taken together, one of the contributing mechanisms to the suppressed influence of continuous exposure to IGF-1 or TGF-β1 on construct development may be attributed to the accumulation of exogenous and endogenous growth factors in the culture environments which elicits a negative feedback response that inhibits cellular expression of specific surface receptors and probably accelerates subsequent catabolic activities (Morales and Roberts 1988; Lima, Bian et al. 2007). On the contrary, transient exposure to IGF-1 or TGF-β1 is likely to maintain chondrocyte homeostasis and thus promotes their anabolic functions under hydrodynamic stimuli.

The formation of a fibrous capsule at the construct periphery is believed to result from the direct contact of chondrocytes with medium supplements that induce fibrotic processes (Ignotz and Massagué 1986; Lohmann, Schwartz et al. 2000; Kelly, Fisher et al. 2008), and is further promoted as rounded articular chondrocytes deform into a flattened, elongated fibroblast-like shape under fluid agitation (Vunjak-Novakovic, Freed et al. 1996) and thus produce more type I collagen, but less GAG (Guh, Yang et al. 1996; Darling and Athanasiou 2005). We also reported that sufficient fibrosis-promoting soluble factors are necessary to initiate the process of the capsule formation even in hydrodynamic cultivation (Chapter 3). Although one of the two hypotheses of the present study was that engineered tissues treated with TGF-β1, a molecule capable of facilitating fibrosis of different tissues and organs (Ignotz and Massagué 1986; Dobaczewski, Bujak et al. 2010; Meng, Huang et al. 2010; Fragiadaki, Ikeda et al. 2011), will form a thicker

fibrous capsule in comparison with the untreated ones, we found that it was valid only when constructs were exposed to static conditions (data included in the next paragraph). Conversely, a capsule was eliminated from hydrodynamic neocartilage transiently or continuously nourished with exogenous TGF-β1 (Figure 4.4). One possible explanation is that elongated cells at the periphery of the TGF-β1 constructs expressed a minimal level of TGF-βRII (Figure 4.7B), the molecule which is associated with the initial binding of TGF-β and triggers subsequent intracellular reactions (Gebken, Feydt et al. 1999), so they were blocked from receiving TGF-β1 signals and thus acted like normal chondrocytes. In addition, discontinuation of TGF-β1 supplementation at day 15 did not rescue the fibrous capsule in hydrodynamic constructs, indicating that this fibrotic process is mostly governed and influenced by environmental factors present in early neocartilage development. In combination with the findings reported in Chapter 3, we suggest a biphasic dose-dependent effect of TGF-β on the capsule formation in hydrodynamic cultivation of tissue-engineered cartilage. Given that the concentration of TGF-β in FBS is approximately 16 ng/mL after being activated (Danielpour, Kim et al. 1989; Danielpour 1993), a fibrous capsule can be eliminated from hydrodynamic cartilage constructs when they are cultured with a TGF-β level lower than 0.032 ng/mL (i.e. 0.2% FBS) or higher than 10.32 ng/mL (2% FBS + 10 ng/mL TGF-β1). Supportively, a recent study revealed that high doses of TGF-β (10 ng/mL) could suppress type I collagen synthesis by fibroblasts via up-regulation of *CUX1*, a transcription factor (Fragiadaki, Ikeda et al. 2011). Regulation of chondrocyte-related fibrosis by TGF-β at the transcriptional level requires further investigations. It is also noteworthy that chondrocytes in the TGF-β1 constructs did not accumulate at the outer edges of the

constructs, where a fibrous capsule usually occurs. It has been demonstrated in several cell types including mast cells, fibroblasts and lymphocytes that cell aggregation can cause fibrosis of various tissues and organs such as bone marrow (Chiu, Nanaji et al. 2009), lung (Katzenstein 1985; Bantsimba-Malanda, Marchal-Sommé et al. 2010) and liver (Carthew, Edwards et al. 1991). Therefore, it is possible that a lower degree of aggregation of fibroblast-mimicking chondrocytes would suppress the fibrosis of the construct periphery.

Table 4.2 Biochemical Properties and Capsule Thickness of 28-Day Static and Hydrodynamic Constructs

	Static			Dynamic		
	Control (w/o TGF-β1)	**Transient TGF-β1**	**Continuous TGF-β1**	**Control (w/o TGF-β1)**	**Transient TGF-β1**	**Continuous TGF-β1**
Total Collagen Content (% of ww)	1.01 ± 0.13^	1.01 ± 0.15^	1.33 ± 0.13^*$^{\#}$	2.52 ± 0.19	4.30 ± 0.13*	3.75 ± 0.26*$^{\#}$
GAG Content (% of ww)	1.27 ± 0.13^	1.42 ± 0.21^	1.74 ± 0.17^*	2.43 ± 0.25	3.67 ± 0.15*	3.61 ± 0.31*
Capsule Thickness (μm)	12.43 ± 4.25	16.71 ± 4.12^	23.44 ± 6.19†*	78.28 ± 8.56†	ND	ND

- Total collagen and GAG contents: ^significant decrease versus the corresponding dynamic group; *significant increase versus the control group under the same loading conditions; $^{\#}$significant difference from the transient group under the same loading conditions; $p < 0.05$; n = 4 (static) or 7 (dynamic). WW: wet weight.
- Capsule thickness: ^significance versus the static control group ($p < 0.05$); †significance versus the static control group ($p < 0.001$); *significance versus the transient group under the same loading conditions ($p < 0.001$); n = 20. ND: non-detectable.

We further investigated regulation of predominant cytoplasmic mediators in TGF-β signaling by TGF-β1 and/or fluid shear stress and attempted to connect their expression to neocartilage development and capsule formation. Amongst these biomolecules, both Smad2 and Smad3 are receptor-regulated proteins while Smad7 is an inhibitory factor (Derynck and Zhang 2003; Shi and Massagué 2003). We found that TGF-β1 or fluid shear stress alone increased the phosphorylation of both Smad2 and Smad3 (Figure 4.8), leading to enhanced cartilage growth and capsule formation (Table 4.2 and Figure 4.9). Compared with shear stress alone, incorporation of TGF-β1 into the dynamic system

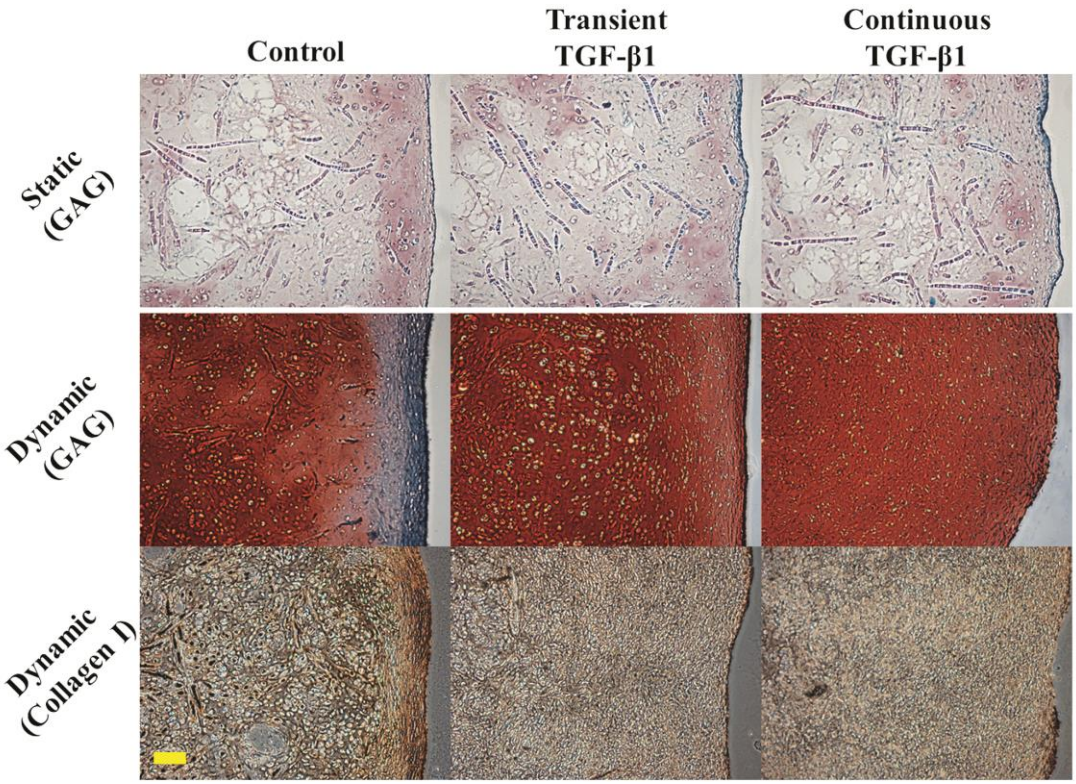

Figure 4.9 Staining of GAG and type I collagen in 28-day constructs cultured under the specified conditions. 1st and 2nd rows: GAG and cytoplasm are stained pink/red and green, respectively. 3rd row: type I collagen is stained brown. Images were taken with the same optical parameters for each molecule. Scale bar = 100 μm (10X magnification).

amplified pSmad2 signals, but lowered pSmad3 intensity, yielding improved cartilage quality, but reduced capsule structure. Evaluation of Smad7 (Figure 4.8) indicated that the reduction in pSmad3 was likely due to the direct action of Smad7 on Smad3 signaling in the early dynamic cultivation, but might be managed by other mechanisms in the later stage. Previously, Brown and coworkers identified the diverse roles Smad2 and Smad3 play in epithelial cells and fibroblasts (Brown, Pietenpol et al. 2007). We herein suggest that Smad2 and Smad3 primarily dominate chondrocyte- and fibroblast-specific phenotypes, respectively, in articular chondrocytes and both the pathways are potently promoted by TGF-β or fluid shear stress. However, TGF-β reversely regulates Smad2 and Smad3 signaling pathways in the presence of hydrodynamic stimuli partially through Smad7. Table 4.3 summarizes fluid shear stress/TGF-β-regulated Smad expression in relation to chondrocyte and cartilage development.

Table 4.3 Summary of Potential Smad Regulation on Chondrocyte Activities in Response to TGF-β1 and/or Fluid Shear Stress

Culture Conditions (Control)	**Extracellular Stimulation**	**Intracellular Regulation (versus Control)**	**Cell/Tissue Responses (versus Control)**
Static	TGF-β1 or Fluid shear stress	pSmad2 ↑ pSmad3 ↑	Cartilage matrix ↑ Capsule formation ↑
Hydrodynamic	TGF-β1	pSmad2 ↑ pSmad3 ↓ Smad7* ↑	Cartilage matrix ↑ Capsule formation ↓

*Smad7 inhibits phosphorylation of Smad3 in the early development of tissue-engineered cartilage. ↑: enhanced synthesis; ↓: reduced synthesis.

This chapter demonstrates a cost-efficient tissue engineering strategy for cartilage repair by combining transient exposure to exogenous growth factors with a hydrodynamic culture system. With this system, we identified a potential mechanism related to homeostasis between growth factor secretion and receptor expression to explain increased ECM production by chondrocytes cultured under transient stimulation of exogenous IGF-1 or TGF-β1. A biphasic response to concentrations of fibrosis-promoting soluble molecules such as TGF-β was also recognized in the process of the capsule formation during the development of hydrodynamically engineered cartilage. Finally, we gained a preliminary understanding of chondrogenesis and fibrosis of chondrocytes governed by Smad2 and Smad3, respectively. Since the current study is limited to a single drug dose and one fluid agitation rate, future investigations are required to determine how varied combinations of growth factor concentration and shear stress magnitude impact the "transient" phenomenon, capsule formation and Smad expression. The strategy reported here holds promise for tissue engineering applications that utilize allogeneic chondrocytes harvested from healthy young donors. These juvenile cells may be preferred because they are thought to possess a stronger ability to regenerate cartilage tissues (Tran-Khanh, Hoemann et al. 2005) and can be isolated without causing further damage to patients. Collectively, our findings provide valuable insights for establishment of a better growth factor supplementation protocol, capsule formation and Smad regulation on chondrocyte activities, all of which can effectively contribute to the achievement of clinically relevant cartilage tissue replacements.

CHAPTER 5

DIVERSE EFFECTS OF A FIBROUS CAPSULE ON TISSUE HOMOGENEITY AND INTEGRATION CAPABILITY OF HYDRODYNAMICALLY ENGINEERED CARTILAGE[††]

5.1 Introduction

Articular cartilage which covers the surfaces of synovial joints is designed to allow smooth contact between long bones and to absorb shock induced during joint movement. The load-bearing function of articular cartilage is built upon a combination of its unique ECM components and properties which are both inhomogeneous and anisotropic. Aging, disease or abnormal loading (overloaded or immobilized) conditions applied to diarthrodial joints may cause degeneration of articular cartilage. To date, only a few therapeutic strategies aimed to restore the function of damaged cartilage tissues exist. Among the common surgical treatments for cartilage defects are abrasion arthroplasty, subchondral drilling, microfracture, transplantation of autografts or allografts and total joint replacement (Brittberg, Lindahl et al. 1994; Andres, Mears et al. 2001; Hangody, Feczkó et al. 2001; Sgaglione, Miniaci et al. 2002; Bos and Ellermann 2003; Hand, Lobo et al. 2003; Huntley, Bush et al. 2005; Jakobsen, Engebretsen et al. 2005; Saris, Vanlauwe et al. 2008; Ronn, Reischl et al. 2011). Yet, formation of fibrocartilage or scar tissues at the defect site, which usually accompanies natural and

[††]Adapted and modified from Yang, Y.-H. and Barabino, G.A. (*in press*) Differential Morphology and Homogeneity of Tissue-Engineered Cartilage in Hydrodynamic Cultivation with Transient Exposure to Insulin-Like Growth Factor-1 and Transforming Growth Factor-β1. *Tissue Engineering Part A*.

reparative cartilage healing processes, persists as a major issue in cartilage regeneration (Shapiro, Koide et al. 1993; Andres, Mears et al. 2001; Knutsen, Engebretsen et al. 2004; Ronn, Reischl et al. 2011). Although these fibrous tissues comfort patients by alleviating pain, they are composed of abundant type I collagen fibrils and therefore are biochemically and mechanically compromised relative to healthy articular cartilage (Knutsen, Engebretsen et al. 2004). Evidently, inhomogeneous mechanical properties owned by the regenerated cartilage tissue may elicit severe disruption within the tissue (Ahsan and Sah 1999) and lead to recurrence of tissue degeneration (Shapiro, Koide et al. 1993; Khan, Gilbert et al. 2008). Tissue engineering as a means of producing high quality tissue substitutes by combining appropriate cell sources, materials, engineering tools and stimulating agents holds considerable promise for diminishing variations in functional properties between the implant and the surrounding host tissues. Nevertheless, tissue heterogeneity may also arise within each engineered construct (Kelly, Ng et al. 2006; Kelly, Ng et al. 2009; Sheehy, Buckley et al. 2011) and thus needs to be reviewed prior to implantation.

A successful tissue-engineered construct also needs to integrate strongly and stably with native tissues to maintain the integrity of the regenerated tissue since poor integration can cause an altered property of the implant and ultimately its degradation (Khan, Gilbert et al. 2008). The quality of tissue integration depends on a variety of factors such as the developmental stage of the implant (Obradovic, Martin et al. 2001; Dimicco, Waters et al. 2002), architecture and composition of the implant and the adjacent tissues (Tognana, Chen et al. 2005), and choices of scaffolding materials (Hunter and Levenston 2004) and cell sources (Vinardell, Thorpe et al. 2009) for tissue-

engineered constructs. Although many have demonstrated that a structure similar to fibrocartilage usually forms at the implant-cartilage interfaces (Shapiro, Koide et al. 1993; Fujisato, Sajiki et al. 1996; Khan, Gilbert et al. 2008; Vinardell, Thorpe et al. 2009), several approaches have been developed to improve integrative repair of articular cartilage. For instance, pre-incubation of the implant with Z-VAD-FMK or Necrostatin-1 which inhibits cell apoptosis and necrosis, respectively, at the wound edge was found to strengthen its ability to integrate with native cartilage (Khan, Gilbert et al. 2008; Gilbert, Singhrao et al. 2009). A study reported by Djouad et al. further revealed that the blockage of extracellular regulated kinase (ERK) signaling pathways by an inhibitor, U0126, prevented the production of proteinases induced by pro-inflammatory cytokines such as interleukin-1β (IL-1β) and tumor necrosis factor-α (TNF-α) and thus doubled the adhesive stress at the integration site (Djouad, Rackwitz et al. 2009). Obradovic and coworkers showed that treatment of host cartilage with trypsin promoted its fusion with immature (5-day) engineered tissues, but had no apparent effects on the integration with mature (5-week) constructs or with intact cartilage explants (Obradovic, Martin et al. 2001). In addition, cartilage tissue integration can also be improved by the use of biological glues like tissue transglutaminase (Jürgensen, Aeschlimann et al. 1997) and fibrin-based gels (Silverman, Bonasser et al. 2000; Peretti, Zaporojan et al. 2003; Peretti, Campo-Ruiz et al. 2006). A fibrin glue gel (made up of fibrinogen and thrombin) seeded with chondrocytes was utilized to join two separate pieces of cartilage to yield a thick tissue complex (~ 4 mm) (Silverman, Bonasser et al. 2000) and the sandwiched construct grew more homogeneously when the incorporated cartilage slices were decellularized

(Peretti, Campo-Ruiz et al. 2006). This evidence substantiates that the extent of tissue integration is greatly influenced by both extrinsic and intrinsic elements.

A fibrous capsule represents a unique characteristic of tissue-engineered cartilage and is usually found at the outer edge of neocartilage (Vunjak-Novakovic, Freed et al. 1996; Kisiday, Kurz et al. 2005; Bueno, Bilgen et al. 2008; Kelly, Fisher et al. 2008). The capsule consists of rich type I collagen and sparse GAG molecules and thereby resembles fibrocartilage (Guh, Yang et al. 1996; Darling and Athanasiou 2005). The formation of a fibrous capsule is modulated by the complex interactions of environmental factors present in culture, such as medium supplements and mechanical stimuli. We have demonstrated that the initiation of the capsule formation relies on the concentration of serum (Chapter 3). Specifically, when engineered cartilage is nourished with media containing a minimal FBS content of 2%, one can expect a fibrous capsule at the end of a 4-week cultivation, whose thickness is at least 12 μm in static cultures or 74 μm in hydrodynamic cultures. As described in the previous chapters, engineered constructs exposed to turbulent flow-induced shear conditions display a solid capsule potentially due to the deformation of articular chondrocytes at the construct periphery, which leads to a phenotypic change of the cells from the chondrocytic nature to the fibroblastic nature (Vunjak-Novakovic, Freed et al. 1996). It has been suggested that it may be necessary to remove the capsule and only retain the central portion of tissue-engineered cartilage for further biochemical evaluations (Kisiday, Kurz et al. 2005) or implantation procedures (Moyer, Wang et al. 2010) in order to minimize the nonchondrocytic phenotype of the product. However, the mechanical integrity of the construct may be sacrificed due to the ECM damage created around and/or at the cut surface of the construct during capsule

removal. Besides, the role of the fibrous capsule in cartilage tissue integration remains unclear.

Collectively, the present study was aimed to investigate how the presence of the fibrous capsule affects the homogeneity of tissue-engineered cartilage and alters the construct capability to integrate with native cartilage. We have previously utilized the WWB system in combination with exogenous growth factors, IGF-1 and TGF-β1, to produce two types of hydrodynamically engineered constructs, both of which exhibit comparable biochemical and mechanical properties, but different tissue morphologies (Chapter 4). Specifically, the properties of the IGF-1 and the TGF-β1 hydrodynamic constructs (transiently treated) are 4.21 ± 0.11% and 3.67 ± 0.15% of wet weight in GAG content, 3.66 ± 0.20% and 4.30 ± 0.13% of wet weight in total collagen content, and 87.82 ± 8.48 kPa and 136.43 ± 29.99 kPa in equilibrium modulus, respectively. Morphologically, engineered tissues nourished with IGF-1 have a solid capsule with an average thickness of about 80 μm whereas treatment with TGF-β1 yields constructs without a capsule. This allows us to test the hypothesis that the capsule-containing (CC) (IGF-1) constructs will demonstrate compromised tissue homogeneity and have a less strong inner core compared with the capsule-free (CF) (TGF-β1) constructs. Moreover, the ability of the intact hydrodynamic neocartilage with or without a fibrous capsule to integrate with native cartilage tissues was assessed using an established *in-vitro* cartilage explant model (Obradovic, Martin et al. 2001; Dimicco, Waters et al. 2002; Hunter and Levenston 2004; Djouad, Rackwitz et al. 2009; Gilbert, Singhrao et al. 2009; Vinardell, Thorpe et al. 2009).

5.2 Materials and Methods

5.2.1 Materials

Unless specified otherwise, reagents were purchased from VWR (West Chester, PA), Sigma (St. Louis, MO), Thermo Fisher Scientific (Waltham, MA) or Life Technologies (Grand Island, NY).

5.2.2 Bioreactor and Scaffold Preparation

Conventional spinner flasks were purchased from Bellco Glass, Inc. (Vineland, NJ) and sent to G. Finkenbeiner, Inc. (Waltham, MA) for WWB fabrication based on the configuration described in Chapter 2.3.2.5. Prior to each experiment, the interiors of bioreactors, needles, and stir bars were treated with Sigmacote® to prevent cell adherence. After evaporation of Sigmacote®, the assembled bioreactors were washed gently, air-dried and steam-sterilized.

10-mm (for the tissue homogeneity experiments) or 5-mm (for the tissue integration experiments) PGA discs (Biomedical Structures, Warwick, RI) (2 mm thick, 85 mg/mL bulk density, 97% void volume) were sterilized by a series of rinses in sterile 70% ethanol and deionized water, followed by a 30-minute exposure to ultraviolet light. Two of the sterilized PGA discs were threaded onto each of the 21 gauge needles and separated by a silicone spacer, resulting in totally eight scaffolds per bioreactor. The WWBs were then filled with 120-mL hgDMEM and allowed to stabilize overnight with a stir bar spinning at 50 rpm inside a humidified, 37°C, 5% CO_2 incubator.

5.2.3 Cell Isolation, Cell Seeding and WWB Cultivation

Articular chondrocytes were isolated from femoropatellar grooves of freshly slaughtered 2-week-old calves (Research 87, Marlborough, MA) by digestion with type II collagenase as previously described (Freed, Marquis et al. 1993). Cell number and viability (> 85%) were determined using a trypan blue exclusion assay. A small aliquot of cells in suspension was added to each of the sterilized WWBs at a density of 5 million live cells per scaffold. Cell seeding was carried out in the BM (hgDMEM, 2% FBS, 1% ITS, 100 U/mL penicillin/streptomycin, 10 mM HEPES, 0.4 mM L-proline, 0.1 mM NEAA, 3.6 mg/mL sodium bicarbonate, 2.5 µg/mL fungizone and 50 µg/mL ascorbic acid) and allowed to proceed for 4 days under fluid agitation (50 rpm) until 95% of the cells achieved attachment.

Following the cell seeding process, chondrocyte-seeded PGA scaffolds were cultivated in the WWBs agitated at 50 rpm for an additional 28 days and were nourished with either 100 ng/mL IGF-1 or 10 ng/mL TGF-β1 (R&D Systems, Minneapolis, MN) for the first 15 days of the culture. Herein, we only employed constructs transiently exposed to exogenous growth factors since these engineered tissues were previously demonstrated to exhibit better biochemical and mechanical properties than those continuously treated with the same molecules (Chapter 4). Culture media were completely renewed every 3 days and the growth factors were added to fresh BM during medium exchanges. Tissue-engineered constructs were harvested at the end of the cultivation for further processing.

5.2.4 Experimental Design

5.2.4.1 Tissue Homogeneity

A 5-mm central core was punched out of each of the 28-day hydrodynamic constructs (Ø10~11 mm) and variations in tissue properties between the inner core and the outer annulus (radial variations) were quantified to determine the homogeneity of tissue-engineered cartilage (Figure 5.1A).

5.4.2.2 Tissue Integration

The ability of the 28-day hydrodynamic constructs (Ø~5 mm x ~2.5 mm thick) to integrate with native cartilage was evaluated using a cartilage explant model (Figure 5.1B). Briefly, native cartilage explants were harvested from bovine donors and shaped into discs (Ø10 mm × 3 mm thick) by aseptically removing both superficial and deep zone cartilage tissues. A 5-mm central core was then punched out of each of the discs to yield a cartilage plug (Ø5 mm) and a cartilage outer ring (inner and outer diameters were 5 mm and 10 mm, respectively). The thickness of the cartilage plugs was then reduced to 2.5 mm. A disc/ring hybrid tissue composite was formed by randomly incorporating each of the three types of grafts, i.e. native cartilage plug, CF construct and CC construct, into one of the created cartilage rings by press-fit. The assembled hybrid composites were cultivated with a serum-free ITS-supplemented medium (hgDMEM, 1% ITS, 100 U/mL penicillin/streptomycin, 10 mM HEPES, 0.4 mM L-proline, 0.1 mM NEAA, 3.6 mg/mL sodium bicarbonate, 2.5 µg/mL fungizone and 50 µg/mL ascorbic acid) for 4 weeks under static conditions and were maintained in transwells (top and bottom compartments contained 3 mL of the medium each) to increase the diffusion efficiency of nutrients.

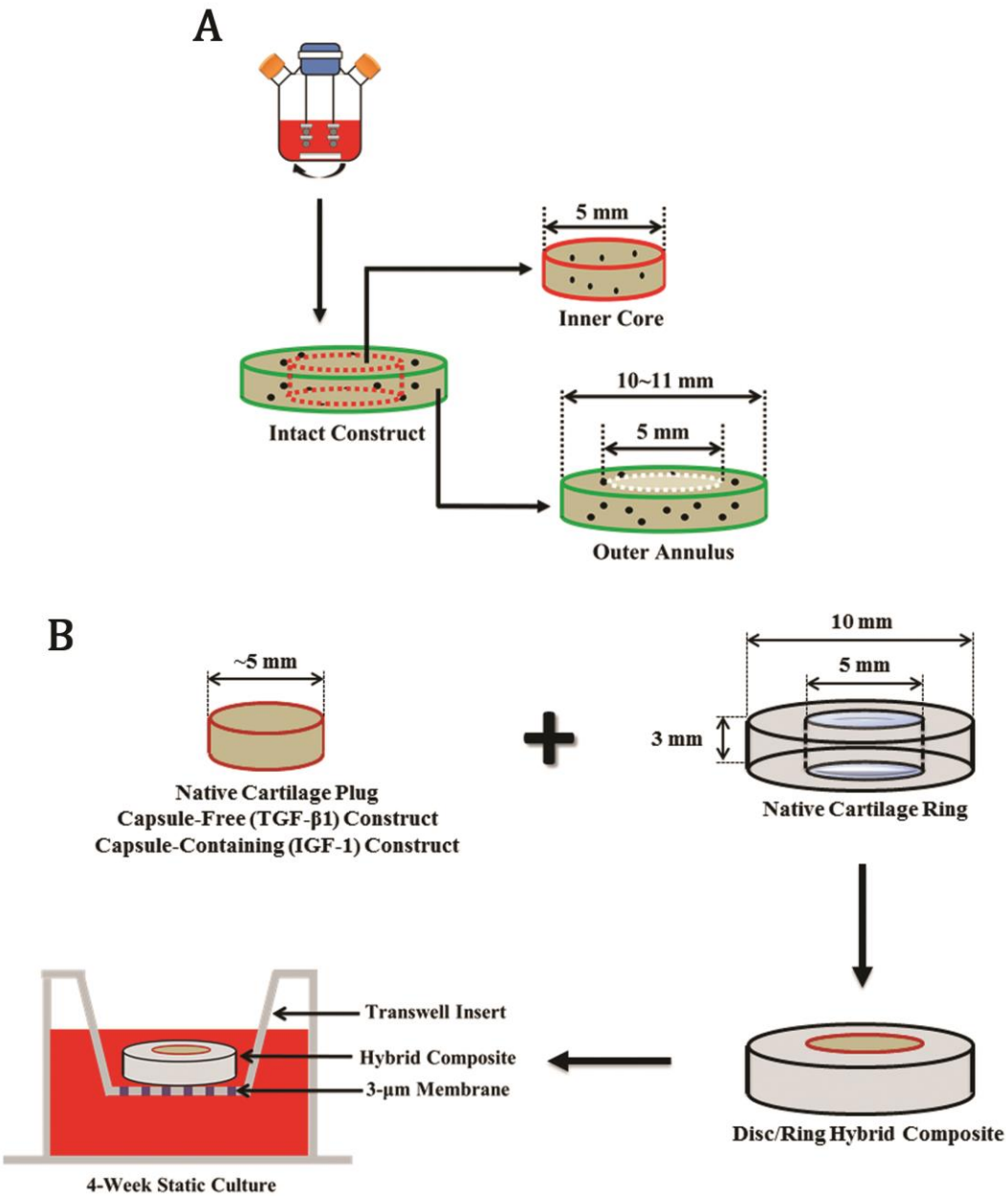

Figure 5.1 Schematic overview of the tissue homogeneity (A) and the tissue integration (B) studies. (A) Tissue homogeneity of 28-day hydrodynamic constructs was determined by evaluating radial variations in tissue properties (inner core versus outer annulus). (B) A disc/ring hybrid composite was formed by incorporating each graft into a created native cartilage ring by press-fit and was cultured in a transwell for 4 weeks under static conditions.

5.2.5 Biomechanics

Equilibrium compressive moduli of engineered tissues were determined using an unconfined compression test. During examination, a preload of 0.01 N was applied to samples until equilibrium was achieved. A stress relaxation test was carried out at strains of 5, 10, 15, 20 and 25%, after which samples were allowed to equilibrate. Equilibrium moduli were obtained from the slope of the plot of equilibrium force normalized to the cross-sectional area of the construct versus the strains.

Adhesive strength is defined as the stress that fractures a hybrid composite at the integration site during a push-through test (Figure 5.2A). Briefly, the inner disc of a composite was gradually pushed out by a 4-mm plunger at a rate of 10 μm/s while the composite was placed on a custom-designed rigid annular ring with a 6-mm center hole. The force at ultimate failure (Figure 5.2B) was normalized to the lateral area of the inner disc to obtain adhesive strength.

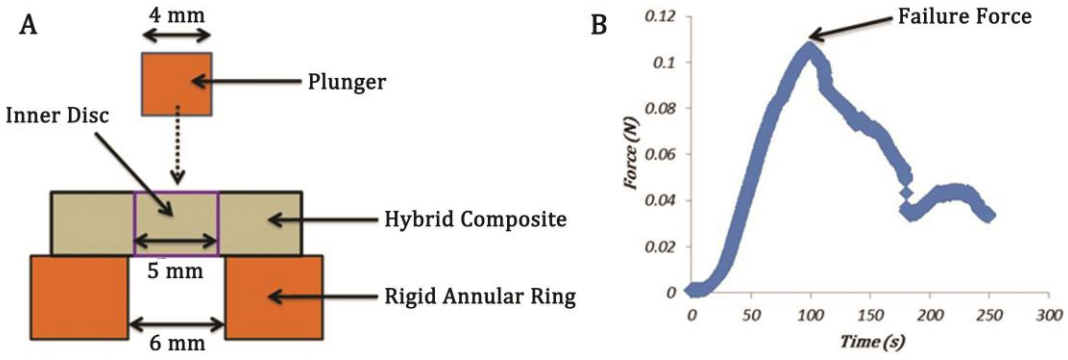

Figure 5.2 Push-out test (A) and a representative force vs. time curve during a push-out test (B). Adhesive strength of a hybrid composite at the integration site was calculated by normalizing the failure force to the lateral area of the inner disc.

5.2.6 Biochemistry

Prior to the biochemical assays, constructs were weighed (wet weight), frozen, lyophilized and then digested with papain enzyme. DNA weights were quantified using a PicoGreen dsDNA kit and the manufacturer's instructions were followed. Sulfated GAG contents were assessed using a DMMB dye-binding assay (Farndale, Buttle et al. 1986). Chondroitin sulfate was used to create a standard curve and a chondroitin sulfate-to-GAG ratio of 1 was assumed. For compositional analysis of collagen, papain-digested samples were further incubated with 1 mg/mL pancreatic elastase in 1X Tris-buffered saline solution for 48 hours at 4˚C to cleave intra- and inter-molecular cross-linkages of collagen. Type I and II collagen contents were measured using enzyme-linked immunosorbent assay (ELISA)-based detection kits (Chondrex, Redmond, WA) and the manufacturer's instructions were followed. GAG and type I and II collagen contents are presented in values normalized to the wet weight or the DNA weight of constructs.

5.2.7 Histology and Immunohistochemistry

Constructs or hybrid composites were fixed, embedded in paraffin and sectioned in 5-μm thick slices. The slices were deparaffinized and stained for GAG and collagen using safranin-O/fast green and Masson's trichrome methods, respectively.

Type I and II collagen molecules were stained immunohistochemically. Briefly, deparaffinized sections were incubated with citrate buffer heated to 99°C for 25 minutes to retrieve antigens, followed by a 20-minute cooling at room temperature. The samples were then incubated with 0.3% hydrogen peroxide for 30 minutes, blocking buffer for 20 minutes, and primary rabbit anti-bovine antibodies (1:1500, Abcam, Cambridge, MA)

overnight. Finally, the sections were treated with biotinylated secondary antibodies (1:200, Vector Labs, Burlingame, CA) for 30 minutes and streptavidin-conjugated horseradish-peroxidase complex (Vector Labs) for another 30 minutes, followed by the incubation with diaminobenzidine chromogen reagent until optimal staining was developed. Samples incubated with normal rabbit serum substituted for primary antibodies were used as negative controls and no non-specific staining was observed. Color images were captured under a light microscope (Nikon Eclipse Ti, Japan).

5.2.8 Electron Microscopy

Harvested hybrid composites were fixed in 2% glutaradehyde solution in 0.1 M cacodylic acid buffer for 48 hours at 4ºC, followed by several rinses in the buffer and deionized water. For scanning electron microscopy (SEM), samples were dehydrated in a graded ethanol series (30%, 50%, 75%, 95% and 100%) and dried in a critical point dryer (Autosamdri-814, Tousimis, Rockville, MD). The dried samples were mounted onto aluminum stubs (Electron Microscopy Sciences, Hatfield, PA) and then coated with a thin layer of gold (SPI-Module Sputter, SPI Supplies, West Chester, PA). Images were captured using an SEM (Aquila, Topcon Positioning Systems, Livermore, CA).

For transmission electron microscopy (TEM), rinsed composites were further fixed in 1% osmium tetroxide for 2 hours at room temperature and incubated with 0.5% uranyl acetate for another hour. After several washes, samples were dehydrated in a graded ethanol series (30%, 50%, 75%, 95% and 100%), followed by an Epon infiltration process to embed specimens in resin (Electron Microscopy Sciences). The resin blocks were then sectioned in 60-nm thick slices that were mounted onto meshed gilder grids

(Electron Microscopy Sciences) and post-stained with methanolic uranyl acetate and Reynold's lead citrate. The grids were viewed under a TEM (JEM-1210, Jeol, Japan) and images captured at 25000X were collected for image analysis using AMT Capture Engine Software V602 (Advanced Microscopy Techniques, Woburn, MA) to measure the diameter of collagen fibrils at the integration sites.

5.2.9 Statistical Analyses

In the tissue homogeneity study, statistical data were obtained from experiments repeated twice with two replicates per group per experiment and knee chondrocytes harvested from three bovine donors (donors X, Y and Z) were pooled together and used in the entire study.

The tissue integration study was repeated three times and chondrocytes isolated from five donors (donors A, B, C, D and E) were mixed to grow different implanted tissue constructs required in all the three experiments. Prior to each experiment, fresh cartilage explants were collected from three donors (experiment 1: donors F, G and H; experiment 2: donors I, J and K; experiment 3: donors L, M and N) to prepare cartilage outer rings for the study. Similar trends were detected in all the three experiments and data shown here represent one of the experiments.

Statistical data are presented as means ± one standard deviation and statistical analyses were performed by one-way or two-way ANOVA in conjunction with the Bonferroni post test for multiple comparisons with significance at a p value of less than 0.05.

5.3 Results

5.3.1 Radial Variations

Evaluation of radial variations showed that the CC (1.45 ± 0.11% of wet weight) and the CF (2.65 ± 0.20% of wet weight) inner cores reached 51% and 79% of the collagen II contents achieved by the respective intact constructs and either inner core value was also lower than the corresponding outer annulus level (*p < 0.05) (Figure 5.3A). When values were normalized to DNA weight (Figure 5.3B), chondrocytes in the CC outer annuli produced a greater amount of collagen including both type II (39.53 ± 2.79 µg/µg DNA) and type I (20.72 ± 1.93 µg/µg DNA) relative to those in the inner cores (*p < 0.05) whereas comparable collagen synthetic activities were detected throughout the CF constructs. A significant difference in collagen I-to-II ratio (Figure 5.3C) between outer annuli and inner cores was identified in the CC group (annulus: 0.52 ± 0.12; core: 0.34 ± 0.03) (*p < 0.05).

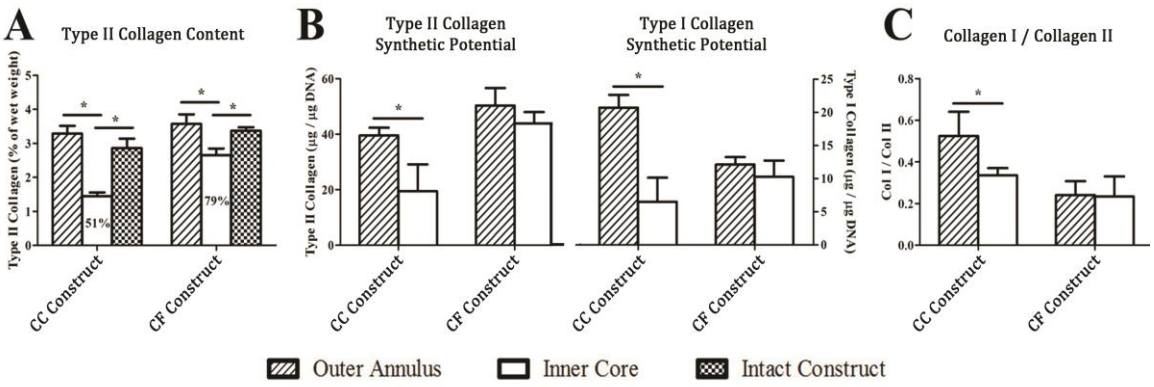

Figure 5.3 Type II collagen content (A), type II and I collagen synthetic potential (B) and collagen I to II ratio (C) of outer annuli and inner cores of 28-day hydrodynamic constructs transiently treated with IGF-1 (CC) or TGF-β1 (CF). Percentages represent the inner core values normalized to the corresponding intact construct values. *indicates statistical significance between the groups; p < 0.05; n = 4. CC: capsule-containing; CF: capsule-free.

In GAG analysis, the CF inner cores (3.82 ± 0.25% of wet weight) contained a GAG composition equivalent to that of the intact CF constructs (3.48 ± 0.20% of wet weight) whereas the CC inner cores (2.75 ± 0.04% of wet weight) had a compromised GAG content in comparison with both the outer annulus (4.11 ± 0.33% of wet weight) and the intact construct (3.73 ± 0.19% of wet weight) values (*$p < 0.05$) (Figure 5.4A). While cells in the CF inner cores (36.03 ± 8.53 μg/μg DNA) exhibited significantly weaker GAG synthetic potential than those in the outer annuli (50.80 ± 1.44 μg/μg DNA), opposite behavior was recognized in the CF group (*$p < 0.05$) (Figure 5.4B). Biomechanically, equilibrium moduli of the CC (33.72 ± 7.61 kPa) and the CF (76.40 ± 14.44 kPa) inner cores matched 37% and 59% of the corresponding intact construct values, respectively (Figure 5.4C).

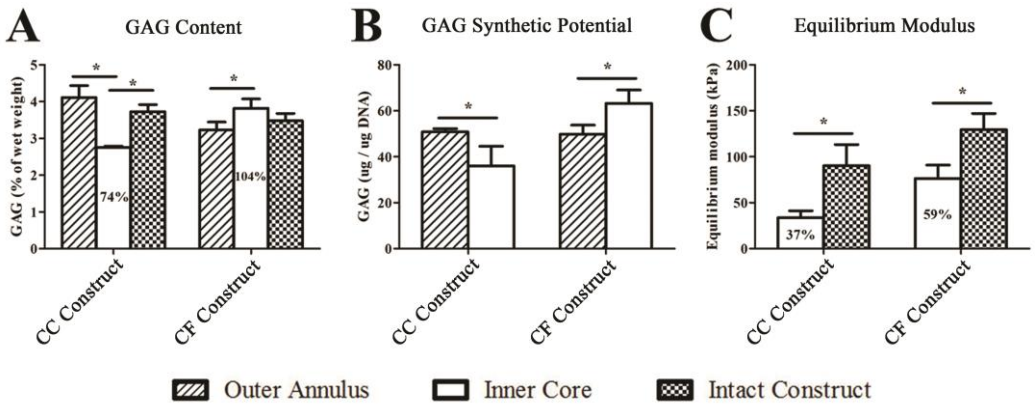

Figure 5.4 GAG content (A), GAG synthetic potential (B) and equilibrium compressive modulus (C) of outer annuli and/or inner cores of 28-day hydrodynamic constructs transiently treated with IGF-1 (CC) or TGF-β1 (CF). Percentages represent the inner core values normalized to the corresponding intact construct values. *indicates statistical significance between the groups; $p < 0.05$; n = 4. CC: capsule-containing; CF: capsule-free.

Histologically, the CF specimens were more intensely stained for type II collagen than the CC specimens in both the outer annulus and the inner core regions (Figure 5.5A). Abundant type I collagen molecules were present in the CC outer annuli. Figure 5.5B reveals that intense GAG staining was observed throughout the CF constructs while the CC specimens confirmed that the fibrous capsule consisted mainly of type I collagen (Figure 5.5).

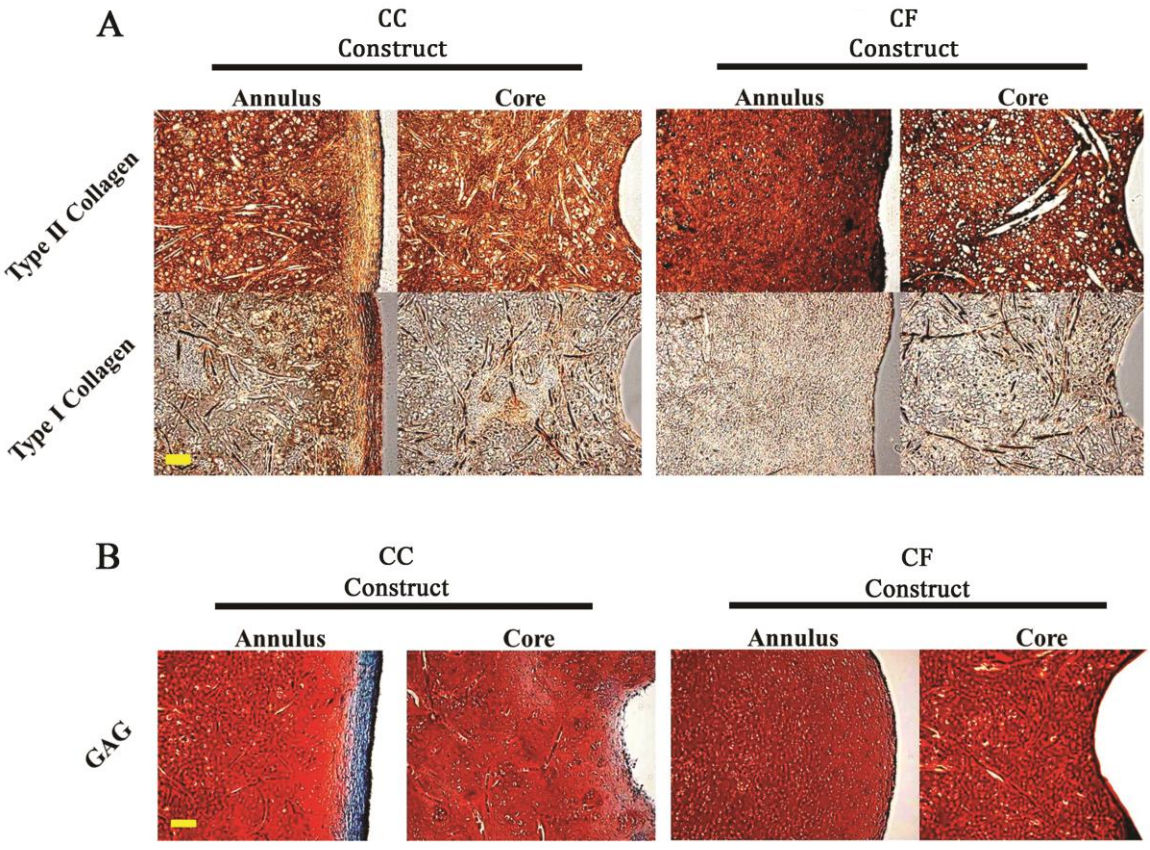

Figure 5.5 Immunohistochemical staining of type II and type I collagen (A) and histological staining of GAG (B) in 28-day hydrodynamic constructs transiently treated with IGF-1 (CC) or TGF-β1 (CF). (A) Collagen molecules are stained brown. (B) GAG and cytoplasm are stained red and green, respectively. Images were taken under the same optical conditions for each molecule. Scale bar = 100 μm (10X magnification). CC: capsule-containing; CF: capsule-free.

5.3.2 Tissue Integration

5.3.2.1 Tissue Morphology of Grafts Used to Form Hybrid Composites

Prior to preparation of hybrid composites, tissue morphologies of the three types of grafts, i.e. native cartilage plug, CF construct and CC construct, were confirmed by histology and immunohistochemistry. Figure 5.6 shows that a fibrous capsule was only present in the constructs treated with exogenous IGF-1 (CC).

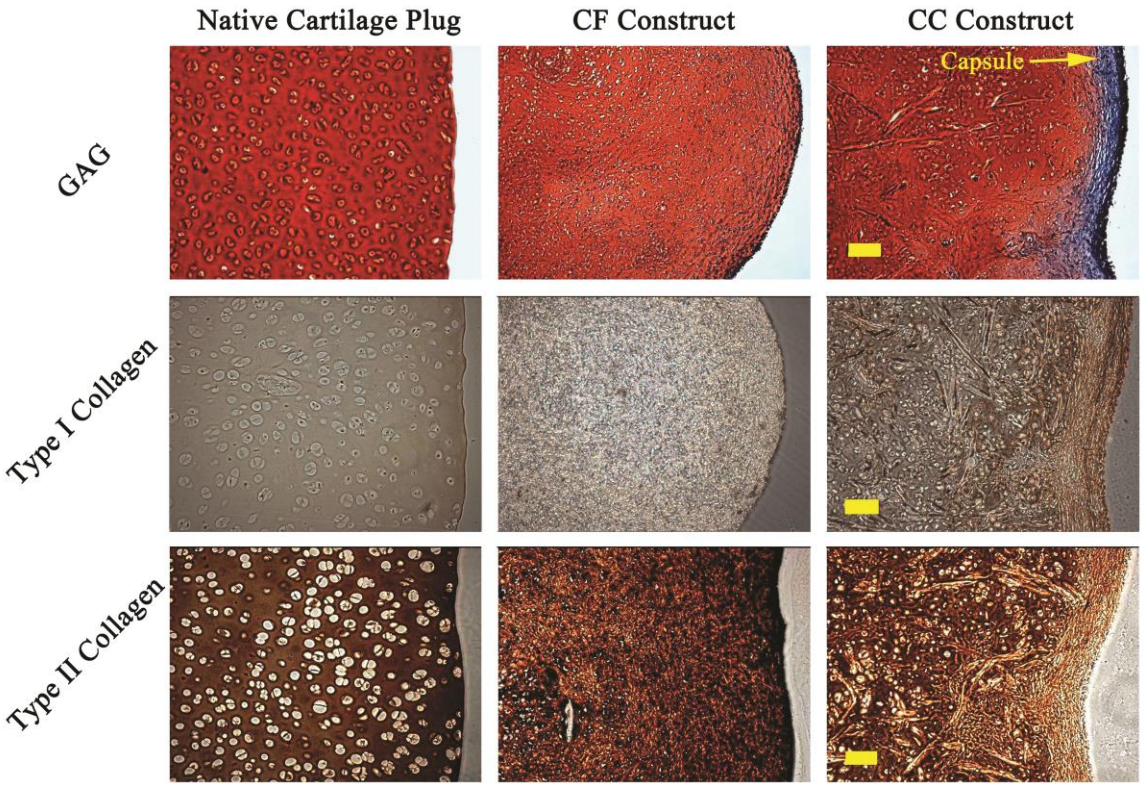

Figure 5.6 Histology and immunohistochemistry of tissue grafts for implantation. (1st row) GAG and cytoplasm are stained red and green, respectively. (2nd row) type I collagen molecules are stained brown. (3rd row) type II collagen molecules are stained brown. Images were taken under the same optical conditions for each molecule. Scale bar = 100 µm (10X magnification). CC: capsule-containing; CF: capsule-free.

5.3.2.2 Adhesive Strength

At the end of the 4-week static cultivation, harvested hybrid composites were subjected to a push-out test to determine the adhesive strength at the cartilage-cartilage or the construct-cartilage interface. The results (Figure 5.7) revealed that the CC constructs (10.93 ± 0.76 kPa) possessed the strongest capability to integrate with the surrounding articular cartilage tissues, followed by the CF constructs (6.95 ± 0.25 kPa) and then the native cartilage controls (3.81 ± 0.31 kPa) (***$p < 0.001$).

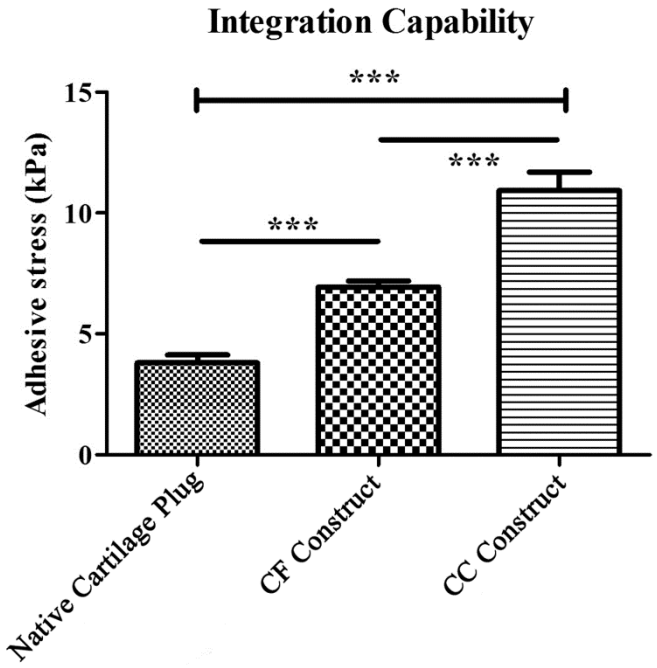

Figure 5.7 Adhesive strength of hybrid composites at the integration site. The CC and the CF constructs represented the engineered cartilage tissues transiently treated with IGF-1 and TGF-β1, respectively, in the pre-hydrodynamic cultivation. ***indicates significant difference between the groups; $p < 0.001$; n = 8 (cartilage plugs) or 9 (CC and CF constructs). CC: capsule-containing; CF: capsule-free.

5.3.2.3 Electron Microscopy and Histology

SEM (Figure 5.8) indicated that all the three types of hybrid composites demonstrated a certain level of integration on and/or close to the surface of the composite and highly cross-linked matrix meshes were identified at the integration sites.

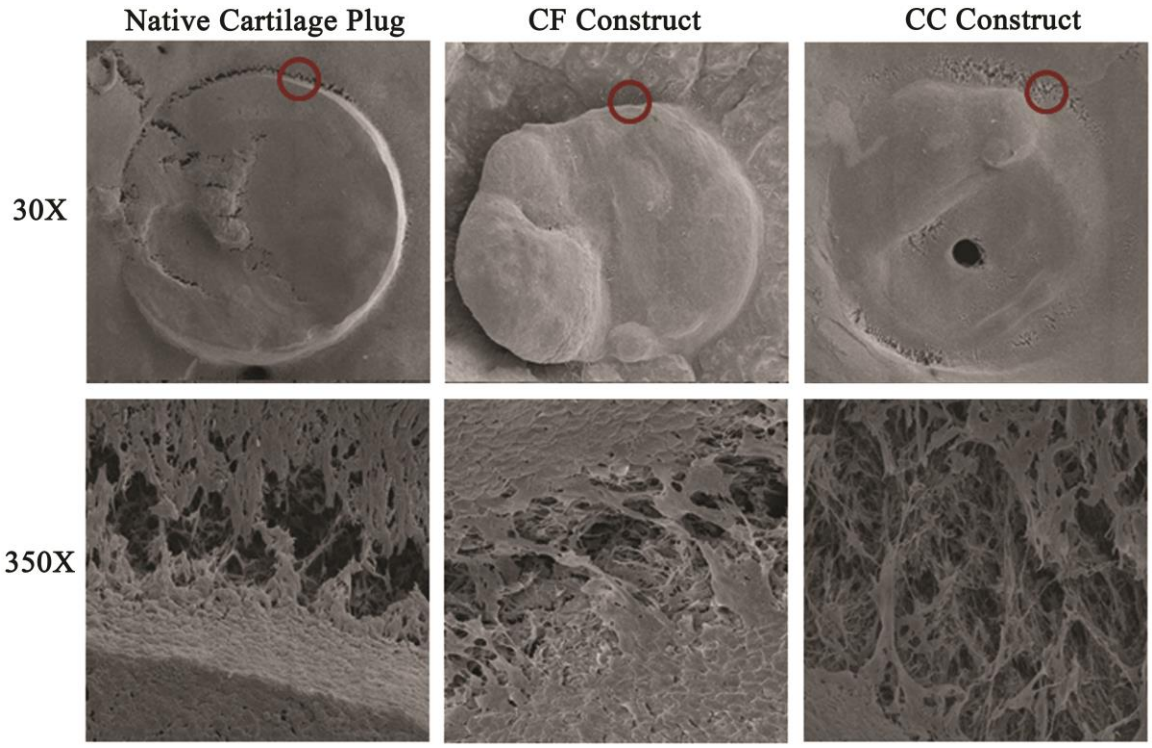

Figure 5.8 Scanning electron microscopy of 28-day hybrid composites. Images were captured at 30X (1st row) or 350X (2nd row). The 350X images represent the enlarged regions defined by the red cycles in the corresponding group. CC: capsule-containing; CF: capsule-free.

Histology and immunohistochemistry were used to visualize tissue integration at the disc-ring interface throughout the full depth of hybrid composites (Figure 5.9). Although most interfacial regions remained separate in all the cases, the CC and the CF

groups had some areas that showed integration. More cells and denser ECM components were accumulated at the integration site of the construct-cartilage composites in the CC group. Conversely, the implant and the adjacent native tissue were still intact in the native cartilage controls and a continuous gap (> 50 μm) existed at the disc-ring interface. In addition, moderate type I collagen staining was observed at and around the interface in all the groups.

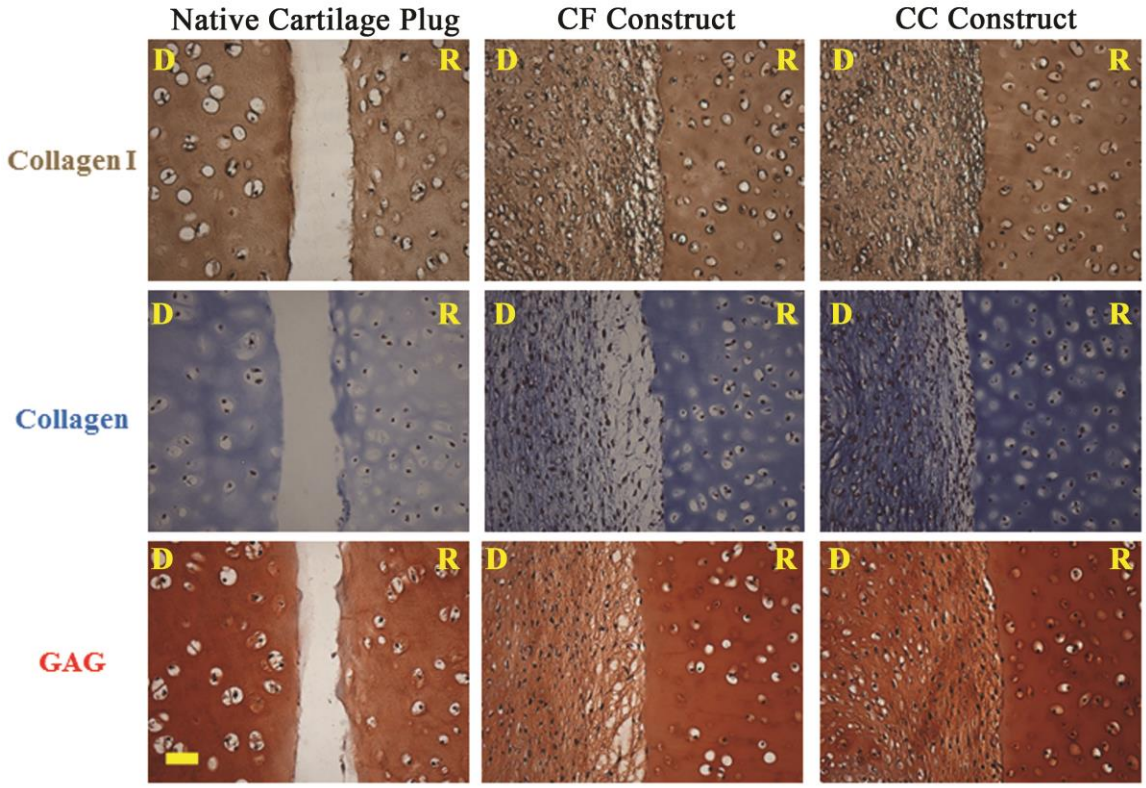

Figure 5.9 Histology and immunohistochemistry of 28-day hybrid composites. (1st row) Type I collagen molecules are stained brown. (2nd row) Collagen molecules are stained blue. (3rd row) GAG molecules are stained red. Scale bar = 50 μm (20X magnification). CC: capsule-containing; CF: capsule-free; D: disc; R: ring.

The deposition of collagen fibrils at the integration sites of the CC and the CF hybrid composites was detected by TEM (Figure 5.10). These collagen fibrils were found to highly align in the same direction parallel to the disc-ring interface. Specifically, the CC group contained an organization composed of tightly packed collagen fibrils while the CF group demonstrated a relatively low level of collagen alignment and sparse collagen molecules. In contrast, no collagen fibrils were identified at the disc-ring interface of the cartilage-cartilage composites since the gaps were not filled with any ECM components and stayed unclosed.

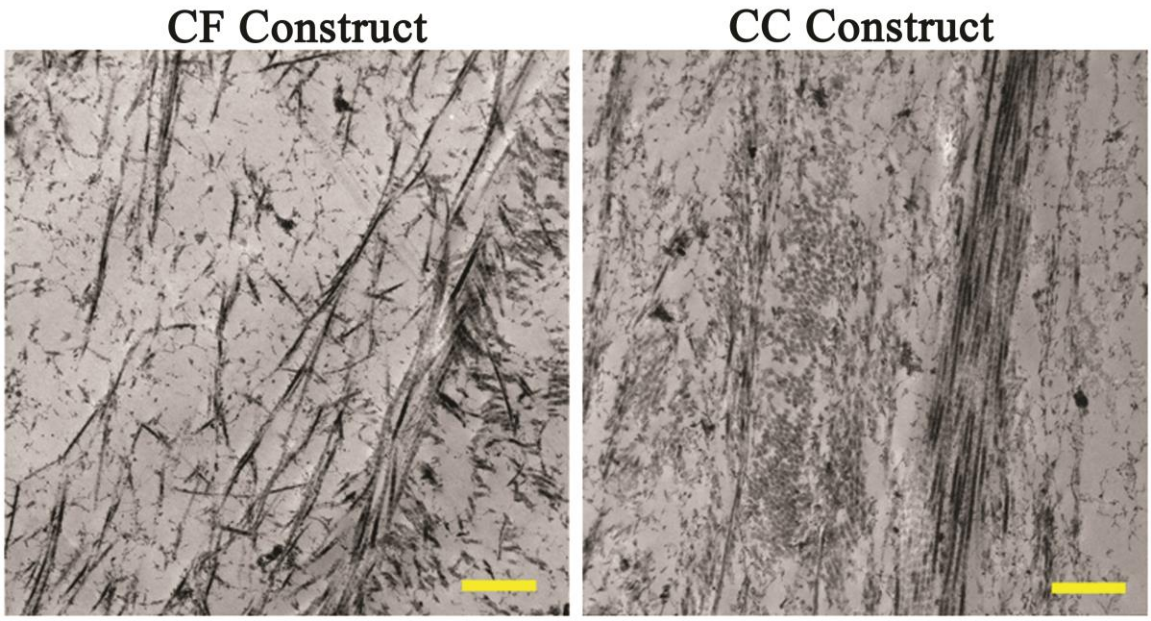

Figure 5.10 Transmission electron microscopy of 28-day hybrid composites. Images represent the regions at the integration sites and were captured at 12000X. Scale bar = 500 nm. CC: capsule-containing; CF: capsule-free.

5.3.2.4 Collagen Fibril Diameter

Twenty 25000X TEM images per group were collected to calculate the average diameters of collagen fibrils found at the integration sites and at least fifteen (CF) or twenty-five (CC) random fibrils were measured per image. The results showed that the average value of the CC group (25.58 ± 7.27 nm) was significantly higher than that of the CF group (18.08 ± 6.29 nm) while both of them were compromised relative to the average diameter of collagen fibrils (46.50 ± 13.69 nm) located in freshly harvested articular cartilage tissues (Figure 5.11A). In the diameter distribution (Figure 5.11B), about 59% of the collagen fibrils in the CC group had a diameter ranged from 20 nm to 30 nm and at least 79% of the fibrils were thicker than 20 nm. Conversely, the majority of the collagen diameters in the CF group fell in the range between 10 nm and 20 nm (60%) and only about 32% of the fibrils were thicker than 20 nm.

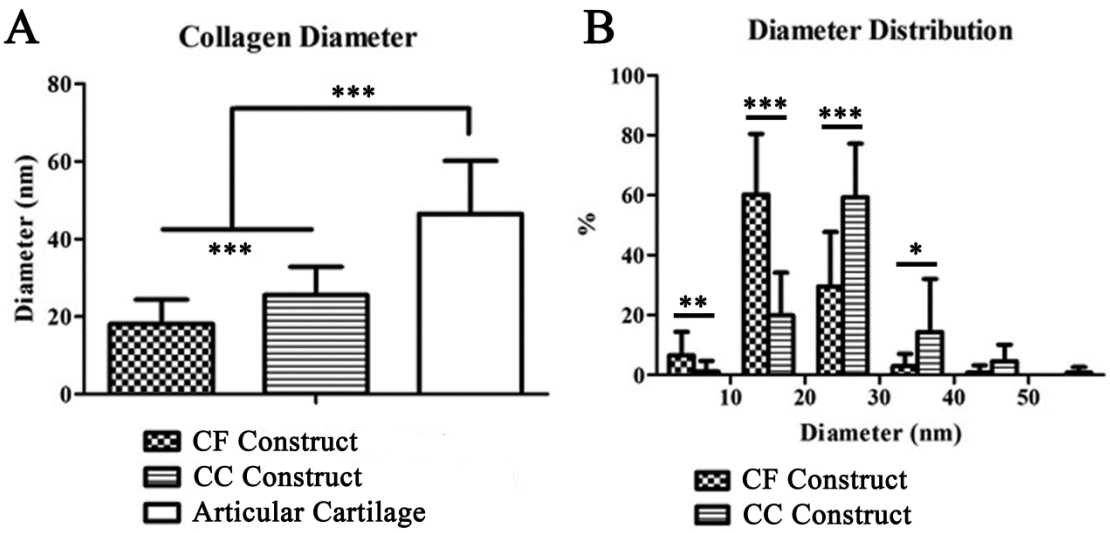

Figure 5.11 Diameter (A) and diameter distribution (B) of collagen fibrils at the integration sites. (A) ***indicates significant difference between the groups; $p < 0.001$; n = 120 (articular cartilage) or > 300 (engineered constructs). (B) *$p < 0.05$; **$p < 0.01$; ***$p < 0.001$; n = 20 (images). CC: capsule-containing; CF: capsule-free.

5.4 Discussion

Development of engineered cartilage with spatially homogeneous tissue properties remains challenging. Many studies have been focused on improving nutrient transport efficiency to yield better tissue homogeneity. For example, Kelly and coworkers cultivated chondrocyte-laden agarose gels under either free-swelling or compressively loaded conditions and found that a more even ECM synthetic potential was achieved by cells encapsulated in the loaded samples (Kelly, Ng et al. 2009). Under fluid agitation, similar hydrogel constructs embedded with microchannels also demonstrated greater tissue uniformity than those without channels (Sheehy, Buckley et al. 2011). To our best knowledge, however, no reported studies have evaluated the capsule effects on tissue homogeneity of engineered cartilage, probably due to the lack of techniques to produce intact capsule-free constructs.

The CC and the CF engineered tissues were produced in the WWB system combined with the previously established growth factor supplementation protocols utilizing IGF-1 and TGF-β1, respectively (Chapter 4). The divergent tissue morphologies of the two types of the constructs due to the presence of a type I collagen-based fibrous layer covering the construct did influence the tissue homogeneity. Specifically, superior biochemical homogeneity was observed in the constructs without a capsule whereas the inner cores of the CC constructs exhibited significantly decreased type II collagen (Figure 5.3A) and GAG (Figure 5.4A) contents compared with their own outer annuli. This reduction is likely due to compromised collagen (Figure 5.3B) and GAG (Figure 5.4B) synthetic abilities of the cells occupying the inner cores of the CC constructs. Suggestively, the fibrous capsule which is composed of abundant cells may block the

chondrocytes in the interiors of the constructs from receiving medium supplements, which thus demonstrate suppressed potential to synthesize ECM components. This blockage can be attributed to the capsule acting as a shield to hinder molecular transport similar to that observed on the exterior of embryoid bodies (Bratt-Leal, Carpenedo et al. 2009) or as a sink to consume the majority of nutrients. Noteworthily, the increased production of type I collagen by the cells in the outer annuli of the CC constructs may be organized into the formation of the fibrous capsule (Figure 5.3C). In contrast, cells in the CF engineered tissues possessed uniform potential for collagen deposition throughout the constructs (Figure 5.3B & C) and slightly better GAG synthesis in the inner cores of the constructs (Figure 5.4B). Although greater biochemical homogeneity ultimately led to better mechanical strength exhibited by the CF constructs which had stronger inner cores in comparison with the CC constructs, the stiffness of the inner core was lower than that of the intact construct in both the CC and the CF cases (Figure 5.4C). This observation substantiates that even though a uniform biochemical composition is detected throughout a tissue construct, extraction of the inner core from the construct by a punch biopsy is likely to damage its matrix network at the cut surfaces, suggesting that removal of construct periphery, i.e. capsule, will compromise the mechanical integrity of the engineered tissue.

Successful cartilage repair requires integration of implanted engineered constructs with surrounding host tissues to sustain the overall integrity and the long-term functionality of the restored joint when exposed to external loads (Khan, Gilbert et al. 2008). The second part of the current study was aimed to evaluate the potential of the fibrous capsule to contribute to cartilage integration. The *in-vitro* cartilage explant model

employed here allows us to retain control over environmental variables (Obradovic, Martin et al. 2001; Hunter and Levenston 2004; Djouad, Rackwitz et al. 2009; Gilbert, Singhrao et al. 2009) and thus to concentrate on the capsule effects. Previous studies in which the same cartilage model was utilized suggested the possible formation of a fibrous tissue covering the surfaces of the cultured hybrid composites, resulting in overestimation of integrative strength at the disc-ring interface (Moretti, Wendt et al. 2005; Gilbert, Singhrao et al. 2009). We speculated that the basic mechanism that drives the creation of this fibrous layer is similar to that involved in the capsule formation, i.e. through the direct contact of cultured chondrocytes with medium supplements that induce fibrotic processes (Ignotz and Massagué 1986; Lohmann, Schwartz et al. 2000; Kelly, Fisher et al. 2008). Therefore, hybrid composites were cultivated with a serum-free ITS-supplemented medium in the present study since we have previously demonstrated that this medium combination can potentially eliminate the formation of a fibrous capsule and simultaneously support cartilage development under loading-free conditions (Chapter 3). The SEM images confirm that the fibrous cell outgrowth on the composite surfaces was impeded or minimized as the implanted grafts were still distinguishable after 4 weeks in culture with native cartilage rings (Figure 5.8).

While tissue integration occurred at the disc-ring interface on and/or close to the composite surfaces, different wound gap sizes were observed within the composite in all the three groups, with some regions in which the gaps were narrower or closed. This is in agreement with other studies (Obradovic, Martin et al. 2001; Hunter and Levenston 2004; Tognana, Chen et al. 2005; Gilbert, Singhrao et al. 2009; Theodoropoulos, De Croos et al. 2011), suggesting that the cultivation time of 3 to 8 weeks is too short to achieve full

integration. The strongest and weakest integrative strengths were found in the CC and the native control groups, respectively (Figure 5.7). This outcome may be attributed to a combination of multiple factors. Sprouting of ECM components in the interfacial zone is a key indicator of tissue integration (Obradovic, Martin et al. 2001; Peretti, Zaporojan et al. 2003). Buds of new cartilage matrix, however, were only detected in the CC and the CF hybrid composites (Figure 5.9), which verified that native cartilage tissues barely bound to each other. Furthermore, one can expect that a greater extent of ECM penetration into the adjacent tissues will be accomplished when a longer culture period is applied (Peretti, Zaporojan et al. 2003).

The initial affinity to host cartilage tissues may predominantly depend on the GAG content of the implant (Obradovic, Martin et al. 2001; Tognana, Chen et al. 2005). Rationally, negatively charged GAG molecules form the branches of aggrecan monomers present in articular cartilage and tend to generate repelling forces against each other (Knudson and Knudson 2004). The lack of GAG in the region of the capsule present at the periphery of the CC constructs (Figure 5.6) might decrease the initial resistance to the surrounding native tissues. Conversely, the cartilage plugs had the most abundant GAG amounts that theoretically yielded the strongest force opposing the cartilage rings and thereby suppressed the integration. Supportively, Tognana and coworkers revealed that the integrative affinity of engineered cartilage to bone, a tissue containing little GAG, was significantly higher than that to cartilage, suggesting a negative correlation between tissue GAG content and construct adhesion (Tognana, Chen et al. 2005). As a result, several bioactive agents such as trypsin and chondroitinase have been utilized to reduce

GAG concentrations at tissue edges in order to promote cartilage integration (Lee, Sung et al. 2000; Obradovic, Martin et al. 2001; Khan, Gilbert et al. 2008).

Native cartilage rings used in this cartilage explant model are created by mechanical dissociation and cell death is then introduced at the cut surfaces that mimic surgical wounds (Tew, Kwan et al. 2000). Cell death occurring at the edges of both the inner disc and the outer ring may also account for the compromised adhesive strength determined at the cartilage-cartilage interface (Hunter and Levenston 2004; Theodoropoulos, De Croos et al. 2011). It has been demonstrated that this poor tissue integration can be improved by treating damaged articular cartilage with anti-apoptosis molecules such as Z-VAD-FMK during wound repair which increase the number of viable cells at the wound edge and prevent matrix loss (Gilbert, Singhrao et al. 2009). Thus, one of the benefits of implanting intact engineered cartilage is to maintain high cell viability such that cells at the implant periphery can migrate across the interfacial zone and facilitate tissue integration (Theodoropoulos, De Croos et al. 2011). In comparison with the CF composites, the high cellularity of the fibrous capsule is likely to further enhance the fusion of the CC constructs with native cartilage since more proliferating chondrocytes were observed at the integration site (Figure 5.9), leading to higher adhesive stress (Figure 5.7).

In agreement with previous reports (Shapiro, Koide et al. 1993; Fujisato, Sajiki et al. 1996; Khan, Gilbert et al. 2008; Vinardell, Thorpe et al. 2009), deposition of type I collagen was identified at the wound edge and/or at the integration site in all the groups (Figure 5.9), suggesting the induction of fibrocartilage. Therefore, another contributing factor to the superior composite integration in the case in which a fibrous capsule was

included may be the accumulation of thicker collagen fibrils at the construct-cartilage interface (Figure 5.11). This observation is confirmed by Moretti et al. who found that more mature (thicker) collagen fibrils were only present within the narrowest interfacial regions (Moretti, Wendt et al. 2005). Interestingly, the newly synthesized collagen fibrils at the integration sites were approximately aligned in the same direction along the wound edge (Figure 5.10). One possible explanation is that the initial gaps between the implanted constructs and the adjacent native tissues were too wide for cells to cross so they had to migrate along the construct edges and simultaneously laid down new matrix components to narrow the fissures. The formation of denser and thicker collagen fibrils in the CC composites can be attributed to the combined effects of increased cell density and a decreased GAG content that are usually determined in the fibrous capsule (Figure 5.6). In the cartilage-cartilage composites, such collagen organization was not found and most interfacial areas remained void or contained sparse and scattered ECM molecules (images not shown).

In this chapter, we report experiments that were designed to investigate the potential roles of a solid fibrous capsule in the development of tissue-engineered cartilage by employing two types of constructs with comparable bulk properties, but significantly divergent tissue morphologies. Our results suggest that the presence of a fibrous capsule potentially decreases tissue homogeneity of engineered cartilage such that the inner cores of the CC constructs demonstrate relatively compromised biochemical and mechanical properties. In contrast, the CF constructs exhibit greater material homogeneity and have stronger inner cores. Moreover, the inclusion of a fibrous capsule in engineered tissues effectively improves early (4 weeks) cartilage tissue integration. This outcome can result

from the combined effects of (1) the absence of GAG molecules and (2) increased cell contents in the capsule area and (3) deposition of thicker collagen fibrils at the integration site. Although the *in-vitro* cartilage explant model utilized in the current study represents a powerful template to evaluate and manipulate variables contributing to tissue integration, the findings will ultimately need to be verified in controlled *in-vivo* systems. In conclusion, the work summarized in this chapter provides a tool to study capsule functions and mechanics and indicates that the fibrous capsule is essential to enhance construct integration with native cartilage tissues even though its presence reduces construct homogeneity. Therefore, further refinement of bioprocessing conditions is necessary in order to maximize tissue homogeneity of engineered cartilage while retaining a minimal capsule thickness that is beneficial for cartilage tissue integration.

CHAPTER 6

CONCLUSIONS AND FUTURE WORK

Tissue engineering is a multidisciplinary subject that bridges engineering, material science, biology and medicine, all of which together hold promise for generation of functional and implantable substitutes to repair or restore damaged tissues including articular cartilage. Continuous refinement of tissue engineering strategies is required to optimize bioprocessing conditions for achievement of viable tissue replacements. The wavy-walled bioreactor (WWB, Chapter 2) employed here not only provides a hydrodynamic environment for cultivation of engineered constructs but also enables researchers to manipulate and study environmental factors that are vital to cultured cells and tissues. The type I collagen-based fibrous capsule which resembles fibrocartilage (Guh, Yang et al. 1996; Darling and Athanasiou 2005) represents a unique characteristic of tissue-engineered cartilage and is likely to be modulated by the synergy between environmental factors, yet its formation and function have not been thoroughly explored. In this dissertation, a better understanding of (1) the complex interplay between hydrodynamic forces and soluble biochemical cues in the capsule formation and (2) the roles of the capsule in the development of tissue-engineered cartilage was sought while the effort to systematically establish a novel low-serum/growth factor supplementation protocol for the WWB system was obtained. The findings, conclusions and recommendations drawn from this thesis work are recapitulated in this chapter.

6.1 Specific Aim 1

6.1.1 Findings

Chapter 3 summarizes the study that was aimed to evaluate (1) the feasibility of reduced serum contents to support hydrodynamic cultivation of tissue-engineered constructs and (2) the serum effects on the capsule formation. The results indicated that a serum-free ITS-supplemented culture medium was sufficient to maintain neocartilage quality under loading-free conditions. The presence of shear-sensitive serum constituents, however, may be required in order for cultured chondrocyte-seeded PGA scaffolds to benefit from turbulent flow-induced hydrodynamic forces. The evidence suggests that fluid shear stress is likely to stimulate chondrocyte growth and cartilage development via mediation of shear-sensitive soluble molecules such as TGF-β (Malaviya and Nerem 2002). On the other hand, the serum concentration was recognized to be a key factor that activated and modulated the fibrotic process of the capsule formation. Based on our data, 2% FBS or higher seemed to secure the capsule formation while fluid shear stress further promoted its development. The study outlined in Chapter 3 substantiates the importance of shear-sensitive signals derived from serum constituents in the development of hydrodynamically engineered cartilage and distinguishes potential mechanisms that drive the capsule formation and development.

6.1.2 Limitations and Future Work

In Specific Aim 1, the serum concentration was reduced by 80% (from 10% to 2%) to produce hydrodynamic constructs morphologically, compositionally and mechanically comparable to the traditional high-serum constructs. While minimized,

uncertain soluble constituents (present in 2% FBS) still exist in culture, which persists as one of the major concerns of this study. The developed approach combining a low-serum content and an FBS substitute, ITS, represents a chemically more reliable, but still somewhat undefined media preparation protocol. A solution to this issue is to uncover the unidentified shear-sensitive and fibrosis-promoting soluble molecules that contribute to neocartilage development and capsule formation, respectively, by decomposition of serum constituents using ELISA, protein microarray or mass spectrometry. The process that decouples serum components is expected to be time-consuming and costly. However, it will be greatly helpful to formulate a chemically defined serum-free medium suitable for hydrodynamic cultivation of tissue-engineered cartilage.

6.2 Specific Aim 2

6.2.1 Findings

Chapter 4 describes the experiments that were designed to investigate (1) the feasibility of transient exposure of hydrodynamically engineered cartilage to exogenous growth factors and (2) the effects of shear-sensitive growth factors on the capsule formation. Two shear-sensitive soluble molecules, TGF-β1 (fibrosis-promoting factor) and IGF-1 (non-fibrosis-promoting factor) (Ohno, Cooke et al. 1995; Sakai, Mohtai et al. 1998; Negishi, Lu et al. 2001; Malaviya and Nerem 2002; Jin, Emkey et al. 2003; Lau, Kapur et al. 2006) were employed in this study. The key findings derived from this part of the thesis are as follows. Based on the low-serum culture medium formulated in Chapter 3, transient exposure to either TGF-β1 or IGF-1 potently supported and facilitated the development of hydrodynamic constructs, suggesting that the reduced

supplementation of shear-sensitive exogenous growth factors is an effective and economical tissue engineering strategy. One of the potential contributing mechanisms to the "transient" phenomenon, which is related to homeostasis between growth factor secretion and receptor expression by cultured chondrocytes, was proposed.

The capsule formation in hydrodynamic cultures was identified as a biphasic fibrotic process in response to concentrations of fibrosis-promoting molecules (i.e. TGF-β1 in this study). The elimination of the fibrous capsule from hydrodynamic constructs due to treatment with TGF-β1 (10 ng/mL) may be attributed to a combination of several reasons. For example, when elongated fibroblast-like chondrocytes occupying the capsule region were exposed to exogenous TGF-β1 at the specified concentration, they tended to suppress the expression of the corresponding receptors to block themselves from further receiving TGF-β signals and thus stopped acting like fibroblasts, which potentially impeded the capsule formation. Given that aggregation of fibroblasts is found to promote fibrosis of different tissues and organs (Katzenstein 1985; Carthew, Edwards et al. 1991), the disappearance of the capsule may also result from a reduced level of cell accumulation at the periphery of the TGF-β1 constructs.

Modulation of intracellular Smad proteins associated with TGF-β signaling by TGF-β and Fluid shear stress was also uncovered. Specifically, both Smad2 and Smad3 pathways were potently promoted by TGF-β or fluid shear stress while TGF-β reversely regulated Smad2 and Smad3 phosphorylation under hydrodynamic stimuli partially via Smad7. In combination with analyses of tissue morphology and properties of engineered cartilage, the Smad results provide valuable insights which suggest that Smad2 and Smad3 possibly dominate chondrocyte- and fibroblast-specific phenotypes, respectively,

in articular chondrocytes and that controlled neocartilage development and capsule formation may be achieved through manipulation of intracellular signals.

The work outlined in Chapter 4 further combines the developed low-serum ITS-supplemented culture medium with the use of exogenous growth factors in a cost-efficient manner. The utilization of transient growth factor supplementation is expected to be applicable to other shear-sensitive growth factors that are vital to articular chondrocytes, such as BMPs (Khalafi, Schmid et al. 2007; Kim and Im 2008; Shen, Wei et al. 2008; An, Cheng et al. 2010). In addition, the creation of a robust capsule-free engineered construct by using the WWB system coupled with TGF-β1 will greatly benefit future studies (including the one summarized in Chapter 5) and tissue engineering applications.

6.2.2 Limitations and Future Work

In Specific Aim 2, the understanding of the "transient" phenomenon, capsule formation and Smad regulation is confined to one fluid agitation rate and one concentration for each growth factor, which needs to be broadened further. Results obtained from experiments that evaluate multiple combinations of fluid shear stress magnitude and growth factor concentration can be incorporated into the previously developed artificial neural network mathematical model (Bilgen, Uygun et al. 2009) to optimize the WWB culture conditions and to predict the capsule formation. An in-depth analysis of Smad expression by cells populating in different regions in a construct (for example, capsule versus core) needs to be carried out in order to confirm the diverse roles Smad2 and Smad3 may play in articular chondrocytes and their relation to cartilage

matrix production and capsule formation. In addition, the responses of Smad2, Smad3 and Smad7 signaling to fluid shear stress and TGF-β or other soluble molecules can also be acquired by utilizing simple perfusion systems (Yeatts and Fisher 2010) or microfluidic hydrogel devices (Choi, Cabodi et al. 2007; Ling, Rubin et al. 2007; Borenstein, Megley et al. 2010) that provide controllable fluid shear and require relatively small amounts of growth factors and medium supplements.

6.3 Specific Aim 3

6.3.1 Findings

Chapter 5 elucidates the potential effects of the presence of the capsule on tissue homogeneity of engineered cartilage and on construct capability to integrate with native cartilage. One of advantages of the use of the WWB system in combination with the growth factor supplementation protocol developed in Chapter 4 is to fabricate two types of cartilage constructs that have similar biochemical and mechanical properties, but exhibit different tissue morphologies. This benefit allows us to thoroughly focus on the capsule functions. In the evaluation of tissue homogeneity, the difference in tissue biochemical and mechanical properties between inner core and outer annulus of engineered cartilage was found to be relatively minor in the CF constructs. In contrast, the outer annuli of the CC constructs had significantly higher ECM contents and stronger mechanical strength in comparison with their own inner cores. On a per cell basis, the chondrocytes in the inner cores of the CC constructs exhibited weaker matrix synthetic potential than those in the outer annuli. The evidence suggests that the fibrous capsule

may block the cells in the interiors of the constructs from receiving medium supplements and nutrients and thereby hinders the development of the inner cores.

Analyses of tissue integration revealed that constructs with a fibrous outer capsule had a stronger integrative affinity to native cartilage than those without a capsule while the poorest integration was found at the cartilage-cartilage interface. The improved integration of the CC constructs with the surrounding native tissues is likely to be attributed to a combination of (1) the absence of GAG molecules in the capsule which enhances the initial binding of the constructs to native cartilage, (2) a higher number of proliferating cells in the capsule which leads to increased sprouting and production of new matrix components in the interfacial zone and (3) the deposition of thicker and denser collagen fibrils at the integration site. Altogether, the presence of the fibrous capsule at the periphery of engineered constructs effectively accelerates early (4 weeks) cartilage tissue integration. Collectively, we have demonstrated that tissue-engineered cartilage with a fibrous capsule has a better integration capability, but compromised material homogeneity. Thus, further investigations are needed to find the balance between the two indicators.

6.3.2 Limitations and Future Work

In Specific Aim 3, tissue homogeneity of engineered cartilage was determined by quantifying variations between inner cores and outer annuli of constructs. This analysis allowed us to evaluate the bulk properties of construct inner cores for their potential use in future applications, but might only provide a rough estimate of material homogeneity. Therefore, a more thorough investigation should involve serial dissections of a construct

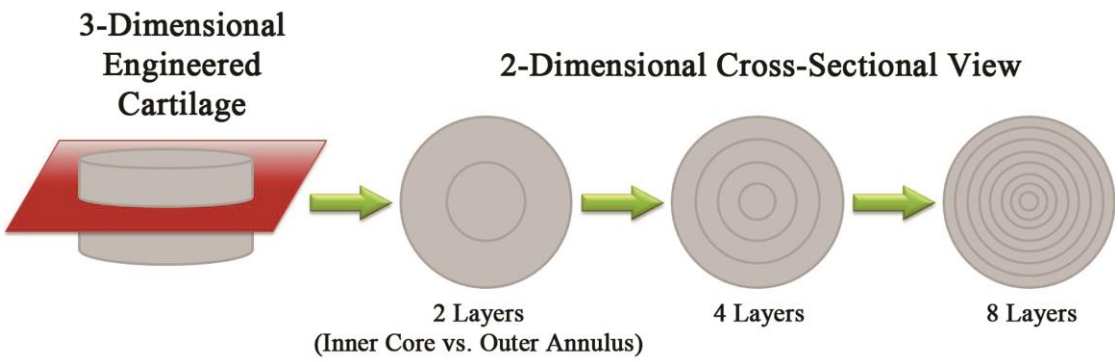

Figure 6.1 Multi-layered evaluation of tissue homogeneity. The method used in the current work to determine tissue homogeneity of engineered cartilage is based on a 2-layered approach (inner core versus outer annulus). A multi-layered analysis should be conducted in the future.

along the radial direction (Figure 6.1) to give a better definition of tissue homogeneity. Similar analyses should also be applied to assessment of variations in the axial direction to obtain a complete understanding of the capsule effects on distribution of ECM components within an engineered tissue. Homogeneity and distribution of tissue solid matrix can also be detected using other techniques such as micro-computed tomography (Case, Duty et al. 2003; Xie, Lin et al. 2009). Another limitation of this aim is the short culture period (4 weeks) applied to the tissue integration study, which resulted in poor integration detected in all the groups (large gaps still remained). This shortcoming can be overcome by extending the incubation time (Peretti, Zaporojan et al. 2003) or exposing hybrid composites to dynamic culture conditions (Obradovic, Martin et al. 2001). Either approach has been shown to greatly improve the adhesive strength at the integration site. Finally, although the cartilage explant model employed in the present work represents a useful tool to study cartilage tissue integration through manipulation of environmental parameters, it is also important to validate the findings reported here in controlled *in-vivo*

systems in order to determine the long-term stability of the capsule-improved cartilage integration. Available animal models include mice and rats (non-load-bearing) or mini-pigs and goats (load-bearing) (Chu, Szczodry et al. 2009).

6.4 Conclusions

This dissertation work is built upon the use of juvenile cells isolated from bovine donors, given that the access to human primary chondrocytes is limited and passaged chondrocytes constantly experience rapid phenotypic changes (Darling and Athanasiou 2005; Otero, Favero et al. 2012). While it may not be ideal, the use of these animal cells does enable researchers to study different environmental factors and conditions that can contribute to repair or regeneration of various tissues. Clinically however, investigations utilizing human cells will be required to verify the conclusions drawn from animal cells and studies. Additionally, general considerations that have to be kept in mind include factors like age (Tran-Khanh, Hoemann et al. 2005) and health status (Mohtai, Gupta et al. 1996; Fukui, Zhu et al. 2003) of donors that are also likely to influence the experimental outcome.

In this dissertation, we have demonstrated that tissue morphology and properties of engineered constructs can be manipulated by altering environmental factors such as loading conditions and biochemical parameters. A chemically reliable media preparation protocol involving the use of a low serum concentration and transient growth factor supplementation has been established for the WWB cultivation of tissue-engineered cartilage, which is also expected to be applicable to other types of load-bearing tissues. The overall significance of this thesis work consists in characterization of capsule

formation, development and function. The findings suggest the need to incorporate the fibrous capsule into the design of neocartilage and provide important insights for future tissue engineering studies aimed to optimize bioprocessing conditions for the development of clinically relevant cartilage tissue replacements.

APPENDIX A

BIOCHEMICAL ASSAYS AND PROTOCOLS

A.1 DNA

Reagent Preparation

1. Diluted tris-EDTA buffer
   - ❖ Dilute 20X tris-EDTA solution to 1X with deionized water.

2. PicoGreen working solution
   - ❖ Mix 100 µL of PicoGreen stock solution with 19.9 mL of diluted tris-EDTA buffer.
   - ❖ Avoid placing the mixture in direct light.
   - ❖ The solution is stable for 1 day.

3. DNA working standards
   - ❖ Dilute 30 µL of Lambda DNA standard with 1.47 mL of diluted tris-EDTA buffer (DNA stock solution: 2 µg/mL).
   - ❖ Prepare the working standards based on the table below (Table A.1).

DNA stock volume (µL)	Diluted tris-EDTA volume (µL)	Final concentration (µg/mL)
1000	0	2
500	500	1
300	700	0.6
100	900	0.2
10	990	0.02
1	999	0.002
0	1000	0

Assay Procedure

1. Dilute samples and controls with diluted tris-EDTA buffer (dilution factor = 1:60 ~ 1:120).

2. Add 100 µL of working standards, diluted samples and controls to each well of a 96-well plate in duplicate.

3. Add 100 µL of PicoGreen working solution to each well.

4. Incubate the plate in the dark at room temperature for 5 minutes.

5. Read the plate using a fluorescence plate reader with an excitation wavelength of 480 nm and an emission wavelength of 520 nm.

A.2 Glycosaminoglycan

Reagent Preparation

1. DMMB dye solution
    - ❖ Add 16 mg of DMMB to 5 mL of 100% ethanol and mix the solution for at least 12 hours until the DMMB is fully dissolved.
    - ❖ Mix the dissolved DMMB solution with 950 mL of deionized water, 8.7 mL of 1 N hydrogen chloride, 3.04 g of glycine and 2.367 g of sodium chloride.
    - ❖ Adjust pH to 3.0 using 1 N hydrogen chloride or sodium hydroxide.
    - ❖ Thoroughly mix using a stir bar.
    - ❖ Measure the absorbance of the DMMB dye solution using a spectrophotometer.
        - ✓ $0.30 < A_{525} < 0.34$
        - ✓ $1.25 < A_{592} < 1.33$
            - o If the readings are too high, dilute the dye solution with deionized water.
            - o If the readings are too low, add one grain of DMMB to the dye solution and stir it for 12 hours.
            - o Re-measure the absorbance.
    - ❖ Store in the dark for up to 3 months.

2. PBS-EDTA-cysteine solution
    - ❖ Dissolve 0.372 g of EDTA and 0.175 g of cysteine in 100 mL of PBS.
    - ❖ The solution is stable for 1 day.

3. Chondroitin sulfate working standards
    - ❖ Dissolve 50 mg of chondroitin sulfate in 10 mL of PBS-EDTA-cysteine solution (chondroitin sulfate solution: 5 mg/mL).
    - ❖ Mix 2 mL of chondroitin sulfate solution with 48 mL of PBS-EDTA-cysteine solution (chondroitin sulfate stock solution: 200 μg/mL).
    - ❖ Prepare the working standards based on the table below (Table A.2).

Chondroitin sulfate stock volume (μL)	PBS volume (μL)	Final concentration (μg/mL)
0	1000	0
125	875	25
250	750	50
375	625	75
500	500	100
625	375	125
750	250	150
875	125	175
1000	0	200

Assay Procedure

1. Dilute samples and controls with PBS (dilution factor = 1:15 ~ 1:50).

2. Add 8 μL of working standards, diluted samples and controls to each well of a 96-well plate in duplicate.

3. Add 200 μL of DMMB dye solution to each well.

4. Incubate the plate at room temperature for 2 minutes.

5. Read the plate using a spectrophotometer at 525 nm.

6. Assume a ratio of chondroitin sulfate to glycosaminoglycan of 1:1.

A.3 Total Collagen

Reagent Preparation

1. Assay stock buffer
   - ❖ Dissolve 25.217 g of monohydrate citric acid and 60 g of sodium acetate trihydrate in 423.17 mL of deionized water.
   - ❖ Add 6 mL of acetic acid, 70.83 mL of 6 N sodium hydroxide and 5 drops of toluene to the solution.

2. Assay working buffer
   - ❖ Mix 10 mL of deionized water, 15 mL of isopropanol and 50 mL of assay stock buffer together.
   - ❖ Adjust pH to 6.0 using 1 N hydrogen chloride or sodium hydroxide.
   - ❖ Store at room temperature for up to several months.

3. Chloramine-T solution
   - ❖ Mix 2 mL of deionized water, 2 mL of isopropanol and 16 mL of assay working buffer together.
   - ❖ Dissolve 0.282 g of Chloramine-T in the mixture.
   - ❖ Store in the dark at 4˚C for up to 1week.

4. pDAB solution
   - ❖ Dissolve 3 g of pDAB in 12 mL of isopropanol.
   - ❖ Add 5.2 mL of 60% perchloric acid slowly.
   - ❖ Add 2.8 mL of n-propanol to the mixture.
   - ❖ The solution is stable for 1 day.

5. Hydroxyproline working standards
   - ❖ Dissolve 10 mg of hydroxyproline in 100 mL of deionized water (hydroxyproline stock solution: 100 μg/mL).
   - ❖ Prepare the working standards based on the table below (Table A1.3).

Hydroxyproline stock volume (μL)	Deionized water volume (μL)	Final concentration (μg/mL)
0	1000	0
100	900	10
200	800	20
300	700	30
400	600	40
500	500	50
600	400	60
700	300	70
800	200	80
900	100	90
1000	0	100

Assay Procedure

1. Take 120 μL of working standards, samples and controls and place them in glass test tubes.

2. Add 120 μL of 12 N hydrogen chloride to each tube and vortex.

3. Cover the tubes with marbles and incubate them at 100˚C for 3 hours, followed by an 18-hour incubation at 95˚C using an oven in a fume hood.

4. Cool samples at room temperature.

5. Re-suspend the dried standards, samples and controls in 1 mL of deionized water and vortex.

6. Dilute samples and controls with deionized water (dilution factor = 1:2 ~ 1:10).

7. Add 50 μL of standards and diluted samples and controls to each well of a 96-well plate in duplicate.

8. Add 50 μL of chloramine-T solution to each well and incubate the plate in the dark at room temperature for 20 minutes.

9. Add 50 μL of pDAB solution to each well and incubate the plate in water bath at 60˚C for 30 minutes.

10. Cool the plate at room temperature for 15 minutes.

11. Read the plate using a spectrophotometer at 550 nm.

12. Assume a ratio of hydroxyproline to total collagen of 1:10.

A.4 Western Blot

Reagent Preparation

1. 1X running buffer
    - ❖ Dissolve 10 g of sodium dodecyl sulfate, 30 g of tris base and 144 g of glycine in 1 L of deionized water.
    - ❖ Adjust pH to 8.3 using 1 N hydrogen chloride or sodium hydroxide (10X running buffer).
    - ❖ Dilute 10X running buffer to 1X with deionized water.

2. 1X transfer buffer
    - ❖ Dissolve 30 g of tris base and 144 g of glycine in 1 L of deionized water.
    - ❖ Adjust pH to 8.3 using 1 N hydrogen chloride or sodium hydroxide (10X transfer buffer).
    - ❖ Dilute 10X transfer buffer to 1X with deionized water.

3. Diluted blocking buffer
    - ❖ Mix Li-Cor blocking solution with PBS at a ratio of 1:2.

4. Diluted primary and secondary antibodies
    - ❖ Mix primary antibodies with diluted blocking buffer at a desired ratio.
    - ❖ Mix secondary antibodies (IRDye 800CW) with diluted blocking buffer at a ratio of 1:5000.

Assay Procedure

1. Add 20 µg of total proteins to 2 µL of 5X tracking dye solution and balance with lysis buffer to obtain a final volume of 10 µL.

2. Load 10 µL of protein ladder and diluted samples into each channel of a 10% polyacrylamide gel and fill empty channels with 1X tracking dye solution diluted in lysis buffer.

3. Run electrophoresis at 100 volts in 1X running buffer for at least 1 hour until the dye reaches the bottom of the gel.

4. Rinse the gel with 1X transfer buffer.

5. Soak 3 extra thick filter papers and 1 nitrocellulose membrane in 1X transfer buffer for 20 minutes.

6. Transfer proteins from the gel to the membrane at 10 volts for 30 minutes.

7. Incubate the membrane with diluted blocking buffer at room temperature for 1 hour under shaking.

8. Incubator the membrane with diluted primary antibodies at 4˚C overnight under shaking.

9. Wash the membrane with 1X PBS/Tween-20 buffer diluted with deionized water at room temperature under shaking (3 times, 20 minutes each).

10. Incubate the membrane with diluted secondary antibodies in the dark at room temperature for 1 hour under shaking.

11. Wash the membrane with 1X PBS/Tween-20 buffer diluted with deionized water at room temperature under shaking (3 times, 20 minutes each).

12. Image the membrane with Odyssey Infrared Scanner.

APPENDIX B

HISTOLOGY AND IMMUNOHISTOCHEMISTRY

B.1 Hematoxylin and Eosin

Table B.1 Hematoxylin and Eosin Staining Protocol

Step	Reagent	Time (min : sec)
1	Distilled water	01 : 00
2	Hematoxylin	00 : 45
3	Distilled water	01 : 00
4	1% acid alcohol	00 : 01
5	Distilled water	01 : 00
6	Scott's	00 : 30
7	Deionized water	02 : 00
8	95% alcohol	01 : 00
9	Eosin, alcoholic	03 : 00
10	95% alcohol	00 : 30
11	100% alcohol	01 : 00
12	100% alcohol	02 : 00
13	100% alcohol	02 : 00
14	Xylene substitute	02 : 00
15	Xylene substitute	02 : 00
16	Xylene	01 : 00

Results:
Cell nuclei are blue-purple.

B.2 Safranin-O and Fast Green

Table B.2 Safranin-O and Fast Green Staining Protocol

Step	Reagent	Time (min : sec)
1	Distilled water	01 : 00
2	Weigert's hematoxylin working solution	02 : 00
3	Distilled water	05 : 00
4	0.2% aqueous fast green	01 : 00
5	1% acetic acid	00 : 03
6	0.5% safranin-O	05 : 00
7	95% alcohol	01 : 00
8	100% alcohol	01 : 00
9	100% alcohol	01 : 00
10	100% alcohol	01 : 00
11	Xylene substitute	01 : 00
12	Xylene substitute	01 : 00
13	Xylene	01 : 00

Results:
GAG, nuclei and cytoplasm are stained pink/red, black and green, respectively.

B.3 Masson's Trichrome

Table B.3 Masson's Trichrome Staining Protocol

Step	Reagent	Time (min : sec)
1	Distilled water	01 : 00
2	Bouin's solution (56˚C)	60 : 00
3	Distilled water	05 : 00
4	Weigert's hematoxylin working solution	02 : 00
5	Distilled water	05 : 00
6	Biebrich scarlet-acid fuchsin solution	05 : 00
7	Distilled water	01 : 00
8	Phosphomolybdic-phosphotungstic acid	01 : 00
9	2.5% aniline blue	05 : 00
10	1% acetic acid	05 : 00
11	95% alcohol	01 : 00
12	100% alcohol	01 : 00
13	100% alcohol	01 : 00
14	100% alcohol	01 : 00
15	Xylene substitute	01 : 00
16	Xylene substitute	01 : 00
17	Xylene	01 : 00

Results:
Collagen and nuclei are blue and black, respectively.

B.4 Immunohistochemistry

Reagent Preparation

1. Sodium citrate solution
   - ❖ Dissolve 2.94 g of sodium citrate in 1 L of deionized water.
   - ❖ Adjust pH to 6.0 using 1 N hydrogen chloride or sodium hydroxide.
   - ❖ Add 500 µL of 20X PBS/Tween-20 solution.
   - ❖ Store at room temperature for 3 months or at 4˚C for longer storage.

2. 0.3% hydrogen peroxide solution
   - ❖ Dilute 1 mL of 3% hydrogen peroxide with 9 mL of DI water.

3. Blocking buffer
   - ❖ Mix 150 µL of (goat) serum with 10 mL of PBS.

4. Diluted primary and secondary antibodies
   - ❖ Mix primary antibodies with blocking buffer at a desired ratio.
   - ❖ Mix avidin-biotinylated secondary antibodies with blocking buffer at a ratio of 1:200.

5. Avidin-biotin complex (ABC)
   - ❖ Add 100 µL of avidin and 100 µL of biotinylated horseradish peroxidase to 10 mL of PBS and incubate for 30 minutes before use.

6. Diaminobenzidine working solution
   - ❖ Add 100 µL of diaminobenzidine stock solution and 50 µL of hydrogen peroxide to 1 mL of PBS.
   - ❖ Avoid placing the mixture in direct light.

Staining Procedure

1. Rinse sectioned samples with deionized water for 5 minutes.

2. Incubate sections with 0.3% hydrogen peroxide solution at room temperature for 30 minutes.

3. Rinse sections 2 times with PBS, 2 minutes each.

4. Antigen retrieval
   - ❖ Pre-heat sodium citrate solution to 100˚C.
   - ❖ Incubate sections with 100˚C sodium citrate solution for 30 minutes.
   - ❖ Cool sections at room temperature for 20 minutes.

5. Rinse sections 2 times with PBS, 2 minutes each.

6. Incubate sections with blocking buffer at room temperature for 20 minutes and remove excess blocking solution from slides.

7. Incubate sections with diluted primary antibodies at 4˚C for 17 hours.

8. Rinse sections 2 times with PBS, 2 minutes each.

9. Incubate sections with diluted secondary antibodies at room temperature for 30 minutes.

10. Rinse sections 2 times with PBS, 2 minutes each.

11. Incubate sections with ABC solution at room temperature for 30 minutes.

12. Rinse sections 2 times with PBS, 2 minutes each.

13. Incubate sections with diaminobenzidine working solution at room temperature for 12 minutes or until optimal staining developed.

14. Rinse sections 3 times with deionized water, 1 minute each.

APPENDIX C

ELECTRON MICROSCOPY

C.1 Scanning Electron Microscopy

Reagent Preparation

1. 0.1 M cacodylic acid buffer
   - ❖ Dissolve 13.8 g of cacodylic acid in 1 L of deionized water.
   - ❖ Adjust pH to 7.3 using 1 N hydrogen chloride or sodium hydroxide.

2. Fixing solution
   - ❖ Mix 10 mL of 25% glutaradehyde with 115 mL of 0.1 M cacodylic acid buffer.

Sample Processing Procedure

1. Wash samples 3 times with 0.1 M cacodylic acid buffer, 10 minutes each.

2. Incubate samples with fixing solution at 4˚C for 48 hours.

3. Rinse samples 3 times with 0.1 M cacodylic acid buffer, 25 minutes each.

4. Rinse samples 3 times with deionized water, 20 minutes each.

5. Dehydrate samples in a graded ethanol series based on the table below (Table C.1).

Step	Reagent	Time (min)
1	30% ethanol	25
2	50% ethanol	25
3	75% ethanol	25
4	95% ethanol	25
5	95% ethanol	25
6	100% ethanol	25
7	100% ethanol	25
8	100% ethanol	25

6. Dry samples in a critical point dryer.

7. Mount the dried samples onto aluminum stubs with carbon stickers.

8. Coat the mounted samples with a thin layer of gold using a sputter coater.

9. Microscopy.

C.2 Transmission Electron Microscopy

Reagent Preparation

1. 0.1 M cacodylic acid buffer
   - ❖ Dissolve 13.8 g of cacodylic acid in 1 L of deionized water.
   - ❖ Adjust pH to 7.3 using 1 N hydrogen chloride or sodium hydroxide.

2. Primary fixing solution
   - ❖ Mix 10 mL of 25% glutaradehyde with 115 mL of 0.1 M cacodylic acid buffer.

3. Secondary fixing solution
   - ❖ Mix 2%, w/v osmium tetroxide diluted with deionized water with 0.1 M cacodylic acid buffer at a ratio of 1:1.

Sample Processing Procedure

1. Wash samples 3 times with 0.1 M cacodylic acid buffer, 10 minutes each.

2. Incubate samples with primary fixing solution at 4˚C for 48 hours.

3. Rinse samples 3 times with 0.1 M cacodylic acid buffer, 15 minutes each.

4. Post-fix samples in secondary fixing solution at room temperature for 2 hours.

5. Rinse samples with 0.1 M cacodylic acid buffer for 20 minutes.

6. Rinse samples 4 times with deionized water, 15 minutes each.

7. Incubate samples with 0.5% uranyl acetate diluted with 0.1 M cacodylic acid buffer in the dark for 1 hour.

8. Rinse samples 3 times with deionized water, 10 minutes each.

9. Dehydrate samples based on the table below (Table C.2).

Step	Reagent	Time (min)
1	30% ethanol	20
2	50% ethanol	20
3	75% ethanol	20
4	95% ethanol	20
5	95% ethanol	20
6	100% ethanol	20
7	100% ethanol	20
8	100% acetone	10
9	100% acetone	10
10	100% propylene oxide	15
11	100% propylene oxide	15

10. Infiltrate samples with Epon/Araldite-DDSA-DMP30 (EA mixture).
    - ❖ Incubate samples with EA mixture and propylene oxide mixed at a ratio of 1:1 for 2 hours.
    - ❖ Incubate samples with fresh 100% EA mixture for 2 hours.
    - ❖ Incubate samples with fresh 100% EA mixture for an additional 2 hours.

11. Embed samples in 100% EA mixture at 60˚C for 24 hours.

12. Section resin blocks in 60-nm thick slices.

13. Mount slices onto meshed gilder grids.

14. Incubate grids with 5% methanolic uranyl acetate for 5 minutes.

15. Rinse grids 2 times with deionized water, 1 minute each.

16. Incubate grids with Reynold's lead citrate for 8 minutes.

17. Rinse grids 2 times with deionized water, 1 minute each.

18. Microscopy.

REFERENCES

Agrawal, C. M., Athanasiou, K. A., et al. (1997). "Biodegradable PLA-PGA Polymers for Tissue Engineering in Orthopaedics." Materials Science Forum **250**: 115-128.

Agrawal, C. M., Mckinney, J. S., et al. (2000). "Effects of Fluid Flow on the in Vitro Degradation Kinetics of Biodegradable Scaffolds for Tissue Engineering." Biomaterials **21**(23): 2443-2452.

Ahamed, J., Burg, N., et al. (2008). "In Vitro and in Vivo Evidence for Shear-Induced Activation of Latent Transforming Growth Factor-β1." Blood **112**(9): 3650-3660.

Ahsan, T. and Sah, R. L. (1999). "Biomechanics of Integrative Cartilage Repair." Osteoarthritis and Cartilage **7**(1): 29-40.

An, C., Cheng, Y., et al. (2010). "IGF-1 and BMP-2 Induces Differentiation of Adipose-Derived Mesenchymal Stem Cells into Chondrocytes-Like Cells." Annals of Biomedical Engineering **38**(4): 1647-1654.

Andres, B. M., Mears, S. C., et al. (2001). "Surgical Treatment Options for Cartilage Defects within the Knee." Orthopaedic Nursing **20**(3): 27-31.

Angelidis, I. K., Thorfinn, J., et al. (2009). "Tissue Engineering of Flexor Tendons: The Effect of a Tissue Bioreactor on Adipoderived Stem Cell-Seeded and Fibroblast-Seeded Constructs." Journal of the American College of Surgeons **209**(3, Supplement 1): S75-S76.

Bantsimba-Malanda, C., Marchal-Sommé, J., et al. (2010). "A Role for Dendritic Cells in Bleomycin-Induced Pulmonary Fibrosis in Mice?" American Journal of Respiratory and Critical Care Medicine **182**(3): 385-395.

Barabino, G. A., Metghalchi, M., et al. (1993). "Mammalian Cell Culture in a Novel Bioreactor." American Society of Mechanical Engineers (Bioprocess Engineering Symposium) **27**: 1-4.

Barron, V., Lyons, E., et al. (2003). "Bioreactors for Cardiovascular Cell and Tissue Growth: A Review." Annals of Biomedical Engineering **31**(9): 1017-1030.

Basalo, I. M., Chahine, N. O., et al. (2007). "Chondroitin Sulfate Reduces the Friction Coefficient of Articular Cartilage." Journal of Biomechanics **40**(8): 1847-1854.

Bian, L., Lima, E. G., et al. (2008). "Mechanical and Biochemical Characterization of Cartilage Explants in Serum-Free Culture." Journal of Biomechanics **41**(6): 1153-1159.

Bian, L., Kaplun, M., et al. (2009). "Influence of Chondroitin Sulfate on the Biochemical, Mechanical and Frictional Properties of Cartilage Explants in Long-Term Culture." Journal of Biomechanics **42**(3): 286-290.

Bilgen, B., Chang-Mateu, I. M., et al. (2005). "Characterization of Mixing in a Novel Wavy-Walled Bioreactor for Tissue Engineering." Biotechnology and Bioengineering **92**(7): 907-919.

Bilgen, B., Sucosky, P., et al. (2006). "Flow Characterization of a Wavy-Walled Bioreactor for Cartilage Tissue Engineering." Biotechnology and Bioengineering **95**(6): 1009-1022.

Bilgen, B. and Barabino, G. A. (2007). "Location of Scaffolds in Bioreactors Modulates the Hydrodynamic Environment Experienced by Engineered Tissues." Biotechnology and Bioengineering **98**(1): 282-294.

Bilgen, B., Orsini, E., et al. (2007). "Fetal Bovine Serum Suppresses Transforming Growth Factor-β1-Induced Chondrogenesis in Synoviocyte Pellet Cultures While Dexamethasone and Dynamic Stimuli Are Beneficial." Journal of Tissue Engineering and Regenerative Medicine **1**(6): 436-442.

Bilgen, B., Uygun, K., et al. (2009). "Tissue Growth Modeling in a Wavy-Walled Bioreactor." Tissue Engineering Part A **15**(4): 761-771.

Bilodeau, K. and Mantovani, D. (2006). "Bioreactors for Tissue Engineering: Focus on Mechanical Constraints. A Comparative Review." Tissue Engineering **12**(8): 2367-2383.

Blunk, T., Sieminski, A. L., et al. (2002). "Differential Effects of Growth Factors on Tissue-Engineered Cartilage." Tissue Engineering **8**(1): 73-84.

Böhme, K., Winterhalter, K. H., et al. (1995). "Terminal Differentiation of Chondrocytes in Culture Is a Spontaneous Process and Is Arrested by Transforming Growth Factor-β2 and Basic Fibroblast Growth Factor in Synergy." Experimental Cell Research **216**(1): 191-198.

Borenstein, J. T., Megley, K., et al. (2010). "Tissue Equivalents Based on Cell-Seeded Biodegradable Microfluidic Constructs." Materials **3**(3): 1833-1844.

Bos, L. and Ellermann, A. (2003). "Indication and Results of Autologous Osteochondral Transplantation of the Knee." Deutsche Zeitschrift Fur Sportmedizin **54**(6): 222-224.

Bouffi, C., Thomas, O., et al. (2010). "The Role of Pharmacologically Active Microcarriers Releasing TGF-β3 in Cartilage Formation in Vivo by Mesenchymal Stem Cells." Biomaterials **31**(25): 6485-6493.

Bratt-Leal, A. M., Carpenedo, R. L., et al. (2009). "Engineering the Embryoid Body Microenvironment to Direct Embryonic Stem Cell Differentiation." Biotechnology Progress **25**(1): 43-51.

Brittberg, M., Lindahl, A., et al. (1994). "Treatment of Deep Cartilage Defects in the Knee with Autologous Chondrocyte Transplantation." New England Journal of Medicine **331**(14): 889-895.

Brown, K. A., Pietenpol, J. A., et al. (2007). "A Tale of Two Proteins: Differential Roles and Regulation of Smad2 and Smad3 in TGF-β Signaling." Journal of Cellular Biochemistry **101**(1): 9-33.

Brown, T. D., Johnston, R. C., et al. (2006). "Posttraumatic Osteoarthritis: A First Estimate of Incidence, Prevalence, and Burden of Disease." Journal of Orthopaedic Trauma **20**(10): 739-744.

Buckwalter, J., Mow, V., et al. (1994). "Restoration of Injured or Degenerated Articular Cartilage." Journal of the American Academy of Orthopaedic Surgeons **2**(4): 192-201.

Bueno, E. M., Bilgen, B., et al. (2004). "Increased Rate of Chondrocyte Aggregation in a Wavy-Walled Bioreactor." Biotechnology and Bioengineering **88**(6): 767-777.

Bueno, E. M., Bilgen, B., et al. (2005). "Wavy-Walled Bioreactor Supports Increased Cell Proliferation and Matrix Deposition in Engineered Cartilage Constructs." Tissue Engineering **11**(11-12): 1699-1709.

Bueno, E. M., Laevsky, G., et al. (2007). "Enhancing Cell Seeding of Scaffolds in Tissue Engineering through Manipulation of Hydrodynamic Parameters." Journal of Biotechnology **129**(3): 516-531.

Bueno, E. M., Bilgen, B., et al. (2008). "Hydrodynamic Parameters Modulate Biochemical, Histological, and Mechanical Properties of Engineered Cartilage." Tissue Engineering Part A **15**(4): 773-785.

Byers, B. A., Mauck, R. L., et al. (2008). "Transient Exposure to Transforming Growth Factor-β3 under Serum-Free Conditions Enhances the Biomechanical and Biochemical Maturation of Tissue-Engineered Cartilage." Tissue Engineering Part A **14**(11): 1821-1834.

Carthew, P., Edwards, R. E., et al. (1991). "Rapid Induction of Hepatic Fibrosis in the Gerbil after the Parenteral Administration of Iron-Dextran Complex." Hepatology **13**(3): 534-539.

Cartmell, S. H., Porter, B. D., et al. (2003). "Effects of Medium Perfusion Rate on Cell-Seeded Three-Dimensional Bone Constructs in Vitro." Tissue Engineering **9**(6): 1197-1203.

Case, N. D., Duty, A. O., et al. (2003). "Bone Formation on Tissue-Engineered Cartilage Constructs in Vivo: Effects of Chondrocyte Viability and Mechanical Loading." Tissue Engineering **9**(4): 587-596.

Caterson, E. J., Nesti, L. J., et al. (2001). "Three-Dimensional Cartilage Formation by Bone Marrow-Derived Cells Seeded in Polylactide/Alginate Amalgam." Journal of Biomedical Materials Research **57**(3): 394-403.

Chen, F. H., Rousche, K. T., et al. (2006). "Technology Insight: Adult Stem Cells in Cartilage Regeneration and Tissue Engineering." Nature Clinical Practice Rheumatology **2**(7): 373-382.

Cheng, Y. J., Hootman, J. M., et al. (2010). "Prevalence of Doctor-Diagnosed Arthritis and Arthritis-Attributable Activity Limitation--United States, 2007 2009." Morbidity and Mortality Weekly Report **59**(39): 1261-1265.

Cheung, W.-H., Lee, K.-M., et al. (2001). "TGF-β1 Is the Factor Secreted by Proliferative Chondrocytes to Inhibit Neo-Angiogenesis." Journal of Cellular Biochemistry **81**(S36): 79-88.

Childs, C. B., Proper, J. A., et al. (1982). "Serum Contains a Platelet-Derived Transforming Growth Factor." Proceedings of the National Academy of Sciences of the United States of America **79**(17): 5312-5316.

Chiu, A., Nanaji, N. M., et al. (2009). "The Stromal Composition of Mast Cell Aggregates in Systemic Mastocytosis." Modern Pathology **22**(7): 857-865.

Chiu, J. B., Luu, Y. K., et al. (2005). "Electrospun Nanofibrous Scaffolds for Biomedical Applications." Journal of Biomedical Nanotechnology **1**(2): 115-132.

Choi, N. W., Cabodi, M., et al. (2007). "Microfluidic Scaffolds for Tissue Engineering." Nature materials **6**(11): 908-915.

Chu, C. R., Szczodry, M., et al. (2009). "Animal Models for Cartilage Regeneration and Repair." Tissue Engineering Part B: Reviews **16**(1): 105-115.

Chua, K. H., Aminuddin, B. S., et al. (2005). "Insulin-Transferrin-Selenium Prevent Human Chondrocyte Dedifferentiation and Promote the Formation of High Quality Tissue Engineered Human Hyaline Cartilage." European Cells and Materials **9**: 58-67.

Chung, C. and Burdick, J. A. (2008). "Influence of Three-Dimensional Hyaluronic Acid Microenvironments on Mesenchymal Stem Cell Chondrogenesis." Tissue Engineering Part A **15**(2): 243-254.

Chung, C. and Burdick, J. A. (2008). "Engineering Cartilage Tissue." Advanced Drug Delivery Reviews **60**(2): 243-262.

Clemmons, D. R., Busby, W. H., et al. (2002). "Inhibition of Insulin-Like Growth Factor Binding Protein 5 Proteolysis in Articular Cartilage and Joint Fluid Results in Enhanced Concentrations of Insulin-Like Growth Factor-1 and Is Associated with Improved Osteoarthritis." Arthritis and Rheumatism **46**(3): 694-703.

Cohen, N. P., Foster, R. J., et al. (1998). "Composition and Dynamics of Articular Cartilage: Structure, Function, and Maintaining Healthy State." The Journal of Orthopaedic and Sports Physical Therapy **28**(4): 203-215.

Cole, B. J. and Malek, M. M. (2004). Articular Cartilage Lesions : A Practical Guide to Assessment and Treatment. New York, Springer.

Danielpour, D., Kim, K.-Y., et al. (1989). "Sandwich Enzyme-Linked Immunosorbent Assays (Selisas) Quantitate and Distinguish Two Forms of Transforming Growth Factor-β (TGF-β1 and TGF-β2) in Complex Biological Fluids." Growth Factors **2**(1): 61-71.

Danielpour, D. (1993). "Improved Sandwich Enzyme-Linked Immunosorbent Assays for Transforming Growth Factor-β1." Journal of Immunological Methods **158**(1): 17-25.

Darling, E. M. and Athanasiou, K. A. (2003). "Articular Cartilage Bioreactors and Bioprocesses." Tissue Engineering **9**(1): 9-26.

Darling, E. M. and Athanasiou, K. A. (2005). "Rapid Phenotypic Changes in Passaged Articular Chondrocyte Subpopulations." Journal of Orthopaedic Research **23**(2): 425-432.

Das, P., Schurman, D. J., et al. (1997). "Nitric Oxide and G Proteins Mediate the Response of Bovine Articular Chondrocytes to Fluid-Induced Shear." Journal of Orthopaedic Research **15**(1): 87-93.

Davies, L. C., Blain, E. J., et al. (2008). "The Potential of Insulin-Like Growth Factor-1 and Transforming Growth Factor-Beta1 for Promoting "Adult" Articular Cartilage Repair: An in Vitro Study." Tissue Engineering Part A **14**(7): 1251-1261.

Davies, P. F. (1995). "Flow-Mediated Endothelial Mechanotransduction." Physiological Reviews **75**(3): 519-560.

Davisson, T., Kunig, S., et al. (2002). "Static and Dynamic Compression Modulate Matrix Metabolism in Tissue Engineered Cartilage." Journal of Orthopaedic Research **20**(4): 842-848.

Defail, A. J., Chu, C. R., et al. (2006). "Controlled Release of Bioactive TGF-β1 from Microspheres Embedded within Biodegradable Hydrogels." Biomaterials **27**(8): 1579-1585.

Derynck, R., Lindquist, P. B., et al. (1988). "A New Type of Transforming Growth Factor-β, TGF-β3." EMBO Journal **7**(12): 3737-3743.

Derynck, R. and Zhang, Y. E. (2003). "Smad-Dependent and Smad-Independent Pathways in TGF-β Family Signalling." Nature **425**(6958): 577-584.

Dimicco, M. A., Waters, S. N., et al. (2002). "Integrative Articular Cartilage Repair: Dependence on Developmental Stage and Collagen Metabolism." Osteoarthritis and cartilage **10**(3): 218-225.

Djouad, F., Rackwitz, L., et al. (2009). "ERK1/2 Activation Induced by Inflammatory Cytokines Compromises Effective Host Tissue Integration of Engineered Cartilage." Tissue Engineering Part A **15**(10): 2825-2835.

Dobaczewski, M., Bujak, M., et al. (2010). "Smad3 Signaling Critically Regulates Fibroblast Phenotype and Function in Healing Myocardial Infarction." Circulation Research **107**(3): 418-428.

Dunkelman, N. S., Zimber, M. P., et al. (1995). "Cartilage Production by Rabbit Articular Chondrocytes on Polyglycolic Acid Scaffolds in a Closed Bioreactor System." Biotechnology and Bioengineering **46**(4): 299-305.

Dupont, J., Khan, J., et al. (2001). "Insulin and IGF-1 Induce Different Patterns of Gene Expression in Mouse Fibroblast NIH-3T3 Cells: Identification by Cdna Microarray Analysis." Endocrinology **142**(11): 4969-4975.

Duraine, G., Neu, C. P., et al. (2009). "Regulation of the Friction Coefficient of Articular Cartilage by Transforming Growth Factor-β1 and Interleukin-1β." Journal of Orthopaedic Research **27**(2): 249-256.

Duty, A. O., Oest, M. E., et al. (2007). "Cyclic Mechanical Compression Increases Mineralization of Cell-Seeded Polymer Scaffolds in Vivo." Journal of Biomechanical Engineering **129**(4): 531-539.

Elder, B. D. and Athanasiou, K. A. (2009). "Effects of Temporal Hydrostatic Pressure on Tissue-Engineered Bovine Articular Cartilage Constructs." Tissue Engineering Part A **15**(5): 1151-1158.

Elder, B. D. and Athanasiou, K. A. (2009). "Hydrostatic Pressure in Articular Cartilage Tissue Engineering: From Chondrocytes to Tissue Regeneration." Tissue Engineering Part B: Reviews **15**(1): 43-53.

Emin, N., Koç, A., et al. (2008). "Engineering of Rat Articular Cartilage on Porous Sponges: Effects of TGF-β1 and Microgravity Bioreactor Culture." Artificial Cells, Blood Substitutes, & Biotechnology **36**(2): 123-137.

Engler, A. J., Sen, S., et al. (2006). "Matrix Elasticity Directs Stem Cell Lineage Specification." Cell **126**(4): 677-689.

Erickson, I. E., Huang, A. H., et al. (2009). "Differential Maturation and Structure–Function Relationships in Mesenchymal Stem Cell- and Chondrocyte-Seeded Hydrogels." Tissue Engineering Part A **15**(5): 1041-1052.

Farndale, R. W., Buttle, D. J., et al. (1986). "Improved Quantitation and Discrimination of Sulphated Glycosaminoglycans by Use of Dimethylmethylene Blue." Biochimica et biophysica acta **883**(2): 173-177.

Farooque, T. M. (2008). Biochemical and Mechanical Stimuli for Improved Material Properties and Preservation of Tissue-Engineered Cartilage. Ph.D., Georgia Institute of Technology.

Fischer, J., Dickhut, A., et al. (2010). "Human Articular Chondrocytes Secrete Parathyroid Hormone–Related Protein and Inhibit Hypertrophy of Mesenchymal Stem Cells in Coculture During Chondrogenesis." Arthritis and Rheumatism **62**(9): 2696-2706.

Fitzsimmons, J. S., Sanyal, A., et al. (2004). "Serum-Free Media for Periosteal Chondrogenesis in Vitro." Journal of Orthopaedic Research **22**(4): 716-725.

Fragiadaki, M., Ikeda, T., et al. (2011). "High Doses of TGF-β Potently Suppress Type I Collagen via the Transcription Factor CUX1." Molecular Biology of the Cell **22**(11): 1836-1844.

Freed, L. E., Marquis, J. C., et al. (1993). "Neocartilage Formation in Vitro and in Vivo Using Cells Cultured on Synthetic Biodegradable Polymers." Journal of Biomedical Materials Research **27**(1): 11-23.

Freed, L. E. and Vunjak-Novakovic, G. (1995). "Cultivation of Cell-Polymer Tissue Constructs in Simulated Microgravity." Biotechnology and Bioengineering **46**(4): 306-313.

Friedrich, N., Haring, R., et al. (2009). "Mortality and Serum Insulin-Like Growth Factor (IGF)-1 and IGF Binding Protein 3 Concentrations." Journal of Clinical Endocrinology and Metabolism **94**(5): 1732-1739.

Fu, K., Pack, D. W., et al. (2000). "Visual Evidence of Acidic Environment within Degrading Poly(Lactic-Co-Glycolic Acid) (PLGA) Microspheres." Pharmaceutical Research **17**(1): 100-106.

Fujisato, T., Sajiki, T., et al. (1996). "Effect of Basic Fibroblast Growth Factor on Cartilage Regeneration in Chondrocyte-Seeded Collagen Sponge Scaffold." Biomaterials **17**(2): 155-162.

Fukui, N., Zhu, Y., et al. (2003). "Stimulation of BMP-2 Expression by Pro-Inflammatory Cytokines IL-1 and TNF-α in Normal and Osteoarthritic Chondrocytes." The Journal of Bone and Joint Surgery **85**(Supplement 3): 59-66.

Garcia, A. M., Frank, E. H., et al. (1996). "Contributions of Fluid Convection and Electrical Migration to Transport in Cartilage: Relevance to Loading." Archives of Biochemistry and Biophysics **333**(2): 317-325.

Garcia, A. M., Lark, M. W., et al. (1998). "Transport of Tissue Inhibitor of Metalloproteinases-1 through Cartilage: Contributions of Fluid Flow and Electrical Migration." Journal of Orthopaedic Research **16**(6): 734-742.

Gebken, J., Feydt, A., et al. (1999). "Ligand-Induced Downregulation of Receptors for TGF-β in Human Osteoblast-Like Cells from Adult Donors." Journal of Endocrinology **161**(3): 503-510.

Gemmiti, C. V. and Guldberg, R. E. (2006). "Fluid Flow Increases Type II Collagen Deposition and Tensile Mechanical Properties in Bioreactor-Grown Tissue-Engineered Cartilage." Tissue Engineering **12**(3): 469-479.

Gigout, A., Buschmann, M. D., et al. (2009). "Chondrocytes Cultured in Stirred Suspension with Serum-Free Medium Containing Pluronic-68 Aggregate and Proliferate While Maintaining Their Differentiated Phenotype." Tissue Engineering Part A **15**(8): 2237-2248.

Gilbert, S. J., Singhrao, S. K., et al. (2009). "Enhanced Tissue Integration During Cartilage Repair in Vitro Can Be Achieved by Inhibiting Chondrocyte Death at the Wound Edge." Tissue Engineering Part A **15**(7): 1739-1749.

Glowacki, J., Yates, K. E., et al. (2005). "In Vitro Engineering of Cartilage: Effects of Serum Substitutes, TGF-β, and IL-1α." Orthodontics and Craniofacial Research **8**(3): 200-208.

Gooch, K. J., Blunk, T., et al. (2001). "Insulin-Like Growth Factor-1 and Mechanical Environment Interact to Modulate Engineered Cartilage Development." Biochemical and Biophysical Research Communications **286**(5): 909-915.

Gray, M. L., Pizzanelli, A. M., et al. (1989). "Kinetics of the Chondrocyte Biosynthetic Response to Compressive Load and Release." Biochimica et Biophysica Acta (BBA) - General Subjects **991**(3): 415-425.

Grodzinsky, A. J., Levenston, M. E., et al. (2000). "Cartilage Tissue Remodeling in Response to Mechanical Forces." Annual Review of Biomedical Engineering **2**(1): 691-713.

Guh, J. Y., Yang, M. L., et al. (1996). "Captopril Reverses High-Glucose-Induced Growth Effects on LLC-PK1 Cells Partly by Decreasing Transforming Growth Factor-β Receptor Protein Expressions." Journal of the American Society of Nephrology **7**(8): 1207-1215.

Hahn, M., Mchale, M., et al. (2007). "Physiologic Pulsatile Flow Bioreactor Conditioning of Poly(Ethylene Glycol)-Based Tissue Engineered Vascular Grafts." Annals of Biomedical Engineering **35**(2): 190-200.

Hall, A., Horwitz, E., et al. (1996). "The Cellular Physiology of Articular Cartilage." Experimental Physiology **81**(3): 535-545.

Hand, C. J., Lobo, J. J. A., et al. (2003). "Osteochondral Autograft Resurfacing." Sports Medicine and Arthroscopy Review **11**(4): 245-263.

Hangody, L., Kish, G., et al. (1998). "Mosaicplasty for the Treatment of Articular Cartilage Defects: Application in Clinical Practice." Orthopedics **21**(7): 751-756.

Hangody, L., Feczkó, P., et al. (2001). "Mosaicplasty for the Treatment of Articular Defects of the Knee and Ankle." Clinical Orthopaedics and Related Research **391**: S328-S336.

Hannouche, D., Terai, H., et al. (2007). "Engineering of Implantable Cartilaginous Structures from Bone Marrow–Derived Mesenchymal Stem Cells." Tissue Engineering **13**(1): 87-99.

Hidaka, C., Cheng, C., et al. (2006). "Maturational Differences in Superficial and Deep Zone Articular Chondrocytes." Cell and Tissue Research **323**(1): 127-135.

Holland, T. A., Tabata, Y., et al. (2005). "Dual Growth Factor Delivery from Degradable Oligo(Poly(Ethylene Glycol) Fumarate) Hydrogel Scaffolds for Cartilage Tissue Engineering." Journal of Controlled Release **101**(1–3): 111-125.

Holland, T. A., Bodde, E. W. H., et al. (2007). "Degradable Hydrogel Scaffolds for in Vivo Delivery of Single and Dual Growth Factors in Cartilage Repair." Osteoarthritis and Cartilage **15**(2): 187-197.

Holmvall, K., Camper, L., et al. (1995). "Chondrocyte and Chondrosarcoma Cell Integrins with Affinity for Collagen Type II and Their Response to Mechanical Stress." Experimental Cell Research **221**(2): 496-503.

Hou, J. S., Mow, V. C., et al. (1992). "An Analysis of the Squeeze-Film Lubrication Mechanism for Articular Cartilage." Journal of Biomechanics **25**(3): 247-259.

Huang, A. H., Stein, A., et al. (2009). "Transient Exposure to Transforming Growth Factor-β3 Improves the Mechanical Properties of Mesenchymal Stem Cell–Laden Cartilage Constructs in a Density-Dependent Manner." Tissue Engineering Part A **15**(11): 3461-3472.

Hunter, C. J. and Levenston, M. E. (2004). "Maturation and Integration of Tissue-Engineered Cartilages within an in Vitro Defect Repair Model." Tissue Engineering **10**(5-6): 736-746.

Huntley, J. S., Bush, P. G., et al. (2005). "Chondrocyte Death Associated with Human Femoral Osteochondral Harvest as Performed for Mosaicplasty." Journal of Bone and Joint Surgery **87**(2): 351-360.

Hwang, W. S., Li, B., et al. (1992). "Collagen Fibril Structure of Normal, Aging, and Osteoarthritic Cartilage." The Journal of Pathology **167**(4): 425-433.

Ignotz, R. A. and Massagué, J. (1986). "Transforming Growth Factor-β Stimulates the Expression of Fibronectin and Collagen and Their Incorporation into the Extracellular Matrix." Journal of Biological Chemistry **261**(9): 4337-4345.

Jakobsen, R. B., Engebretsen, L., et al. (2005). "An Analysis of the Quality of Cartilage Repair Studies." Journal of Bone and Joint Surgery **87A**(10): 2232-2239.

Janjanin, S., Li, W.-J., et al. (2008). "Mold-Shaped, Nanofiber Scaffold-Based Cartilage Engineering Using Human Mesenchymal Stem Cells and Bioreactor." Journal of Surgical Research **149**(1): 47-56.

Jeffery, A., Blunn, G., et al. (1991). "Three-Dimensional Collagen Architecture in Bovine Articular Cartilage." Journal of Bone and Joint Surgery **73B**(5): 795-801.

Jin, M., Emkey, G. R., et al. (2003). "Combined Effects of Dynamic Tissue Shear Deformation and Insulin-Like Growth Factor-1 on Chondrocyte Biosynthesis in Cartilage Explants." Archives of Biochemistry and Biophysics **414**(2): 223-231.

Jürgensen, K., Aeschlimann, D., et al. (1997). "A New Biological Glue for Cartilage-Cartilage Interfaces: Tissue Transglutaminase." The Journal of Bone and Joint Surgery **79**(2): 185-193.

Jurvelin, J., Kiviranta, I., et al. (1986). "Softening of Canine Articular Cartilage after Immobilization of the Knee Joint." Clinical Orthopaedics and Related Research (207): 246-252.

Kapur, S., Mohan, S., et al. (2005). "Fluid Shear Stress Synergizes with Insulin-Like Growth Factor-1 (IGF-1) on Osteoblast Proliferation through Integrin-Dependent Activation of IGF-1 Mitogenic Signaling Pathway." Journal of Biological Chemistry **280**(20): 20163-20170.

Katzenstein, A.-L. A. (1985). "Pathogenesis of "Fibrosis" in Interstitial Pneumonia: An Electron Microscopic Study." Human Pathology **16**(10): 1015-1024.

Kavalkovich, K., Boynton, R., et al. (2002). "Chondrogenic Differentiation of Human Mesenchymal Stem Cells within an Alginate Layer Culture System." In Vitro Cellular & Developmental Biology - Animal **38**(8): 457-466.

Kelly, T.-A. N., Ng, K. W., et al. (2006). "Spatial and Temporal Development of Chondrocyte-Seeded Agarose Constructs in Free-Swelling and Dynamically Loaded Cultures." Journal of Biomechanics **39**(8): 1489-1497.

Kelly, T.-A. N., Fisher, M. B., et al. (2008). "Low-Serum Media and Dynamic Deformational Loading in Tissue Engineering of Articular Cartilage." Annals of Biomedical Engineering **36**(5): 769-779.

Kelly, T.-A. N., Ng, K. W., et al. (2009). "Analysis of Radial Variations in Material Properties and Matrix Composition of Chondrocyte-Seeded Agarose Hydrogel Constructs." Osteoarthritis and Cartilage **17**(1): 73-82.

Khalafi, A., Schmid, T. M., et al. (2007). "Increased Accumulation of Superficial Zone Protein (SZP) in Articular Cartilage in Response to Bone Morphogenetic Protein-7 and Growth Factors." Journal of Orthopaedic Research **25**(3): 293-303.

Khan, I. M., Gilbert, S. J., et al. (2008). "Cartilage Integration: Evaluation of the Reasons for Failure of Integration During Cartilage Repair. A Review." European Cells and Materials **16**: 26-39.

Kim, H.-J. and Im, G.-I. (2008). "Combination of Transforming Growth Factor-Beta2 and Bone Morphogenetic Protein-7 Enhances Chondrogenesis from Adipose Tissue-Derived Mesenchymal Stem Cells." Tissue Engineering Part A **15**(7): 1543-1551.

Kim, M., Erickson, I. E., et al. (2012). "Transient Exposure to TGF-β3 Improves the Functional Chondrogenesis of MSC-Laden Hyaluronic Acid Hydrogels." Journal of the Mechanical Behavior of Biomedical Materials **11**(0): 92-101.

Kim, Y.-J., Sah, R. L. Y., et al. (1988). "Fluorometric Assay of DNA in Cartilage Explants Using Hoechst 33258." Analytical Biochemistry **174**(1): 168-176.

Kim, Y.-J., Grodzinsky, A. J., et al. (1996). "Compression of Cartilage Results in Differential Effects on Biosynthetic Pathways for Aggrecan, Link Protein, and Hyaluronan." Archives of Biochemistry and Biophysics **328**(2): 331-340.

Kish, G., Módis, L., et al. (1999). "Osteochondral Mosaicplasty for the Treatment of Focal Chondral and Osteochondral Lesions of the Knee and Talus in the Athlete: Rationale, Indications, Techniques, and Results." Clinics in Sports Medicine **18**(1): 45-66.

Kisiday, J., Jin, M., et al. (2002). "Self-Assembling Peptide Hydrogel Fosters Chondrocyte Extracellular Matrix Production and Cell Division: Implications for Cartilage Tissue Repair." Proceedings of the National Academy of Sciences of the United States of America **99**(15): 9996-10001.

Kisiday, J. D., Jin, M., et al. (2004). "Effects of Dynamic Compressive Loading on Chondrocyte Biosynthesis in Self-Assembling Peptide Scaffolds." Journal of Biomechanics **37**(5): 595-604.

Kisiday, J. D., Kurz, B., et al. (2005). "Evaluation of Medium Supplemented with Insulin-Transferrin-Selenium for Culture of Primary Bovine Calf Chondrocytes in Three-Dimensional Hydrogel Scaffolds." Tissue Engineering **11**(1-2): 141-151.

Kisiday, J. D., Kopesky, P. W., et al. (2008). "Evaluation of Adult Equine Bone Marrow- and Adipose-Derived Progenitor Cell Chondrogenesis in Hydrogel Cultures." Journal of Orthopaedic Research **26**(3): 322-331.

Klein, T. J., Chaudhry, M., et al. (2007). "Depth-Dependent Biomechanical and Biochemical Properties of Fetal, Newborn, and Tissue-Engineered Articular Cartilage." Journal of Biomechanics **40**(1): 182-190.

Knudson, W. and Knudson, C. B. (2004). "An Update on Hyaluronan and CD44 in Cartilage." Current Opinion in Orthopaedics **15**(5): 369-375.

Knutsen, G., Engebretsen, L., et al. (2004). "Autologous Chondrocyte Implantation Compared with Microfracture in the Knee." Journal of Bone and Joint Surgery **86**(3): 455-464.

Koga, H., Muneta, T., et al. (2008). "Comparison of Mesenchymal Tissues-Derived Stem Cells for in Vivo Chondrogenesis: Suitable Conditions for Cell Therapy of Cartilage Defects in Rabbit." Cell and Tissue Research **333**(2): 207-215.

Kosmakos, F. C. and Roth, J. (1980). "Insulin-Induced Loss of the Insulin Receptor in IM-9 Lymphocytes. A Biological Process Mediated through the Insulin Receptor." Journal of Biological Chemistry **255**(20): 9860-9869.

Krupp, M. and Lane, M. D. (1981). "On the Mechanism of Ligand-Induced Down-Regulation of Insulin Receptor Level in the Liver Cell." Journal of Biological Chemistry **256**(4): 1689-1694.

Kuettner, K. E. (1992). "Biochemistry of Articular Cartilage in Health and Disease." Clinical Biochemistry **25**(3): 155-163.

Lau, K.-H. W., Kapur, S., et al. (2006). "Up-Regulation of the Wnt, Estrogen Receptor, Insulin-Like Growth Factor-1, and Bone Morphogenetic Protein Pathways in C57BL/6J Osteoblasts as Opposed to C3H/HeJ Osteoblasts in Part Contributes to the Differential Anabolic Response to Fluid Shear." Journal of Biological Chemistry **281**(14): 9576-9588.

Lee, M. C., Sung, K. L. P., et al. (2000). "Adhesive Force of Chondrocytes to Cartilage: Effects of Chondroitinase ABC." Clinical Orthopaedics and Related Research **370**: 286-294.

Li, W.-J., Danielson, K. G., et al. (2003). "Biological Response of Chondrocytes Cultured in Three-Dimensional Nanofibrous Poly(ε-Caprolactone) Scaffolds." Journal of Biomedical Materials Research Part A **67A**(4): 1105-1114.

Liang, D., Hsiao, B. S., et al. (2007). "Functional Electrospun Nanofibrous Scaffolds for Biomedical Applications." Advanced Drug Delivery Reviews **59**(14): 1392-1412.

Lim, S., Oh, S., et al. (2010). "Dual Growth Factor-Releasing Nanoparticle/Hydrogel System for Cartilage Tissue Engineering." Journal of Materials Science: Materials in Medicine **21**(9): 2593-2600.

Lima, E. G., Bian, L., et al. (2007). "The Beneficial Effect of Delayed Compressive Loading on Tissue-Engineered Cartilage Constructs Cultured with TGF-β3." Osteoarthritis and Cartilage **15**(9): 1025-1033.

Lima, E. G., Tan, A. R., et al. (2009). "Genipin Enhances the Mechanical Properties of Tissue-Engineered Cartilage and Protects against Inflammatory Degradation When Used as a Medium Supplement." Journal of Biomedical Materials Research Part A **91A**(3): 692-700.

Lin, Z., Willers, C., et al. (2006). "The Chondrocyte: Biology and Clinical Application." Tissue Engineering **12**(7): 1971-1984.

Ling, Y., Rubin, J., et al. (2007). "A Cell-Laden Microfluidic Hydrogel." Lab on a Chip **7**(6): 756-762.

Liu, Y., Shu, X. Z., et al. (2006). "Osteochondral Defect Repair with Autologous Bone Marrow-Derived Mesenchymal Stem Cells in an Injectable, in Situ, Cross-Linked Synthetic Extracellular Matrix." Tissue Engineering **12**(12): 3405-3416.

Lohmann, C. H., Schwartz, Z., et al. (2000). "Pretreatment with Platelet Derived Growth Factor-BB Modulates the Ability of Costochondral Resting Zone Chondrocytes Incorporated into PLA/PGA Scaffolds to Form New Cartilage in Vivo." Biomaterials **21**(1): 49-61.

Macdonald, M., Rodriguez, N. M., et al. (2008). "Release of a Model Protein from Biodegradable Self Assembled Films for Surface Delivery Applications." Journal of Controlled Release **131**(3): 228-234.

Macdonald, M. L., Rodriguez, N. M., et al. (2010). "Characterization of Tunable FGF-2 Releasing Polyelectrolyte Multilayers." Biomacromolecules **11**(8): 2053-2059.

Macdonald, M. L., Samuel, R. E., et al. (2011). "Tissue Integration of Growth Factor-Eluting Layer-by-Layer Polyelectrolyte Multilayer Coated Implants." Biomaterials **32**(5): 1446-1453.

Malaviya, P. and Nerem, R. M. (2002). "Fluid-Induced Shear Stress Stimulates Chondrocyte Proliferation Partially Mediated via Transforming Growth Factor-β1." Tissue Engineering **8**(4): 581-590.

Mandl, E. W., Van Der Veen, S. W., et al. (2002). "Serum-Free Medium Supplemented with High-Concentration Fibroblast Growth Factor-2 for Cell Expansion Culture

of Human Ear Chondrocytes Promotes Redifferentiation Capacity." Tissue Engineering **8**(4): 573-580.

Martin, I., Vunjak-Novakovic, G., et al. (1999). "Mammalian Chondrocytes Expanded in the Presence of Fibroblast Growth Factor-2 Maintain the Ability to Differentiate and Regenerate Three-Dimensional Cartilaginous Tissue." Experimental Cell Research **253**(2): 681-688.

Martin, I., Obradovic, B., et al. (2000). "Modulation of the Mechanical Properties of Tissue Engineered Cartilage." Biorheology **37**(1-2): 141-147.

Mathieu, P. S. and Loboa, E. G. (2012). "Cytoskeletal and Focal Adhesion Influences on Mesenchymal Stem Cell Shape, Mechanical Properties, and Differentiation Down Osteogenic, Adipogenic, and Chondrogenic Pathways." Tissue Engineering Part B: Reviews **18**(6): 436-444.

Mauck, R. L., Soltz, M. A., et al. (2000). "Functional Tissue Engineering of Articular Cartilage through Dynamic Loading of Chondrocyte-Seeded Agarose Gels." Journal of Biomechanical Engineering **122**(3): 252-260.

Mauck, R. L., Hung, C. T., et al. (2003). "Modeling of Neutral Solute Transport in a Dynamically Loaded Porous Permeable Gel: Implications for Articular Cartilage Biosynthesis and Tissue Engineering." Journal of Biomechanical Engineering **125**(5): 602-614.

Mauck, R. L., Nicoll, S. B., et al. (2003). "Synergistic Action of Growth Factors and Dynamic Loading for Articular Cartilage Tissue Engineering." Tissue Engineering **9**(4): 597-611.

Mauck, R. L., Yuan, X., et al. (2006). "Chondrogenic Differentiation and Functional Maturation of Bovine Mesenchymal Stem Cells in Long-Term Agarose Culture." Osteoarthritis and Cartilage **14**(2): 179-189.

Mcbeath, R., Pirone, D. M., et al. (2004). "Cell Shape, Cytoskeletal Tension, and Rhoa Regulate Stem Cell Lineage Commitment." Developmental Cell **6**(4): 483-495.

Mcquillan, D. J., C J Handley, C. J., et al. (1986). "Stimulation of Proteoglycan Biosynthesis by Serum and Insulin-Like Growth Factor-1 in Cultured Bovine Articular Cartilage." Biochemical Journal **240**(2): 423-430.

Meng, X. M., Huang, X. R., et al. (2010). "Smad2 Protects against TGF-β/Smad3-Mediated Renal Fibrosis." Journal of the American Society of Nephrology **21**(9): 1477-1487.

Mo, X.-T., Guo, S.-C., et al. (2009). "Variations in the Ratios of Co-Cultured Mesenchymal Stem Cells and Chondrocytes Regulate the Expression of Cartilaginous and Osseous Phenotype in Alginate Constructs." Bone **45**(1): 42-51.

Mohtai, M., Gupta, M. K., et al. (1996). "Expression of Interleukin-6 in Osteoarthritic Chondrocytes and Effects of Fluid-Induced Shear on This Expression in Normal Human Chondrocytes in Vitro." Journal of Orthopaedic Research **14**(1): 67-73.

Morales, T. I. and Roberts, A. B. (1988). "Transforming Growth Factor-β Regulates the Metabolism of Proteoglycans in Bovine Cartilage Organ Cultures." Journal of Biological Chemistry **263**(26): 12828-12831.

Moretti, M., Wendt, D., et al. (2005). "Structural Characterization and Reliable Biomechanical Assessment of Integrative Cartilage Repair." Journal of Biomechanics **38**(9): 1846-1854.

Moroni, L., De Wijn, J. R., et al. (2006). "3D Fiber-Deposited Scaffolds for Tissue Engineering: Influence of Pores Geometry and Architecture on Dynamic Mechanical Properties." Biomaterials **27**(7): 974-985.

Moyer, H. R., Wang, Y., et al. (2010). "A New Animal Model for Assessing Cartilage Repair and Regeneration at a Nonarticular Site." Tissue Engineering Part A **16**(7): 2321-2330.

Mu¨Ssener, Å., Litton, M. J., et al. (1997). "Cytokine Production in Synovial Tissue of Mice with Collagen-Induced Arthritis (CIA)." Clinical and Experimental Immunology **107**(3): 485-493.

Negishi, M., Lu, D., et al. (2001). "Upregulatory Expression of Furin and Transforming Growth Factor-β by Fluid Shear Stress in Vascular Endothelial Cells." Arteriosclerosis, Thrombosis, and Vascular Biology **21**(5): 785-790.

Nerem, R. M. and Sambanis, A. (1995). "Tissue Engineering: From Biology to Biological Substitutes." Tissue Engineering **1**(1): 3-13.

Nisbet, D. R., Forsythe, J. S., et al. (2009). "Review Paper: A Review of the Cellular Response on Electrospun Nanofibers for Tissue Engineering." Journal of Biomaterials Applications **24**(1): 7-29.

Nixon, A. J., Fortier, L. A., et al. (1999). "Enhanced Repair of Extensive Articular Defects by Insulin-Like Growth Factor-1-Laden Fibrin Composites." Journal of Orthopaedic Research **17**(4): 475-487.

O'connell, G. D., Fong, J. V., et al. (2012). "Trimethylamine N-Oxide as a Media Supplement for Cartilage Tissue Engineering." Journal of Orthopaedic Research **30**(12): 1898-1905.

O'connor-Mccourt, M. D. and Wakefield, L. M. (1987). "Latent Transforming Growth Factor-β in Serum. A Specific Complex with α2-Macroglobulin." Journal of Biological Chemistry **262**(29): 14090-14099.

Obradovic, B., Martin, I., et al. (2001). "Integration of Engineered Cartilage." Journal of Orthopaedic Research **19**(6): 1089-1097.

Ohno, M., Cooke, J. P., et al. (1995). "Fluid Shear Stress Induces Endothelial Transforming Growth Factor-β1 Transcription and Production. Modulation by Potassium Channel Blockade." Journal of Clinical Investigation **95**(3): 1363-1369.

Otero, M., Favero, M., et al. (2012). Human Chondrocyte Cultures as Models of Cartilage-Specific Gene Regulation. Human Cell Culture Protocols. R. R. Mitry and R. D. Hughes, Humana Press. **806:** 301-336.

Pacherník, J., Bryja, V., et al. (2005). "Neural Differentiation of Pluripotent Mouse Embryonal Carcinoma Cells by Retinoic Acid: Inhibitory Effect of Serum." Physiological Research **54**(1): 115-122.

Papoutsakis, E. T. (1991). "Fluid-Mechanical Damage of Animal Cells in Bioreactors." Trends in Biotechnology **9**(1): 427-437.

Park, H., Temenoff, J. S., et al. (2005). "Delivery of TGF-β1 and Chondrocytes via Injectable, Biodegradable Hydrogels for Cartilage Tissue Engineering Applications." Biomaterials **26**(34): 7095-7103.

Park, H., Temenoff, J. S., et al. (2007). "Injectable Biodegradable Hydrogel Composites for Rabbit Marrow Mesenchymal Stem Cell and Growth Factor Delivery for Cartilage Tissue Engineering." Biomaterials **28**(21): 3217-3227.

Pazzano, D., Mercier, K. A., et al. (2000). "Comparison of Chondrogensis in Static and Perfused Bioreactor Culture." Biotechnology Progress **16**(5): 893-896.

Pei, M., Seidel, J., et al. (2002). "Growth Factors for Sequential Cellular De- and Re-Differentiation in Tissue Engineering." Biochemical and Biophysical Research Communications **294**(1): 149-154.

Pelaez, D., Charles Huang, C.-Y., et al. (2008). "Cyclic Compression Maintains Viability and Induces Chondrogenesis of Human Mesenchymal Stem Cells in Fibrin Gel Scaffolds." Stem Cells and Development **18**(1): 93-102.

Peretti, G. M., Zaporojan, V., et al. (2003). "Cell-Based Bonding of Articular Cartilage: An Extended Study." Journal of Biomedical Materials Research Part A **64A**(3): 517-524.

Peretti, G. M., Campo-Ruiz, V., et al. (2006). "Tissue Engineered Cartilage Integration to Live and Devitalized Cartilage: A Study by Reflectance Mode Confocal Microscopy and Standard Histology." Connective Tissue Research **47**(4): 190-199.

Perka, C., Schultz, O., et al. (2000). "The Influence of Transforming Growth Factor-β1 on Mesenchymal Cell Repair of Full-Thickness Cartilage Defects." Journal of Biomedical Materials Research **52**(3): 543-552.

Persson, G. R. (2012). "Rheumatoid Arthritis and Periodontitis – Inflammatory and Infectious Connections. Review of the Literature." Journal of Oral Microbiology **4**.

Ronn, K., Reischl, N., et al. (2011). "Current Surgical Treatment of Knee Osteoarthritis." Arthritis **2011**.

Rosier, R. N., O'keefe, R. J., et al. (1998). "The Potential Role of Transforming Growth Factor Beta in Fracture Healing." Clinical Orthopaedics and Related Research **355**: S294-S300.

Roy, R., Boskey, A. L., et al. (2008). "Non-Enzymatic Glycation of Chondrocyte-Seeded Collagen Gels for Cartilage Tissue Engineering." Journal of Orthopaedic Research **26**(11): 1434-1439.

Sah, R. L., Trippel, S. B., et al. (1996). "Differential Effects of Serum, Insulin-Like Growth Factor-1, and Fibroblast Growth Factor-2 on the Maintenance of Cartilage Physical Properties During Long-Term Culture." Journal of Orthopaedic Research **14**(1): 44-52.

Sah, R. L. Y., Kim, Y.-J., et al. (1989). "Biosynthetic Response of Cartilage Explants to Dynamic Compression." Journal of Orthopaedic Research **7**(5): 619-636.

Sah, R. L. Y., Doong, J.-Y. H., et al. (1991). "Effects of Compression on the Loss of Newly Synthesized Proteoglycans and Proteins from Cartilage Explants." Archives of Biochemistry and Biophysics **286**(1): 20-29.

Sakai, K., Mohtai, M., et al. (1998). "Fluid Shear Stress Increases Transforming Growth Factor-β1 Expression in Human Osteoblast-Like Cells: Modulation by Cation Channel Blockades." Calcified Tissue International **63**(6): 515-520.

Saris, D. B. F., Vanlauwe, J., et al. (2008). "Characterized Chondrocyte Implantation Results in Better Structural Repair When Treating Symptomatic Cartilage Defects of the Knee in a Randomized Controlled Trial Versus Microfracture." The American Journal of Sports Medicine **36**(2): 235-246.

Schlechter, N. L., Russell, S. M., et al. (1986). "Evidence Suggesting That the Direct Growth-Promoting Effect of Growth Hormone on Cartilage in Vivo Is Mediated by Local Production of Somatomedin." Proceedings of the National Academy of Sciences of the United States of America **83**(20): 7932-7934.

Schumacher, R., Mosthaf, L., et al. (1991). "Insulin and Insulin-Like Growth Factor-1 Binding Specificity Is Determined by Distinct Regions of Their Cognate Receptors." Journal of Biological Chemistry **266**(29): 19288-19295.

Sgaglione, N. A., Miniaci, A., et al. (2002). "Update on Advanced Surgical Techniques in the Treatment of Traumatic Focal Articular Cartilage Lesions in the Knee." Arthroscopy-the Journal of Arthroscopic and Related Surgery **18**(2): 9-32.

Shah, N. J., Macdonald, M. L., et al. (2011). "Tunable Dual Growth Factor Delivery from Polyelectrolyte Multilayer Films." Biomaterials **32**(26): 6183-6193.

Shao, X., Goh, J. C. H., et al. (2006). "Repair of Large Articular Osteochondral Defects Using Hybrid Scaffolds and Bone Marrow-Derived Mesenchymal Stem Cells in a Rabbit Model." Tissue Engineering **12**(6): 1539-1551.

Shapiro, F., Koide, S., et al. (1993). "Cell Origin and Differentiation in the Repair of Full-Thickness Defects of Articular Cartilage." The Journal of bone and joint surgery **75**(4): 532-553.

Shapiro, L. E. and Wagner, N. (1988). "Growth of H-35 Rat Hepatoma Cells in Unsupplemented Serum-Free Media: Effect of Transferrin, Insulin and Cell Density." In Vitro Cellular and Developmental Biology. Animal **24**(4): 299-303.

Shapiro, L. E. and Wagner, N. (1989). "Transferrin Is an Autocrine Growth Factor Secreted by Reuber H-35 Cells in Serum-Free Culture " In Vitro Cellular and Developmental Biology. Animal **25**(7): 650-654.

Sheehy, E. J., Buckley, C. T., et al. (2011). "Chondrocytes and Bone Marrow-Derived Mesenchymal Stem Cells Undergoing Chondrogenesis in Agarose Hydrogels of Solid and Channelled Architectures Respond Differentially to Dynamic Culture Conditions." Journal of Tissue Engineering and Regenerative Medicine **5**(9): 747-758.

Shen, B., Wei, A., et al. (2008). "BMP-2 Enhances TGF-β3–Mediated Chondrogenic Differentiation of Human Bone Marrow Multipotent Mesenchymal Stromal Cells in Alginate Bead Culture." Tissue Engineering Part A **15**(6): 1311-1320.

Shi, Y. and Massagué, J. (2003). "Mechanisms of TGF-β Signaling from Cell Membrane to the Nucleus." Cell **113**(6): 685-700.

Shukla, A., Fleming, K. E., et al. (2010). "Controlling the Release of Peptide Antimicrobial Agents from Surfaces." Biomaterials **31**(8): 2348-2357.

Silverman, R. P., Bonasser, L., et al. (2000). "Adhesion of Tissue-Engineered Cartilage to Native Cartilage." Plastic and Reconstructive Surgery **105**(4): 1393-1398.

Smith, R. L., Rusk, S. F., et al. (1996). "In Vitro Stimulation of Articular Chondrocyte Mrna and Extracellular Matrix Synthesis by Hydrostatic Pressure." Journal of Orthopaedic Research **14**(1): 53-60.

Smith, R. L., Trindade, M. C. D., et al. (2000). "Time-Dependent Effects of Intermittent Hydrostatic Pressure on Articular Chondrocyte Type II Collagen and Aggrecan Mrna Expression." Journal of Rehabilitation Research and Development **37**(2): 153-161.

Spiller, K. L., Liu, Y., et al. (2012). "A Novel Method for the Direct Fabrication of Growth Factor-Loaded Microspheres within Porous Nondegradable Hydrogels: Controlled Release for Cartilage Tissue Engineering." Journal of Controlled Release **157**(1): 39-45.

Steinmeyer, J. and Knue, S. (1997). "The Proteoglycan Metabolism of Mature Bovine Articular Cartilage Explants Superimposed to Continuously Applied Cyclic Mechanical Loading." Biochemical and Biophysical Research Communications **240**(1): 216-221.

Suryawan, A. and Hu, C. Y. (1993). "Effect of Serum on Differentiation of Porcine Adipose Stromal-Vascular Cells in Primary Culture." Comparative Biochemistry and Physiology. Comparative Physiology **105**(3): 485-492.

Takeuchi, Y., Nakayama, K., et al. (1996). "Differentiation and Cell Surface Expression of Transforming Growth Factor-B Receptors Are Regulated by Interaction with Matrix Collagen in Murine Osteoblastic Cells." Journal of Biological Chemistry **271**(7): 3938-3944.

Temenoff, J. S. and Mikos, A. G. (2000). "Review: Tissue Engineering for Regeneration of Articular Cartilage." Biomaterials **21**(5): 431-440.

Tew, S. R., Kwan, A. P. L., et al. (2000). "The Reactions of Articular Cartilage to Experimental Wounding: Role of Apoptosis." Arthritis and Rheumatism **43**(1): 215-225.

Theodoropoulos, J., De Croos, J., et al. (2011). "Integration of Tissue-Engineered Cartilage with Host Cartilage: An in Vitro Model." Clinical Orthopaedics and Related Research **469**(10): 2785-2795.

Tognana, E., Chen, F., et al. (2005). "Adjacent Tissues (Cartilage, Bone) Affect the Functional Integration of Engineered Calf Cartilage in Vitro." Osteoarthritis and Cartilage **13**(2): 129-138.

Tran-Khanh, N., Hoemann, C. D., et al. (2005). "Aged Bovine Chondrocytes Display a Diminished Capacity to Produce a Collagen-Rich, Mechanically Functional Cartilage Extracellular Matrix." Journal of Orthopaedic Research **23**(6): 1354-1362.

Tsao, Y. D. and Gonda, S. R. (1999). "A New Technology for Three-Dimensional Cell Culture: The Hydrodynamic Focusing Bioreactor." Advances in Heat and Mass Transfer in Biotechnology **44**: 37-38.

Uchino, M., Izumi, T., et al. (2000). "Growth Factor Expression in the Osteophytes of the Human Femoral Head in Osteoarthritis." Clinical Orthopaedics and Related Research **377**: 119-125.

Valhmu, W. B., Stazzone, E. J., et al. (1998). "Load-Controlled Compression of Articular Cartilage Induces a Transient Stimulation of Aggrecan Gene Expression." Archives of Biochemistry and Biophysics **353**(1): 29-36.

Van Der Kraan, P. M., Glansbeek, H. L., et al. (1997). "Early Elevation of Transforming Growth Factor-β, Decorin, and Biglycan mRNA Levels During Cartilage Matrix Restoration after Mild Proteoglycan Depletion." The Journal of Rheumatology **24**(3): 543-549.

Venkateswaran, V., Klotz, L. H., et al. (2002). "Selenium Modulation of Cell Proliferation and Cell Cycle Biomarkers in Human Prostate Carcinoma Cell Lines." Cancer Research **62**(9): 2540-2545.

Villiger, P. M. and Lotz, M. (1992). "Differential Expression of TGF-β Isoforms by Human Articular Chondrocytes in Response to Growth Factors." Journal of Cellular Physiology **151**(2): 318-325.

Vinardell, T., Thorpe, S., et al. (2009). "Chondrogenesis and Integration of Mesenchymal Stem Cells within an in Vitro Cartilage Defect Repair Model." Annals of Biomedical Engineering **37**(12): 2556-2565.

Vozzi, G., Flaim, C., et al. (2003). "Fabrication of PLGA Scaffolds Using Soft Lithography and Microsyringe Deposition." Biomaterials **24**(14): 2533-2540.

Vunjak-Novakovic, G., Freed, L. E., et al. (1996). "Effects of Mixing on the Composition and Morphology of Tissue-Engineered Cartilage." AIChE Journal **42**(3): 850-860.

Vunjak-Novakovic, G., Obradovic, B., et al. (1998). "Dynamic Cell Seeding of Polymer Scaffolds for Cartilage Tissue Engineering." Biotechnology Progress **14**(2): 193-202.

Vunjak-Novakovic, G., Martin, I., et al. (1999). "Bioreactor Cultivation Conditions Modulate the Composition and Mechanical Properties of Tissue-Engineered Cartilage." Journal of Orthopaedic Research **17**(1): 130-138.

Waldman, S. D., Spiteri, C. G., et al. (2003). "Long-Term Intermittent Shear Deformation Improves the Quality of Cartilaginous Tissue Formed in Vitro." Journal of Orthopaedic Research **21**(4): 590-596.

Waldman, S. D., Spiteri, C. G., et al. (2004). "Long-Term Intermittent Compressive Stimulation Improves the Composition and Mechanical Properties of Tissue-Engineered Cartilage." Tissue Engineering **10**(9-10): 1323-1331.

Woessner, J. F. (1961). "The Determination of Hydroxyproline in Tissue and Protein Samples Containing Small Proportions of This Imino Acid." Archives of Biochemistry and Biophysics **93**(2): 440-447.

Wood, K. C., Chuang, H. F., et al. (2006). "Controlling Interlayer Diffusion to Achieve Sustained, Multiagent Delivery from Layer-by-Layer Thin Films." Proceedings of the National Academy of Sciences of the United States of America **103**(27): 10207-10212.

Xie, L., Lin, A. S. P., et al. (2009). "Quantitative Assessment of Articular Cartilage Morphology via EPIC-μCT." Osteoarthritis and Cartilage **17**(3): 313-320.

Yaeger, P. C., Masi, T. L., et al. (1997). "Synergistic Action of Transforming Growth Factor-β and Insulin-Like Growth Factor-1 Induces Expression of Type II Collagen and Aggrecan Genes in Adult Human Articular Chondrocytes." Experimental Cell Research **237**(2): 318-325.

Yang, Y. -H. and Barabino, G. A. (2011). "Requirement for Serum in Medium Supplemented with Insulin-Transferrin-Selenium for Hydrodynamic Cultivation of Engineered Cartilage." Tissue Engineering Part A **17**(15-16): 2025-2035.

Yang, Y. -H. and Barabino, G. A. (in press). "Environmental Factors in Cartilage Tissue Engineering." Tissue and Organ Regeneration: Advances in Micro and Nanotechnology. Editors: Zhang, L.G., Khademhosseini, A. and Webster T.

Yang, Y. -H. and Barabino, G. A. (in press). "Differential Morphology and Homogeneity of Tissue-Engineered Cartilage in Hydrodynamic Cultivation with Transient Exposure to Insulin-Like Growth Factor-1 and Transforming Growth Factor-β1." Tissue Engineering Part A.

Yeatts, A. B. and Fisher, J. P. (2010). "Tubular Perfusion System for the Long-Term Dynamic Culture of Human Mesenchymal Stem Cells." Tissue Engineering Part C: Methods **17**(3): 337-348.

Yokota, H., Goldring, M. B., et al. (2003). "CITED2-Mediated Regulation of MMP-1 and MMP-13 in Human Chondrocytes under Flow Shear." Journal of Biological Chemistry **278**(47): 47275-47280.

Yokoyama, A., Sekiya, I., et al. (2005). "In Vitro Cartilage Formation of Composites of Synovium-Derived Mesenchymal Stem Cells with Collagen Gel." Cell and Tissue Research **322**(2): 289-298.

Yu, X., Botchwey, E. A., et al. (2004). "Bioreactor-Based Bone Tissue Engineering: The Influence of Dynamic Flow on Osteoblast Phenotypic Expression and Matrix Mineralization." Proceedings of the National Academy of Sciences of the United States of America **101**(31): 11203-11208.

Zhang, E., Li, X., et al. (2005). "Cell Cycle Synchronization of Embryonic Stem Cells: Effect of Serum Deprivation on the Differentiation of Embryonic Bodies in Vitro." Biochemical and Biophysical Research Communications **333**(4): 1171-1177.